

# **Purification and Characterization of Proteoglycan from Bovine Aortic Endothelial Cells Conditioned Media, and Its Interaction with Basic Fibroblast Growth Factor (bFGF)**

Ningling Wang

Thesis submitted to the Faculty of the  
Virginia Polytechnic Institute and State University  
in partial fulfillment of the requirements for the degree of

Master Science  
in  
Chemical Engineering

Kimberly E. Forsten, chair  
R. Michael Akers  
William H. Velander

August 27 , 1997  
Blacksburg, Virginia

Keywords: Proteoglycan, Basic Fibroblast Growth Factor (bFGF), Bovine Aortic Endothelial cells

Copyright 1997, Ningling Wang

# Purification and Characterization of Proteoglycan from Bovine Aortic Endothelial Cells Conditioned Media, and Its Interaction with Basic Fibroblast Growth Factor (bFGF)

Ningling Wang

(ABSTRACT)

Cultured bovine aortic endothelial (BAE) cells were found to synthesize and secrete heparan sulfate proteoglycans (HSPG), which bound basic fibroblast growth factor (bFGF). bFGF is a known mitogen for vascular smooth muscle cells, and is indicated to have a role in some proliferative vascular disorders. In the present study, we have purified proteoglycans from BAE cells conditioned media (BAE PG), and further separated the PG into two fractions, PG-I and PG-II, by ion exchange chromatography on a Q-Sepharose column using a linear salt gradient (0.15 M to 1.2 M). PG-I and PG-II elute at 0.85M salt and 0.1M salt respectively. BAE PG is primarily composed of heparan sulfate, which is accessible to the digestion of Heparinase I/III and nitrous acid treatment; and a small amount of chondroitin sulfate, which can be digested by Chondroitinase ABC. Gel filtration chromatography (Sepharose CL-2B and CL-4B columns) showed that BAE PG consisted of two different sized peaks, and had an average molecular weight of approximately  $5 \times 10^5$  Da. SDS-PAGE with silver staining indicated that BAE PG had two core proteins with estimated sizes of 300kDa and 320kDa, which corresponded to the core protein of PG-I and PG-II respectively. Western blotting with anti-perlecan primary antibody recognized the core proteins of BAE PG. Size exclusion chromatography (Sepharose CL-6B column) following  $\beta$ -elimination showed that BAE PG had GAG chains with an estimated size less than  $2 \times 10^5$  Da.

A protocol to investigate the cell free binding of bFGF with purified BAE PG was established using the BioRad Bio-Dot apparatus - the cationic filtration assay (CAFAS). Using a simple monovalent binding model, we obtained values for the equilibrium dissociation constant,  $K_D$ , of  $(1.6 \pm 0.8) \times 10^{-10}$  M; the dissociation rate constant,  $k_r$ , of

0.01 min<sup>-1</sup>; the association rate constant,  $k_f$ , of  $6.2 \times 10^7 \text{ M}^{-1}\text{min}^{-1}$  and the total binding sites of the proteoglycan,  $R_T$ , of 0.1~0.2 (# of site)/(molecule of PG). The comparison of experimental data with model predictions indicates that when the number of binding sites provided by the PG is similar or greater than that of bFGF, the monovalent binding model is valid. When the number of binding sites is less than that of bFGF, one possibility is that the binding might not be the described simple monovalent reaction, and bFGF might bind to the PG as dimers or oligomers. In addition, a model is proposed for BAE PG, in which 5 ~ 10 BAE PG molecules form a high affinity binding site for bFGF. Experimentally we find that exogenous heparan sulfate competes with BAE PG for binding with bFGF, while chondroitin sulfate seems to facilitate the binding. This result may be a useful consideration when we want to design possible pharmaceutical compounds.

## Acknowledgments

The accomplishment of this thesis is firstly attributed to the help from my advisor, Dr. Kimberly Forsten. From the first day I began my research work at Virginia Tech, she was always helpful, and encouraged me through every failure and success. Many discussions with her were of great benefit. I was impressed by her dedication and enthusiasm to research work, and felt fortunate to have her as my advisor.

Many thanks to Dr. Kathy Terlesky, who taught me about SDS-PAGE technique, and shared with me about her experiences in many experiments. Students in Dr. William Velander's lab and Dr. Richey Davis' lab were very friendly and generous to let me use some equipment in their labs. I also received support from Dr. Michael Akers and Dr. Doug Smiley for letting me use their  $\gamma$ -counter and scintillation counter when we were in need. All of these facilitated the process of my experimental work.

Living in America, I felt it a great pleasure to have friends. They gave me not only the happiness of being young, but also material and spiritual support when I was in trouble. I greatly appreciate their help and care. Christelle Laot, my present roommate and previous officemate, is my intimate companion. We shared sadness, laughter, different cultural backgrounds, and enjoyment of cooking.

Finally, a full heart of thankfulness to my parents and my brother. They have always been very supportive all my life. Without them, I could not be a person like what I am now. It is very interesting and instructive to talk with my brother, sharing daily life, and enjoying of being brother and sister and being friends. He is the greatest brother I could ever have. I love them, and would like to dedicate this thesis to them.

## Table of Contents

List of Figures .....	vi
List of Tables .....	viii
List of Abbreviations .....	ix
Chapter I. Introduction .....	1
1.1 General Background Information .....	2
1.2 Thesis Topic and General Outline .....	6
Chapter II. Structural Characteristics of Proteoglycan from Conditioned Media .....	12
2.1 Introduction .....	12
2.2 Separation and Purification of Proteoglycan from BAE Cells Conditioned Media .....	13
2.2-1 Materials and Methods .....	13
2.2-2 Standard Curves for DMB Assay and Bio-Rad Protein Microassay .....	14
2.3 Ion Exchange Chromatography with Linear Salt Gradient .....	15
2.3-1 Introduction .....	15
2.3-2 Further Purification of PG from BAE P9 Cells Conditioned Media (BAE P9 PG) on Q-Sepharose Column .....	16
2.4 Gel Filtration Chromatography .....	17
2.4-1 Introduction .....	17
2.4-2 Further Purification of BAE P9 PG by Gel filtration Chromatography .....	18
2.5 Structural Characteristics of BAE P9 PG .....	20
2.5-1 Enzyme Digestion .....	20
2.5-2 Nitrous Acid Treatment .....	23
2.5-3 Purification of BAE P9 PG by Ion Exchange Chromatography Following Enzyme Digestion .....	23
2.5-4 Size Evaluation of PG-I and PG-II by Sepharose CL-4B Gel Filtration .....	24
2.5-5 Size Evaluation of GAG Chains by Sepharose CL-6B Gel Filtration after $\beta$ -elimination Reaction .....	24
2.5-6 Characterization of Core Protein(s) of BAE P9 PG .....	25
2.6 Brief comparison of Proteoglycans from Different Cells Conditioned Media .....	31
2.6-1 Introduction of Cell Lines .....	31
2.6-2 Purification by Ion Exchange Chromatography of PGs Produced by Different Cells .....	31

Chapter III. Cell Free Binding Assay .....	53
3.1 Introduction .....	53
3.2 The Establishment of Protocol for Cell Free Binding Assay .....	54
3.3 The Cell Free Binding Assay of <sup>125</sup> I-bFGF with PG .....	68
 Chapter IV. Discussion, Conclusions and Future Work .....	 76
4.1 Discussion .....	76
4.1-1 Purification and Characterization of BAE P9 PG .....	76
4.1-2 Comparison of Experimental Data with Model Data .....	78
4.1-3 Proposed Model for BAE P9 PG.....	80
4.1-4 Effects of CS and Ca <sup>2+</sup> .....	81
4.1-5 Comparison of BAE P9 PG with Similar Molecules .....	82
4.2 Conclusions .....	85
4.3 Future Work .....	87
4.3-1 Purification of PG and the Study of Biological Function of its two Components .....	87
4.3-2 The System of bFGF, HSPG, and FGFR .....	88
4.3-3 Biological Functions of HSPG .....	90
4.3-4 Mathematical Models .....	90
 References .....	 99
 Appendix A .....	 108
 Appendix B .....	 111
 Appendix C .....	 114
 Curriculum Vitae .....	 116

## List of Figures

Chapter I. Introduction .....	1
Figure1-1 Schematic structure of cell receptors .....	8
Figure1-2 Methods of growth factor delivery .....	9
Figure1-3 Repeating disaccharide structure of glycosaminoglycans .....	10
Figure1-4 Structure of an artery wall .....	11
Chapter II. Structural Characteristics of Proteoglycan from Conditioned Media .....	12
Figure 2-1 Model of the domain structure of heparan sulfate .....	39
Figure 2-2 Heparan sulfate (HS) standard curves by DMB assay .....	40
Figure 2-3 Bovine serum albumin (BSA) standard curve by Bio-Rad protein microassay .....	41
Figure 2-4 Separation of BAE P9 PG on Q- Sepharose column with linear salt gradient .....	42
Figure 2-5 Sepharose CL-6B gel filtration of PG-I and PG-II of BAE P9 PG .....	43
Figure 2-6 Gel filtration of BAE P9 PG .....	44
Figure 2-7 Comparison of salt elution of BAE P9 PG with and without enzyme digestion .....	45
Figure 2-8 Comparison of non-fractionated BAE P9 PG, PG-I, and PG-II on Sepharose CL-4B .....	46
Figure 2-9 Comparison of non-fractionated BAE P9 PG and PG-I on Sepharose CL-6B after beta-elimination .....	47
Figure 2-10 Calibration curve of protein standards on SDS-PAGE .....	48
Figure 2-11 Results of SDS-PAGE with silver staining .....	49
Figure 2-12 Western blotting with the primary antibody of anti-perlecan .....	50
Figure 2-13 Comparison of PGs on Q-Sepharose column with the same salt linear gradient .....	51
Figure 2-14 Comparison of PGs on Q-Sepharose column with the optimal salt linear gradient .....	52
Chapter III. Cell Free Binding Assay .....	53
Figure 3-1 Diagram of the assembly of the Bio-Dot apparatus .....	64
Figure 3-2 Transient study of <sup>125</sup> I-bFGF with 1mg/ml BSA+0.15MTBS buffer in Bio-Dot .....	65
Figure 3-3 Effect of BSA concentration on transient study of <sup>125</sup> I-bFGF behavior in Bio-Dot .....	66
Figure 3-4 Study of washing effect on <sup>125</sup> I-bFGF and <sup>35</sup> S-PG behavior in Bio-Dot .....	67
Figure 3-5 Effect of different washing buffers on retention of <sup>125</sup> I-bFGF, <sup>35</sup> S-PG, and <sup>125</sup> I-bFGF-PG in Bio-Dot .....	68
Figure 3-6 Binding retention of <sup>125</sup> I-bFGF with PG in Bio-Dot .....	69

Figure 3-7 Effect of non-labeled bFGF on <sup>35</sup> S-PG retention in Bio-Dot .....	70
Figure 3-8 Transient study of binding of <sup>125</sup> I-bFGF with PG in Bio-Dot .....	71
Figure 3-9 Effect of PG on <sup>125</sup> I-bFGF retention in Bio-Dot .....	72
Figure 3-10 Effect of Ca <sup>2+</sup> on binding retention of PG with <sup>125</sup> I- bFGF in Bio-Dot .....	73
Figure 3-11 Effect of HS and CS on retention of <sup>125</sup> I-bFGF alone and on binding retention of <sup>125</sup> I-bFGF with PG .....	74
Figure 3-12 Effect of HS and CS on retention of 0.1ng <sup>125</sup> I-bFGF alone and on binding retention of 0.1ng <sup>125</sup> I-bFGF with 40ng PG .....	75
Chapter IV. Discussion, Conclusions and Future Work .....	76
Figure 4-1 Effect of PG-I and PG-II on <sup>125</sup> I-bFGF retention in Bio-Dot .....	95
Figure 4-2 Comparison of experimental data with model data - Binding of 10 ng PG with <sup>125</sup> I-bFGF .....	96
Figure 4-3 Comparison of experimental data with model data - Binding of 40 ng PG with <sup>125</sup> I-bFGF .....	97
Figure 4-4 Comparison of experimental data with model data - Binding of 80 ng PG with <sup>125</sup> I-bFGF .....	98



## List of Tables

Chapter II. Structural Characteristics of Proteoglycan from Conditioned Media .....	12
Table 1 Optimal programming method for producing linear salt gradient on standard Econo <sup>®</sup> system for purification of BAE P9 PG .....	33
Table 2 Fractionation range for Sepharose CL gels.....	33
Table 3 Effect of pH and concentration of Ca <sup>2+</sup> on Heparinase I / Heparinase III (Hep I/Hep III) digestion of heparan sulfate .....	34
Table 4 Effect of pH and Ca <sup>2+</sup> on Chondroitin ABC lyase digestion of chondroitin sulfate .....	35
Table 5 Effect of salt concentration of enzyme digestion of GAG .....	36
Table 6 Content percentage of heparan sulfate and chondroitin sulfate in BAE P9 PG .....	37
Table 7 Content percentage of heparan sulfate and chondroitin sulfate in PG-I and PG-II of BAE P9 PG .....	38
Chapter IV. Discussion, Conclusions and Future Work .....	76
Table 8 Comparison of model data with experiment data of the binding between 10 ng PG with <sup>125</sup> I-bFGF (0.1ng ~ 1.5ng) .....	92
Table 9 Comparison of model data with experiment data of the binding between 40 ng PG with <sup>125</sup> I-bFGF (0.1ng ~ 0.25ng).....	93
Table 10 Comparison of model data with experiment data of the binding between 80 ng PG with <sup>125</sup> I-bFGF (0.1ng ~ 1.5ng).....	94

## List of Abbreviations

aFGF: acidic fibroblast growth factor  
BAE cells: bovine aortic endothelial cells  
BAE P5 PG: proteoglycan purified from bovine aortic endothelial cells of passage 5  
BAE P9 PG: proteoglycan purified from bovine aortic endothelial cells of passage 9  
BAE P12 PG: proteoglycan purified from bovine aortic endothelial cells of passage 12  
bFGF: basic fibroblast growth factor  
BCIP/NBT: 5-Bromo-4-Chloro-3-indolyl phosphate/nitro blue tetrazolium  
BSA: bovine serum albumin  
C.ABC: Chondroitinase ABC  
CAFAS: cationic filtration assay  
CS: chondroitin sulfate  
CSR: cell surface receptor  
DMB: dimethylmethylene blue  
DMEM: Dulbecco's modified Eagle's medium  
FGF: fibroblast growth factor  
FGFR: fibroblast growth factor receptor  
GAG: glycosaminoglycan  
Hep I: Heparinase I  
Hep III: Heparinase III  
HS: heparan sulfate  
HSPG: heparan sulfate proteoglycan  
IdoA: iduronic acid  
Kav: distribution coefficient  
KGF: keratinocyte growth factor  
MW: molecular weight  
MWCO: molecular weight cut off  
PAGE: polyacrylamide gel electrophoresis  
PBS: phosphate buffered saline

PG: proteoglycan

SDS: sodium dodecylsulfate

SMC: smooth muscle cells

TBS: tris buffered saline

TEMED: N,N,N',N'-tetramethylethylene diamine

VEGF: vascular endothelium growth factor

# **Chapter I**

## **Introduction**

Cellular bioengineering combines biochemical experimentation and quantitative engineering modeling. We are interested in understanding cell behavior in terms of engineering properties such as transport and kinetics. For example, we are concerned with how cell proliferation is affected by key regulatory binding (kinetic) events involving components in the extracellular matrix with cell variables like growth factor ligand concentration and receptor density. Through mathematical modeling, we hope to gain a better understanding of the biological mechanisms. We can utilize experimental data to test our model's validity, and then exploit its predictive power. As Lauffenburger and Linderman (1993) wrote: "...mathematical modeling is really a way to formulate hypotheses in a framework that allows their full implications to be recognized. It is a proven tool in the quantitative analysis of complicated systems, whether living or not." Having obtained a reliable prediction of the consequences of changes in molecular properties, we can aid the pharmaceutical industry in the design of drugs that mimic, replace, or interfere with natural compounds that regulate cell functions.

Ischemic coronary disease is the leading cause of morbidity and mortality in the western world. Most available therapeutic approaches aim either at relieving symptoms by reducing myocardial oxygen demand, restoring flow to a localized segment of the arterial tree (angioplasty), or entirely bypassing (temporarily) obstruction (bypass surgery). It was proposed that therapeutic angiogenesis may provide new venues for blood supply to the myocardium (Harada, et al., 1996). Angiogenesis is a complex process involving endothelial and smooth muscle cell proliferation and migration, formation of new capillaries, breakdown of existing extracellular matrix and formation of the new one. In addition, following angioplasty and vascular bypass surgery, restenosis usually occurs (Liu, et al., 1989 and Casscells, 1992). Restenosis is a kind of intimal hyperplasia, caused by the proliferation of smooth muscle cells and their accumulation within the intima.

Growth factors, such as fibroblast growth factors (FGFs) and vascular endothelium growth factor (VEGF), and extracellular matrix components of endothelium may play important roles in the regulation of blood vessel homeostasis. Therefore, the study of those molecules will be beneficial for understanding these diseases and creating medicines or treatments for patients.

### **1.1 General Background Information:**

All living cells are surrounded by a lipid bilayer known as the cell membrane. Cell surface receptors are transmembrane proteins with an extracellular domain for binding ligands, such as growth factors, and a cytoplasmic domain, which can transduce a signal to the cell nucleus. Transduction can also occur indirectly through other membrane-associated or soluble cytoplasmic molecules (Fig. 1-1) (Lauffenburger and Linderman, 1993).

Growth factors can be thought of as immediate local signals used by cells to talk to each other locally (paracrine or juxtacrine secretion), to each other over distance (endocrine secretion), and to talk to themselves (autocrine secretion) (Fig. 1-2) (Hadley, 1996). The function of a growth factor then is to couple a cell to its environment and thus to provide the cell with plasticity to respond appropriately to external changes or to changes in its own state (Sporn and Roberts, 1990). Basic fibroblast growth factor (bFGF) was originally identified as an activity in extracts of pituitary and brain that stimulated the growth of 3T3 cells (Akira et al., 1990; Kawano et al., 1988). The FGFs are a family of cytokines, characterized by high affinity to heparin (Vlodavsky et al., 1991). They currently consist of seven members: FGF-1 (acidic FGF, aFGF), FGF-2 (basic FGF, bFGF), FGF-3 (*int-2*), FGF-4 (*Hst-1*, K-FGF), FGF-5, FGF-6 (*Hst-2*) and FGF-7 (keratinocyte GF). They exhibit mitogenic, angiogenic and neurotrophic properties. They have roles in a wide range of normal physiological processes such as wound repair, angiogenesis, neuronal differentiation and embryonic development (Turnbull and Gallagher, 1993). They are also implicated in various pathological processes such as carcinogenesis, Alzheimer's disease, and muscular dystrophy (Hughes and Hall, 1993). It

is thus apparent that FGFs, and agents which can modulate their activity, have important potential therapeutic applications.

Extracellular matrix-associated bFGF induces cell proliferation and differentiation of many cells of ectodermal or mesodermal origin via a high affinity membrane receptor (Turnbull and Gallagher, 1993; Vlodavsky et al., 1991; Moscatelli, 1988, 1987; Neufeld and Gospodarowicz, 1986, 1985). bFGF can also function as an autocrine factor in cultures of endothelial cells (Rifkin and Moscatelli, 1989; Sato and Rifkin, 1988; Schweigerer et al., 1987). Recent evidence suggests that bFGF and its receptors are key players in the development of the heart and vasculature and are involved in angiogenesis, vasculogenesis, and cardiomyogenesis (Hughes and Hall, 1993).

Proteoglycans are ubiquitous macromolecules that contain at least one glycosaminoglycan (GAG) side chain attached to a core protein (Hardingham and Fosang, 1992; Jackson et al., 1991). They are produced by most eukaryotic cells, and are found predominantly on the cell surface and in the extracellular matrix (Schlessinger et al., 1995). GAG chains are large extended structures, which are highly sulfated and negatively charged. They can be thought of as polymers with disaccharide monomers (Fig 1-3), and they dominate the physical properties of the protein to which they are covalently bound (Hardingham and Fosang, 1992). The primary GAG chains in proteoglycans are chondroitin sulfate, dermatan sulfate, heparan sulfate, and keratan sulfate (Ruoslahti, 1989). Different proteoglycans contain distinct protein core molecules with carbohydrate domain structures that may confer specific functional properties (Hardingham and Bayliss, 1990; Gallagher, 1989). Functions can vary from the physical effects of the proteoglycan aggrecan, which binds with link protein to hyaluronan to form multimolecular aggregates in cartilage, to heparan sulfate proteoglycans like syndecan, that provide matrix binding sites and cell surface receptors for growth factors such as bFGF (Hardingham and Fosang, 1992).

bFGF interacts with specific high affinity receptors on the cell surface (Moscatelli, 1987). The FGF receptors (FGFRs) constitute a family of transmembrane tyrosine kinases with

four known members that have overlapping affinities for the various members of the FGF family (Jaye et al., 1992). At least two of the FGFRs, FGFR-1 (the *flg* gene product) and FGFR-2 (the *bek* gene product), are high affinity receptors for bFGF (Dionne et al., 1990; Mansukhani et al., 1990, 1992). All FGFRs are receptor tyrosine kinases which possess three Ig-like domains at the extracellular region, a single transmembrane region, and a cytoplasmic split kinase domain which is activated upon ligand binding (Zimmer et al., 1993). Binding of bFGF to FGFR-1 or FGFR-2 results in autophosphorylation of the receptor and signaling to the cell (Bellot et al., 1991). bFGF also binds with lower affinity to the heparan sulfate moieties of proteoglycans on the cell surface and the extracellular matrix (Moscatelli, 1987; Vigny et al., 1988; Bashkin et al., 1989). The binding of bFGF to heparan sulfates is thought to confer several biological advantages to the growth factor:

- (1) bFGF bound to heparin or heparan sulfates is protected from thermal denaturation and proteolysis by proteinases, which exist at high levels at the site of tumor growth, neovascularization and wound healing (Gospodarowicz and Cheng, 1986; Saksela et al., 1988);
- (2) the heparan sulfate-bound bFGF may serve as a reservoir of growth factor that can provide a continuous source of ligand for the bFGF receptor where the continuous occupancy of the receptor may be required for long term stimulation (Rifkin and Moscatelli, 1989; Flaumenhaft et al., 1989; Presta et al., 1989);
- (3) the heparan sulfates of the tissues may provide a means to localize bFGF to a particular site, limiting its diffusion (Flaumenhaft et al., 1990);
- (4) soluble heparan sulfates can act as carriers of bFGF and by preventing its interaction with fixed heparan sulfates in the tissues assure its dissemination away from its site of release (Flaumenhaft et al., 1990);
- (5) bFGF can be internalized through its interaction with cell-surface heparan sulfates, clearing excess active molecules from the cell surface, perhaps helping to dampen the response to bFGF (Gannoun-Zaki et al., 1991; Roghani and Moscatelli, 1992; Rusnati and Presta, 1993); and

(6) heparin or heparan sulfates can increase the affinity of bFGF for its receptors, by decreasing the dissociation rate of the bFGF-receptor complex (Moscatelli, 1992; Nugent, and Edelman, 1992; Roghani et al., 1994).

This final point suggests that trimolecular complexes of bFGF, receptor, and heparan sulfate are formed and that these complexes are more stable than complexes of bFGF and receptor alone (Flaumenhaft and Rifkin, 1992; Turnbull and Gallagher, 1993; Roghani et al., 1994; Richard et al., 1995; Fannon and Nugent, 1996). Many investigators have examined the role of cell surface heparan sulfate proteoglycans in bFGF binding and activation of cell surface receptors (Cook et al., 1995; Mason, 1994; Roghani et al., 1994; Nugent and Edelman, 1992; Olwin and Rapraeger, 1992; Rapraeger et al., 1991; Yayon et al., 1991). Some early reports indicated that the interaction of bFGF with heparin or heparan sulfates was necessary for interaction of the growth factor with its tyrosine kinase receptor, and the complex of bFGF, heparan sulfate, and FGFR was a prerequisite for signal transduction (Rapraeger et al., 1991; Yayon et al., 1991). However, several recent studies have found that heparin or heparan sulfates were not strictly required for binding of bFGF to its receptor, internalization, or stimulation of mitogenic activity, but increased the affinity of the bFGF-receptor interaction to a moderate degree (Flaumenhaft and Rifkin, 1992; Turnbull and Gallagher, 1993; Roghani et al., 1994; Fannon and Nugent, 1996).

Vascular tissues contain two predominant cell types: endothelial cells and smooth muscle cells (Fig. 1-4) (Luciano et al., 1983). Arterial endothelial cells form a continuous, selectively permeable, nonthrombogenic barrier between circulating blood and the arterial wall. The anatomic continuity of the endothelial monolayer and the underlying vascular smooth muscle cells provides biochemical control of vascular physiology as well as structural integrity. The arterial endothelium serves as a transport barrier, a biochemical filter, and a regulator of many vascular phenomena. The most potent vasodilators, thromboresistant compounds and inhibitors of smooth muscle cell proliferation are endothelially derived (Nathan, et al., 1995). Both endothelial cells and smooth muscle cells have been shown to produce glycosaminoglycans as well as other connective tissue



components in culture (Oohira et al., 1983). Since vessel proteoglycans have been implicated in a variety of vascular functions, such as a maintenance of tissue integrity, permeability of macromolecules and hemostasis, as well as in the pathogenesis of vascular disease (Oohira et al., 1983; Kramer et al., 1982), their study is of considerable interest. In addition, binding of growth factors to proteoglycans is thought to have an important regulatory role (Ruoslahti and Yamaguchi, 1991). Many studies have reported stimulation of bFGF binding and mitogenic activity by heparin (Olwin and Rapraeger, 1992; Ornitz et al., 1992; Rapraeger et al., 1991; Yayon et al., 1991). It has also been shown that heparan sulfate proteoglycans produced by endothelial cells (fetal bovine pulmonary arterial endothelium) can have an inhibitory effects on smooth muscle cell proliferation, and these proteoglycans may mediate endothelial regulation of smooth muscle growth during development or pathologic pulmonary arterial remodeling (Castellot et al., 1981), especially as endothelial proteoglycans have inhibitory activity for both the bFGF binding and bFGF stimulation of vascular smooth muscle cell proliferation (Forsten et al., 1997). The infusion of analogs of endothelial products such as heparin successfully inhibits vascular cell proliferation *in vitro* and proliferative vascular diseases (such as restenosis after coronary angioplasty) in animal models but has not proven effective in human disease to date (Nugent, et al., 1993, Edelman and Karnovsky, 1994). It seems likely that whether proteoglycans, particularly heparan sulfates, inhibit or increase bFGF stimulation depends on the state of the target cell and the specific conditions present. This is where mathematical modeling (evaluation of parameter effects and relative importance of variables) will be of assistance.

## **1.2 Thesis Topic and General Outline:**

The purpose of our study is to clarify the exact consequences with regard to bFGF binding and its action with secreted proteoglycan from bovine aortic endothelial (BAE) cells conditioned media.

The thesis is essentially composed of four parts. In the first chapter, the general background information on proteoglycans and bFGF was introduced. One feature that recurs in proteoglycan biology is that their structure is open to extensive modulation during cellular expression. The major source of structural variation is in the GAG chains. The number of chains and their length can vary, as well as their pattern of sulfation. The change of GAG structure may be used to change the properties of proteoglycans to suit different biological needs (Hardingham and Fosang, 1992). Therefore, in the second chapter, proteoglycans from different cell types were compared briefly, although the emphasis is on exploring the structural characteristics of proteoglycan from BAE cells conditioned media. Linear-gradient ion exchange chromatography and gel filtration chromatography, along with enzymes (heparinase (HepI), heparitinase (HepIII), and chondroitinase ABC (C.ABC)) treatments were used to determine the profile of GAG chains in the proteoglycan. SDS-PAGE and western blotting helped us to identify the core proteins. A protocol for a cell free binding assay using Bio-Dot apparatus was set up, then we discussed and analyzed results from cell free binding assay in the third chapter. The binding studies of bFGF with the proteoglycan were conducted to seek the regulatory functions of the proteoglycan on bFGF binding. A simple mathematical model with several assumptions has been used to analyze the data from cell free binding assay by applying principles of chemical kinetics, such as mass balance and steady-state approximation. Finally, a discussion and our conclusions, along with future work are included in chapter four.

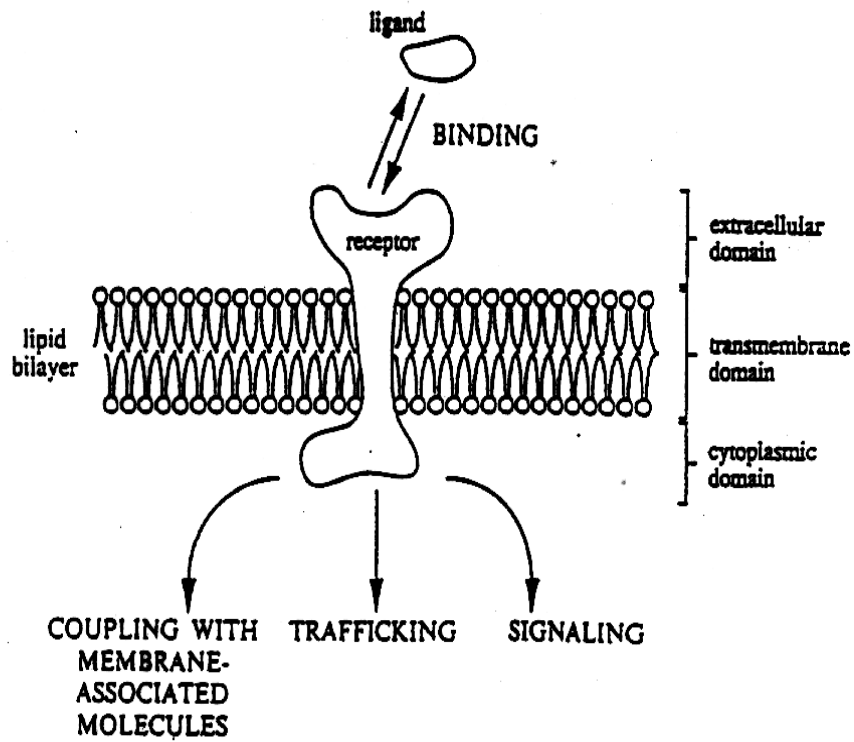
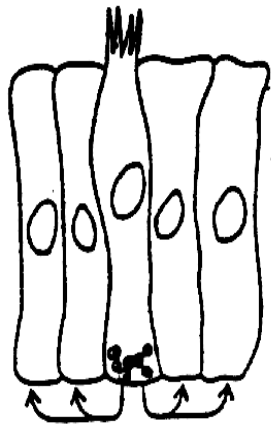
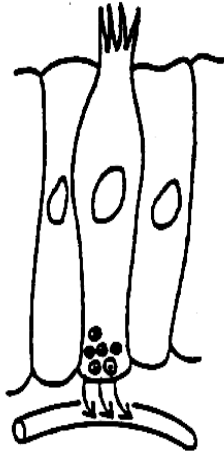


**Figure 1-1 Schematic structure of cell receptors**  
 (Lauffenburger and Landerman, 1993)

Paracrine



Endocrine



Autocrine

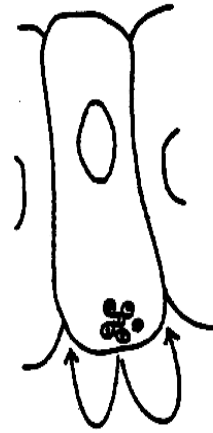


**Figure 1-2 Methods of growth factor delivery**  
(Hadley, 1996)

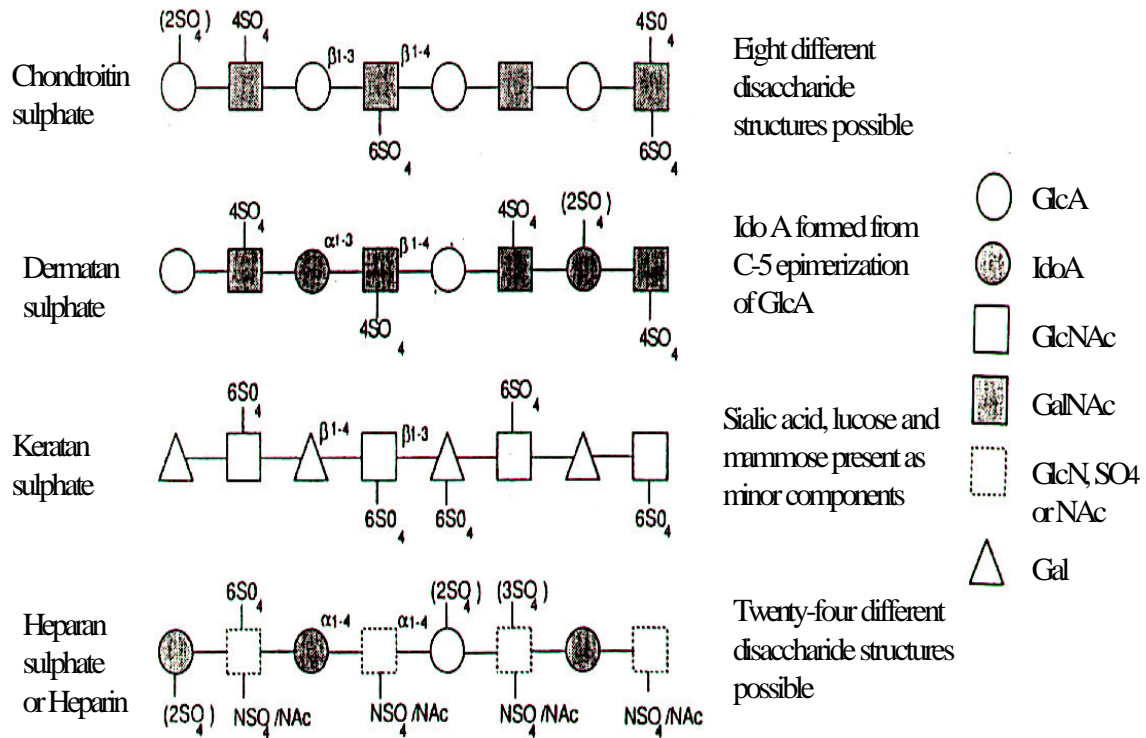


**Figure 1-3 Repeating disaccharide structure of glycosaminoglycans**  
(Hardingham and Fosang, 1992)

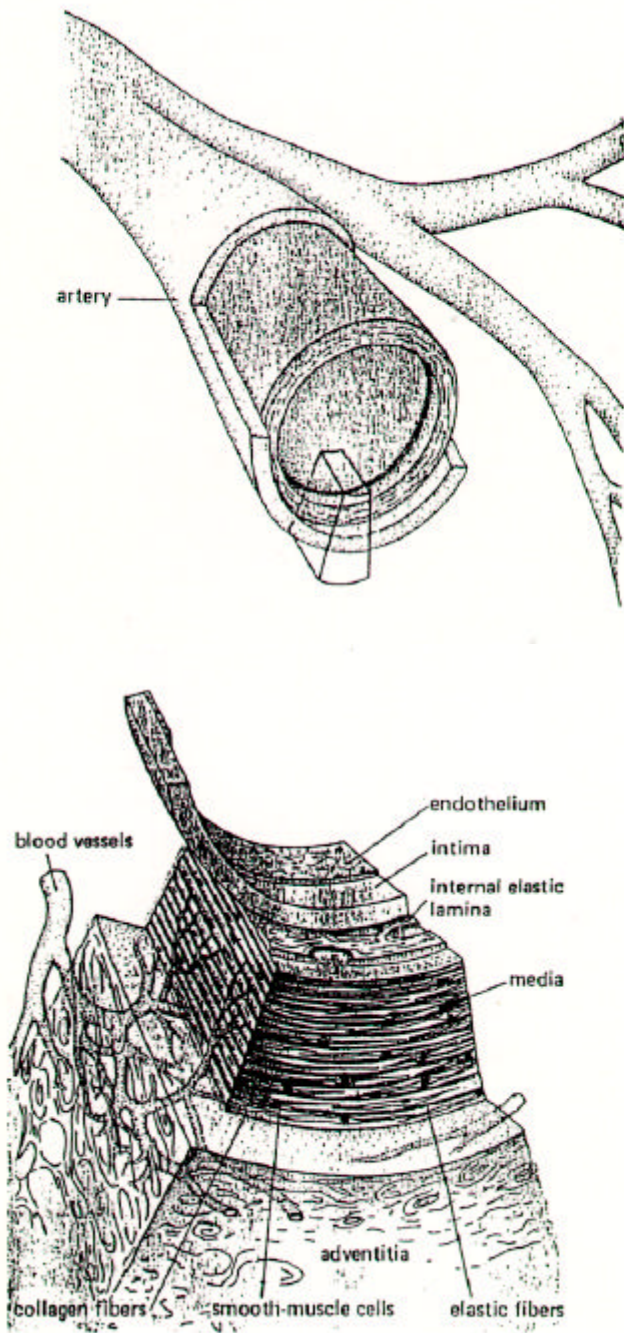


**Figure 1-4 Structure of an artery wall**  
(Luciano et al., 1983)

## **Chapter II**

### **Structural Characteristics of Proteoglycan from Conditioned Media**

#### **2.1 Introduction**

Proteoglycans are produced by most eukaryotic cells and are versatile components of pericellular and extracellular matrices (Schlessinger et al., 1995). They contain at least one glycosaminoglycan (GAG) side chain attached to a core protein (Hardingham and Fosang, 1992; Jackson et al., 1991). The charge and length of the GAG chains contributes to the structural variations of proteoglycans. These are open to extensive modulation during cellular expression which can endow certain properties to the proteoglycans suiting different biological activities (Hardingham and Fosang, 1992).

Heparan sulfates (HS) have an ordered domain structure with N- and O-sulfated regions (enriched in iduronic acid (IdoA) residues) separated by long N-acetyl-rich sequences (Figure 2-1). The N- and O-sulfated polysaccharide chains of HS covalently links to core proteins to form heparan-sulfate proteoglycans (HSPG). It has been reported that the heparinase-cleavage sites are present within the sulfated domains with the most proximal to the protein being on average 16 disaccharides from the protein linkage, whereas the first N-sulfate is approximately ten disaccharides from the protein linkage (Turnbull and Gallagher, 1993). The size, spacing, pattern of sulfation and IdoA content of the sulfated domains varies in a cell-specific manner. These molecules are constituents of most mammalian cells, being found mainly on cell surfaces, in the extracellular matrix and in basement membranes (Turnbull and Gallagher, 1993; Hook et al., 1984). In cultures of endothelial cells, they account for the majority of extracellular sulfated GAGs (Kramer et al., 1982). HS (and heparin) has a much larger number of structural possibilities compared with other glycosaminoglycans which have relatively regular repeat structures. This structural diversity is particularly suited for generating specific domain structures that can be utilized for biological recognition based on specific interactions with proteins (Yanagishita and Hascall, 1992). Many studies have shown that HS can bind bFGF

(Saksela et al., 1988; Baird and Ling, 1987; Moscatelli, D., 1987), and is also involved in bFGF receptor binding and signal transduction (Ornitz et al., 1992; Rapraeger et al., 1991; Yayan et al., 1991). HS has been suggested to play a role in cellular interactions and in growth control during morphogenesis, cell differentiation, and growth (Thesleff, et al., 1989; Iozzo, R., 1988; Castellot et al., 1987; San Antonio et al., 1987). Studies to define the structural characteristics of proteoglycan, especially HSPG from BAE cells conditioned media, will be of considerable interest because they will aid in analysis of the biological functions of HSPG in the extracellular matrix.

## **2.2 Separation and Purification of Proteoglycan from BAE Cells Conditioned Media**

### 2.2-1 Materials and methods

*Cell cultures* - Bovine aortic endothelial (BAE) cells were a generous gift from Dr. Matthew A. Nugent at Boston University School of Medicine. All cells were maintained in 100-mm culture dishes (Corning, Corning, NY) in Dulbecco's modified Eagle's medium (DMEM low glucose; Gibco, Grand Island, NY), supplemented with penicillin (100 units/ml), streptomycin (100 µg/ml), glutamine (2mM) and 10% calf serum (Hyclone, Logan, UT). Confluence was judged to occur when almost all the culture plate was covered with the typical "cobblestone" appearance of endothelial monolayer cells. The cell number was determined by counting trypsinized cells with a Coulter Counter (Model Z1, Coulter Electronics, Inc., Miami, FL).

*Conditioned Medium* - BAE cells at passage 9 (BAE P9 cells) were established in DMEM containing 10% calf serum and grown to confluence. Conditioned medium was prepared by washing the cells for 1 hr in serum-free DMEM at 37°C then incubating the cells for 24 hr in serum-free DMEM at 37°C. Following the 1 hr washing, the medium was collected and stored (1-hr-wash); and conditioned medium was collected after 24-hr incubation. Then media were centrifuged at 750 x g for 30 min at 4°C to remove cell debris. <sup>35</sup>SO<sub>4</sub> (NEN Life Sciences) metabolic labeling was also performed by the same procedures as



above with working concentration between 30 and 40  $\mu\text{Ci/ml}$  in serum-free DMEM during 24-hr incubation.

*Purification of Proteoglycan* - Anionic exchange chromatography was utilized to separate and purify the proteoglycan from BAE cells conditioned medium (BAE P9 PG). A Q-Sepharose (Sigma) column (1.0 x 2.5 cm) was poured and then equilibrated in tris buffered saline (TBS) (50 mM Tris, 0.15 M NaCl, pH 8.0) (referred to as 0.15 M TBS) with 1 M urea. Urea was added to the conditioned media to a final concentration of 1 M. The mixture was put into the refrigerator at 4°C for 30 min allowing the urea to break up proteoglycans aggregates. The mixture was then loaded onto the Q-Sepharose column at a flowrate of 1ml/min. After conditioned media had been loaded, anionic protein and glycoprotein were removed by washing (1ml/min) the column with TBS(0.3 M NaCl) with 1 M urea, and collected the effluent (0.3M-wash). The proteoglycan containing fraction (BAE P9 PG) was then eluted with TBS(1.5M NaCl) with 1M urea, and GAG content was determined using the colorimetric dimethylmethylene blue (DMB) dye binding assay with a heparan sulfate standard (Farnsdale et al., 1986) (DMB was obtained from Aldrich Chemical Co. Milwaukee, WI). Samples with higher value of  $\text{abs}@525$  were collected, pooled, and dialyzed against 0.15M TBS using Spectra/Por cellulose membrane (Spectrum, Houston, TX) with 1,000 molecular weight cut off (MWCO). The nonradioactive sample was further concentrated using lyophilizer (SAVANT®); while the  $^{35}\text{SO}_4$ -labeled sample was concentrated by running on a thin Q-Sepharose column (1.0 x 1.2cm, Sigma) eluted with TBS(1.5M NaCl). The protein concentration was determined using the Bio-Rad Protein Microassay (Bio-Rad Laboratories, Richmond, CA) based on bovine serum albumin (BSA) standards, and the GAG content was determined by DMB assay with heparan sulfate (HS, from bovine kidney, Sigma) standard.

#### 2.2-2 Standard curves for DMB assay and Bio-Rad protein microassay

*DMB assay - Heparan sulfate (HS) standard curve.* The general procedure of Farnsdale et al. was followed (Farnsdale et al., 1986). HS from bovine kidney (Sigma) was used as our

standard heparan sulfate. 1.5 M TBS with 1 M urea or 0.15 M TBS was added to bring the final concentration of HS to 0.1  $\mu\text{g}/\mu\text{l}$ . 1 ml DMB was also added to each 50  $\mu\text{l}$  sample, and samples were measured in the spectrophotometer (HITACHI<sup>®</sup> U-2000 Spectrophotometer, Hitachi Instruments, Inc.) at 525nm wavelength. When 1.5M TBS with 1M urea was used as the baseline, the equation of standard curve was  $y = 16.7x - 0.14$  ( $y$ :  $\mu\text{g}$  HS;  $x$ : abs@525) with  $R^2 = 0.990$ ; while standard curve was  $y = 13.8x - 0.07$  ( $y$ :  $\mu\text{g}$  HS;  $x$ : abs@525) with  $R^2 = 0.997$  when 0.15 M TBS as the baseline (Figure 2-2 ( a ) and ( b )).

*Bio-Rad protein microassay - bovine serum albumin (BSA) standard curve.* BSA was obtained from Fisher Scientific (Fair Lawn, NJ). Deionized water was added to bring the final concentration of BSA to 100  $\mu\text{g}/\text{ml}$ . Then BSA stock and deionized water totaling 800 $\mu\text{l}$  were mixed with 200 $\mu\text{l}$  Protein Microassay Dye (Bio-Rad) for each sample. Sample absorbance reading at 595nm wavelength were measured in the spectrophotometer. The equation for the standard curve was  $y = 22.2x + 0.16$  ( $y$ :  $\mu\text{g}$  BSA;  $x$ : abs@595) with  $R^2 = 0.990$  (Figure 2-3).

## **2.3 Ion Exchange Chromatography with Linear Salt Gradient**

### 2.3-1 Introduction

Chromatography is one of many techniques for separating, purifying, and identifying mixture components, based on differences in partition coefficients between solid-liquid, liquid-liquid or liquid-gas phases. Ion exchange chromatography separates biomolecules based on differences in charge characteristics (cationic/anionic), and is thus dependent on the pH of the system and the isoelectric points (pI) of the biomolecules. It is a separation method in which components with different net charges are separated when a gradient of increasing ionic strength is used as the eluant. The gel matrix can carry either positive or negative groups. In the case of a positively charged gel matrix, sample components with negative charges will be adsorbed. During desorption the negatively charged sample

components are exchanged by the negative ions from the salt gradient. Each sample component is then desorbed at a specific ionic strength and continuously eluted from the column. Proteoglycans, because of their GAG chains, are highly negatively charged molecules. We used Q-Sepharose column to purify the proteoglycan from conditioned media. Q-Sepharose gel, obtained from Sigma (St. Louis, MO), has a functional group of  $-\text{CH}_2\text{N}^+(\text{CH}_3)_3$ , and acts as a strong anion exchanger. At physiological salt concentration (i.e. 0.15 M NaCl), the sample was loaded on the column, and bound with the positive functional group of the gel. By increasing the salt concentration linearly, the binding force between the proteoglycan and the functional group becomes weaker. The proteoglycan is replaced by  $\text{Cl}^-$ , and elutes out of the column with the flowing phase, i.e. TBS buffer. Depending on how charged the molecules are, different proteoglycans will eluted at different stages of separation. The less negative molecule will come out earlier, while the higher negative ones will stay on the column longer.

The standard Econo<sup>®</sup> System from Bio-Rad provided an automated way to produce a linear salt concentration through a gradient proportioning valve and mixer using the programming multi-step method. The system consists of a controller, a plumbing system (pump, gradient proportioning valve and mixer), a gradient monitor with a monitor flow cell on line, a single-pen recorder, and a fraction collector. Two buffers were used as original buffer reservoirs, the buffer A is 0.15M TBS, and the buffer B is 1.5M TBS. The programming method on the standard Econo<sup>®</sup> System has a maximum of five steps defined by six programmable inflection points. Inflection points act as a transition point between each step of the program. And each inflection points corresponds to a certain time value and the percentage of buffer B so that we could know the salt concentration between 0.15 M and 1.5 M at certain time during the linear gradient separation.

2.3-2 Further purification of PG from BAE P9 cells conditioned media (BAE P9 PG) on Q-Sepharose column

A Q-Sepharose column (1.0 x 1.8 cm, Sigma) was used to further purify BAE P9 PG on the standard Econo<sup>®</sup> System with linear salt gradient. The optimal programming method was obtained by trial-and-error. Table 1 shows the optimal programming method for purification of BAE P9 PG on Q-sepharose column with buffer A (0.15M TBS) and buffer B (1.5M TBS). By ion exchange chromatography with a flowrate of 0.5 ml/min and fraction collector setting as 0.5 ml/vial, we obtained two clearly separated peaks (Figure 2-4). The peak I was eluted earlier with the salt concentration of ~ 0.85 M as a sharp spike, and contained more than half of the total amount of PG; while the peak II was eluted with ~1.0 M salt concentration and came out as a plateau. This suggests that there are two components of different charge in BAE P9 PG, and they can be separated by a strong anion exchanger, Q-Sepharose column, with a linear salt gradient. The two peaks were pooled separately as indicated in Fig. 2-4 for further experiments.

## **2.4 Gel Filtration Chromatography**

### 2.4-1 Introduction

Gel filtration, or size exclusion chromatography, is a simple and reliable chromatographic method for separating molecules according to size. Different gels have pores with different controlled range of sizes and act as a molecular sieve separating molecules by differences in size. The gel matrix contains numerous porous beads with an eluant in between. The largest molecules in the sample will often not be able to enter the pores in beads but will pass between them and thus be eluted first. Smaller molecules that have access to the pores are retarded in the gel to a certain extent and will therefore be eluted after the larger molecules in order of decreasing size. Sepharose CL is a cross-linked agarose derivative of Sepharose gel, and is available with three different agarose contents: 2%, 4% and 6%, designated as 2B, 4B, and 6B, respectively. Increasing agarose concentration decreases the matrix porosity, thereby altering the fractionation range while increasing rigidity. Table 2 showed the fraction ranges for Sepharose CL-2B, 4B, and 6B.

One of the most important experimental parameters in the gel filtration chromatography is the distribution coefficient,  $K_d$ , representing the fraction of the stationary phase which is available for diffusion of a given solute species.

$$K_d = \frac{V_e - V_0}{V_s}$$

wherein:

$V_0$  is the void volume, i.e. the volume of the mobile phase;

$V_e$  is the elution volume, which varies with the total volume of the packed bed and with the way the column has been packed;

$V_s$  is the volume of the stationary phase, i.e. the volume of the solvent inside the gel which is available to very small molecules.

Since in practice,  $V_s$  is very difficult to determine,  $K_{av}$  is often used as an expression parameter for normalizing elution behavior.  $K_{av}$ , like  $K_d$ , defines solute behavior independently of the bed dimension and packing.

$$K_{av} = \frac{V_e - V_0}{V_t - V_0}$$

wherein:

$V_e$  is the elution volume;

$V_0$  is the void volume;

$V_t$  is the total volume of the packed bed.

#### 2.4-2 Further purification of BAE P9 PG by gel filtration chromatography

Peak I and peak II of BAE P9 PG, following Q-Sepharose column purification, were separately pooled and run over a Sepharose CL-6B size exclusion column (1.0 x 48 cm, Sigma) in 0.15 M TBS at a flowrate of 0.6 ml/min with a fraction collector setting of 0.5 ml/vial. Both of the peaks were eluted in the void fraction (Figure 2-5). It indicates that the equivalent size  $M_r$  of BAE P9 PG was higher than the upper limit of Sepharose CL-6B fractionation range.

Non-fractionated BAE P9 PG was then run over a Sepharose CL-2B column (1.0 x 48 cm, Sigma) in 0.15 M TBS at a flowrate of 0.4 ml/min with a fraction collector setting of 0.5 ml/vial. BAE P9 PG was in the included volume. There was a distinct peak eluted with a  $K_{av}$  of 0.7 (Figure 2-6 (a)), which had an estimated GAG size equivalent to  $M_r$  of  $2.7 \times 10^5$  (Ohno et al., 1986). A small peak appeared at a  $K_{av}$  of around 0.3, but it was not the major component. The estimated average molecular weight of PG was  $5 \times 10^5$ . It has been reported that BAE PG can be separated on Sepharose CL-2B (1.5 x 41.5 cm, Pharmacia, Piscataway, NJ) into two distinct peaks with the larger part, PG-A, eluted with a  $K_{av}$  of 0.17 and an estimated GAG size equivalent to  $M_r$  of  $2.0 \times 10^6$ , and the second peak, PG-B, eluted with  $K_{av}$  of 0.66 and an estimated size equivalent to  $M_r$  of  $3.1 \times 10^5$  (Forsten et al., 1997). BAE PG was run on the Sepharose CL-2B column with 8M urea, and there was no change indicating that the  $K_{av}$  of 0.3 fraction is likely not an aggregate. The difference is probably because that the BAE cells can adjust their secretion depending on different environments so that the PG-A does not appear obviously as a peak and PG-B is the major component in our preparation.

Sepharose CL-4B was chosen as an intermediate separation gel for BAE P9 PG. BAE P9 PG was loaded onto a Sepharose CL-4B column (1.0 x 48 cm, Sigma), in 0.15 M TBS at a flowrate of 0.4 ml/min with a fraction collector setting of 0.5 ml/vial. Two distinct peaks were observed in the included volume and had  $K_{av}$  values of 0.1 and 0.38 respectively (Figure 2-6 (b)). Compared with the results from Sepharose CL-2B column, we could see that Sepharose CL-4B column “squeezed up” the two parts of the profile we got from Sepharose CL-2B, the first part as a plateau and the second part as a peak, into two distinct peaks. Therefore, it was suggested from gel filtration chromatography that BAE P9 PG was composed of two broad fractions of different size. However, the possibility that either peak represents a tightly associated complex of macromolecules cannot be ruled out at this time, and it is unlikely that the fraction consists of a single homogeneous proteoglycan species. We may further investigate the component characteristics of these two peaks by enzyme digestion with Heparinase I, Heparinase III

and Chondroitinase ABC, identify the core protein by SDS-PAGE with western blotting, and analyze the GAG chains by the enzyme digestion or  $\beta$ -elimination.

## **2.5 Structural Characteristics of BAE P9 PG**

BAE P9 PG can be eluted as two peaks depending on the differences of either charge or size. The two peaks are probably different in the composition. The exploration of structural characteristics of BAE P9 PG requires us to further define the composition of the GAG chains, and molecular weight of core protein(s). Moreover, it will be of great interest to clarify the content percentage of HSPG in BAE P9 PG, because HS plays a significant role in bFGF's binding and subsequent biological functions. Enzyme digestion, nitrous acid treatment and  $\beta$ -elimination were employed to explore the components and size of GAG chains with the help of ion exchange chromatography and gel filtration chromatography. At the same time, molecular weight of core protein(s) can be obtained by SDS-PAGE.

### **2.5-1 Enzyme digestion**

*Enzymes* - Heparinase I (Hep I) from *Flavobacterium*, also known as heparin lyase I or heparinase, selectively cleaves glycosidic linkage between N-sulfated hexosamine and iduronic acid 2-O-sulfate (Linker and Hovingh, 1984). It is an enzyme which preferentially digests high sulfated segments of heparin, resulting in only limited degradation of the less highly sulfated HSPG. Heparinase III (Hep III) from *Flavobacterium*, also known as heparin lyase III or heparitinase I, can cleave glycosidic linkages between sulfated or monosulfated N-acetyl glucosamine and unsulfated iduronic acid or glucuronic acid (Hovingh and Linker, 1974); such linkages are characteristic of HS GAG. It is an enzyme that specifically degrades HS GAG. In addition, chondroitin ABC lyase (C.ABC) from *Proteus* is specific for chondroitin-4-sulfate, chondroitin-6-sulfate, and dermatan sulfate (Suzuki, 1972). It is an enzyme which specifically digests chondroitin sulfate (CS) GAG.

*Conditions for enzyme digestion* - Enzyme digestion, especially digestion with Hep I and Hep III, is very sensitive to conditions, such as the presence of metal ions, pH of the solution, and salt concentration.

(1) Effect of metal ions and pH on Hep I and Hep III digestion:

Hep I is inhibited by  $\text{Hg}^{2+}$ ,  $\text{Cu}^{2+}$ , and  $\text{Fe}^{3+}$ ; and Hep III is inhibited by  $\text{Cu}^{2+}$ ,  $\text{Hg}^{2+}$ ,  $\text{Zn}^{2+}$ , and  $\text{Cd}^{2+}$  (Linker and Hovingh, 1972). The presence of  $\text{Ca}^{2+}$  is necessary to activate the digestion. It was observed that there was no digestion (detection by the DMB difference assay), when there was no  $\text{Ca}^{2+}$  (data not shown).

The effects of pH value and the concentration of  $\text{Ca}^{2+}$  were investigated using six buffers:

- (1) tris/ $\text{CaCl}_2$  with pH 7.52,  $\text{CaCl}_2$  0.2mM;
- (2) tris/ $\text{CaCl}_2$  with pH 7.52,  $\text{CaCl}_2$  0.5mM;
- (3) tris/ $\text{CaCl}_2$  with pH 7.02,  $\text{CaCl}_2$  0.2mM;
- (4) tris/ $\text{CaCl}_2$  with pH 7.02,  $\text{CaCl}_2$  0.5mM;
- (5) tris/ $\text{CaCl}_2$  with pH 8.01,  $\text{CaCl}_2$  0.2mM; and
- (6) tris/ $\text{CaCl}_2$  with pH 8.01,  $\text{CaCl}_2$  0.5mM.

10  $\mu\text{l}$  of HS (Sigma) stock (0.1  $\mu\text{g}/\mu\text{l}$ ) was digested with 5  $\mu\text{l}$  of Hep I (working condition 100U/ml, Sigma) and 7  $\mu\text{l}$  of Hep III (working condition 10U/ml, Sigma) in 30  $\mu\text{l}$  of individual buffers. The DMB assay following enzyme digestion showed buffer (4) allowed the greatest degree of digestion among the buffer tested (Table 3).

(2) Effect of pH and  $\text{Ca}^{2+}$  on C.ABC digestion:

The effect of pH and  $\text{Ca}^{2+}$  on C.ABC digestion was investigated by using 10  $\mu\text{l}$  of CS (Sigma) stock (0.1 $\mu\text{g}/\mu\text{l}$ ) and three different buffers:

- tris/ $\text{CaCl}_2$  buffer with pH 7.02,  $\text{CaCl}_2$  0.5mM (buffer 7.02+);
- tris/ $\text{CaCl}_2$  buffer with pH 8.01,  $\text{CaCl}_2$  0.5mM (buffer 8.01+); and
- tris buffer with pH 8.01, without  $\text{CaCl}_2$  (buffer 8.01-).

Absence of C.ABC was used as control. The digestion percentages for buffer 7.02+, buffer 8.01+ and buffer 8.01- were 81.6%, 83.8% and 80.6% respectively (Table 4). Therefore, the presence of  $\text{Ca}^{2+}$  facilitated the C.ABC digestion, and pH 8.01 was better. On the other hand, the difference between buffer 7.02+ and 8.02+ was not so great as to prevent us using buffer 7.02+.



(3) Effect of salt concentration:

High salt concentration (>0.15M) inhibited both Hep I / Hep III digestion, and C.ABC digestion, with Hep I / Hep III digestion being more sensitive to salt concentration (Table 5).

Therefore, the best conditions employed were: buffer 7.02+ with less than 0.15M NaCl for Hep I and Hep III digestion; buffer 8.01+ with less than 0.15M NaCl for C.ABC digestion; and buffer 7.02+ with less than 0.15M NaCl for Hep I / Hep III and C.ABC digestion.

*Percentage of HS in BAE P9 PG* - 100 µl of BAE P9 PG (17ng GAG/µl) was treated with 12 µl of Hep I (working condition 100U/ml, Sigma) and 14 µl of Hep III (working condition 10U/ml, Sigma), or 7 µl of C.ABC (working condition 10U/ml, Sigma), or 12 µl of Hep I , 14 µl of Hep III and 7 µl of C.ABC (Sigma) at 37 °C for 4 hr under the best conditions. The content percentage of HS was determined by DMB difference assay comparing reading following enzyme digestion with control samples incubated without any enzyme (Table 6). The percentage of HS in BAE P9 PG was ~ 50% ( $49.2 \pm 0.9$  %), and CS was ~ 30% ( $31.3 \pm 0.7$  %). The total percent of HS and CS was ~ 80% ( $79.5 \pm 0.9$  %), which matched the result of digestion with Hep I, Hep III and C.ABC. As a result, HS was the dominant component in BAE P9 PG. There was ~ 20% GAG chains which could not be digested by either Hep I / Hep III or C.ABC. They may be keratan sulfate, Hep I / Hep III resistant, or C.ABC resistant segments accounting for the lack of complete digestion (It was observed that Hep I / Hep III did not digest all the pure HS (Sigma) and C.ABC did not digest all the pure CS (Sigma)).

*GAG components in PG-I and PG-II of BAE P9 PG* - After dialysis against deionized water to reduce the salt concentration, 100 µl of pooled PG-I (1.24ng GAG/µl) or PG-II (2.54ng GAG/µl) was digested with 12 µl of Hep I (working condition 100U/ml, Sigma) and 14 µl of Hep III (working condition 10U/ml, Sigma), or 7 µl of C.ABC (working condition 10U/ml, Sigma), or 12 µl of Hep I , 14 µl of Hep III and 7 µl of C.ABC

(Sigma) at 37 °C for 4 hr under optimal conditions. It was shown by DMB assay that PG-I was primarily composed of HS, while PG-II consisted of HS and CS (Table 7). Because the GAG contents of PG-I and PG-II were quite low, negative data appears in Table 7 due to the detection limit of the spectrophotometer.

#### 2.5-2 Nitrous acid treatment

*Nitrous acid treatment at low pH* - This treatment is used to cleave glycosidic linkages adjacent to N-sulfated hexosamine residues (Shively and Conrad, 1976). It is a specific way of degrading HS GAG. 10 ml of 0.6M nitrous acid (HNO<sub>2</sub>) was produced by mixing 7.4ml of D.I. H<sub>2</sub>O, 2.6ml of glacial acetic acid (HAC, Fisher) and 0.414g of sodium nitrate (NaNO<sub>2</sub>, Sigma) at room temperature. 10 µl of HS (Sigma) stock (0.1 µg/µl) was treated with 40 µl of 0.6M nitrous acid at room temperature for 4 hr. The reaction was terminated by adding 8 µl of 10N NaOH solution. The undigested percentage was determined by DMB assay comparison with control (mixing HNO<sub>2</sub> and NaOH first at room temperature, and then after 4 hr, adding 10 µl of HS (Sigma)). The portion of HS undigested in Hep I / Hep III treated samples was 23%, while 31% in nitrous acid treatment. Compared with Hep I and Hep III digestion under optimal conditions, nitrous acid treatment was not as effective at degrading HS GAG. Therefore, we kept on using enzyme digestion with Hep I / Hep III instead of the nitrous acid treatment.

#### 2.5-3 Purification of BAE P9 PG by ion exchange chromatography following enzyme digestion

BAE P9 PG was treated with Hep I and Hep III, or C.ABC, or the triple combination, under respective optimal conditions at 37°C for 4 hr. Then the digested samples, along with samples without enzyme digestion as a control, were individually applied to Q-Sepharose column (1.0 x 1.8 cm, Sigma) with linear salt gradient provided by the standard Econo<sup>®</sup> system with the optimal programming method. The results are shown in Figure 2-7. Treatment with C.ABC removed the majority of peak II (i.e. PG-II) (Figure 2-7(a)).

When treated with Hep I and Hep III, the peak I (i.e. PG-I) of BAE P9 PG disappeared and shifted as a new peak eluting with 0.75M salt, and peak II (i.e. PG-II) was reduced by a certain amount (Figure 2-7 (b)). In addition, Figure 2-7(c) showed that when BAE P9 PG was treated with enzymes of Hep I, Hep III and C.ABC, the original two peaks disappeared and two new peaks eluted at 0.45M NaCl as free sulfates and 0.75M NaCl as the shifted PG-I. This result confirms our previous conclusion drawn from enzyme digestion that HS and CS are key components of BAE P9 PG. There was still a small amount of GAG chains which were resistant to either Hep I and Hep III or C.ABC, and they were probably keratan sulfate. Alternatively, the remaining GAG may be HS or CS which was not fully digestible. Regardless, that PG-I contained mainly HS, PG-II contained CS and HS, and HS was a major component in GAG chains of BAE P9 PG was verified.

#### 2.5-4 Size evaluation of PG-I and PG II by Sepharose CL-4B gel filtration

<sup>35</sup>S-labeled peak I (i.e. PG-I) and peak II (i.e. PG-II) from Q-Sepharose column separation were pooled separately, as well as non-fractionated BAE P9 PG, and were run over a Sepharose CL-4B column (1.0 x 48 cm, Sigma) individually in 0.15M TBS at a flowrate of 0.4ml/min and the fraction collector setting of 0.5ml/vial. Figure 2-8 shows that PG-I has two components of  $K_{av}$  values as 0.15 and 0.38 respectively; and PG-II has two components of  $K_{av}$  values as 0.1 and 0.4 respectively with a much smaller amount of the larger size component. Should the concept of average molecular weight of polymer apply, the average molecular weight ( or the size) of PG-I was greater than that of PG-II.

#### 2.5-5 Size evaluation of GAG chains from BAE P9 PG and PG-I by Sepharose CL-6B gel filtration after $\beta$ -elimination reaction

*$\beta$ -elimination* - Alkaline borohydride treatment was used to liberate intact GAG chains from PG (Bassols and Massague, 1988). Briefly, PG was incubated in 1M sodium borohydride ( $\text{NaBH}_4$ ) and 0.05M sodium hydroxide ( $\text{NaOH}$ ) at 37°C for 24 hr. The

reaction was quenched through addition of glacial acetic acid to neutrality (pH 7.0).  $\beta$ -elimination provides us with a way to evaluate the chain size of PG.

100  $\mu$ l of  $^{35}\text{S}$ -labeled PG-I (50cpm/ $\mu$ l) pooled from Q-Sepharose column separation and 100  $\mu$ l of  $^{35}\text{S}$ -labeled non-fractionated BAE P9PG were treated with  $\beta$ -elimination reaction, applied to Sepharose CL-6B column (1.0 x 48 cm, Sigma) individually, and then eluted with 0.15M TBS at a flowrate of 0.6ml/min and the fraction collector setting of 0.5 ml/vial. The GAG chain of PG-I had a similar size as those of BAE P9 PG, which had a  $K_{av}$  of 0.3 (Figure 2-9). Due to insufficient quantities of  $^{35}\text{S}$ -labeled PG-II, we could not repeat the process for the GAG chains from PG-II after  $\beta$ -elimination. Theoretically, the GAG chains of PG-II are larger than that of PG-I if we consider GAG chains of PG-I and PG-II as polymer and calculate the average molecular weight based on the elution profile in the Sepharose CL-6B column (Figure 2-9).

#### 2.5-6 Characterization of core protein(s) of BAE P9 PG

*SDS-PAGE* - Sodium dodecylsulfate polyacrylamide gel electrophoresis (SDS-PAGE) was used to determine the molecular weight of BAE P9 PG's core protein(s).

In electrophoresis, sample components can be separated based on their differences in net charge, size, and shape, which affect the mobility rate. Separation usually takes place at a constant pH and ionic strength. Polyacrylamide gel is used as a stabilizing media. The sample is applied as a narrow zone on top of the stabilizing gel and when the electric field is applied, the sample components will migrate into the gel. Separation in the stabilizing media takes place because of different mobilities of the sample components.

The polyacrylamide gel forms when a dissolved mixture of acrylamide and cross-linker monomers polymerize into long chains that are covalently cross-linked. The gel structure is held together by the cross-linker. The most common cross-linker is N,N'-methylene bisacrylamide (i.e. bis-acrylamide). Polymerization of acrylamide is a free-radical catalyzed

reaction, using ammonium persulfate as the initiator and the quaternary amine, N,N,N',N'-tetramethylethylene diamine (TEMED) as the catalyst.

In SDS-PAGE separations, migration is determined not by intrinsic electrical charge of polypeptides, but by molecular weight. Sodium dodecylsulfate (SDS) is an anionic detergent that disrupts non-covalent interactions by wrapping around the polypeptide backbone forming rods of negative charges with equal “charge densities” or charge per unit length. The resulting protein/SDS complex is assumed to be a random coil that has a negative charge dependent on the size of the protein (Hoefer, 1994). Determining the size of a protein by its mobility also requires protein standards of known size for comparison.

A discontinuous buffer system was applied to obtain greater sample resolution. In this system, a stacking gel with nonrestrictive large pores is laid on top of a separating (running) gel. Each gel layer is made with different buffers, and the tank buffer is different from the gel buffers in the composition. The mobility of a protein is intermediate between the mobility of the buffer ion in the stacking gel (leading ion) and the mobility of the buffer ion in the upper tank (tailing ion). When electrophoresis is initiated, the ions and the proteins begin to migrate into the stacking gel. The proteins concentrate in a very thin zone, called the stack, between the leading ion and the trailing ion. The proteins continue to migrate in the stack until they reach the separating gel (Hoefer, 1994).

After the electrophoresis run is complete, the gel may be analyzed qualitatively or quantitatively. The most common analytical procedure is staining. Proteins are usually stained with Coomassie Brilliant Blue or with a silver stain system which is much more sensitive. Radioactively labeled samples separated on a slab gel are commonly detected by autoradiography.

*Methods and materials* - Mini-PROTEAN<sup>®</sup> II Electrophoresis Cell (Bio-Rad) was employed to conduct the separation with slab gel and discontinuous buffer system. Stacking gel was formed with 30% acrylamide solution, 1.0M Tris (pH 6.8) buffer, 10%

SDS (Sigma), 0.01% ammonium persulfate (Sigma) and 0.05% TEMED (Sigma) with a final concentration of 3.5% acrylamide. Separating gel was formed with 30% acrylamide solution, 1.5M Tris (pH 8.8) buffer, 10% SDS, 0.01% ammonium persulfate and 0.05% TEMED with a final concentration of 5% acrylamide. The acrylamide solution was prepared with 30% acrylamide (Sigma) and 0.8% bio-acrylamide (Sigma). Tank buffer contained 0.025M Tris, 0.192M glycine, 0.1% SDS with pH of 8.3. The SDS-PAGE high range of molecular weight standards were used (Bio-Rad).

Gels were run for ~ 45 min at 110V in the Mini-PROTEAN<sup>®</sup> II Electrophoresis Cell (Bio-Rad). Protein bands were visualized by Coomassie Brilliant Blue (Sigma) or silver staining using Silver Stain Kit for polyacrylamide gels (Sigma). Gels were dried with a vacuum gel dryer (model 583, Bio-Rad) at 80 °F for 30 min.

*Calibration curves of protein standards* - The standard protein markers consisted of rabbit skeletal muscle myosin (200 kDa), *E. coli*  $\beta$ -galactosidase (116.25 kDa), rabbit muscle phosphorylase b (97.4 kDa), bovine serum albumin (66.2 kDa) and hen egg white ovalbumin (45 kDa) (Bio-Rad). Relative mobility (Rf) is defined as the ratio of the distance migrated by protein to the distance migrated by the marker, with the lowest-molecular-weight standard protein of 45 kDa serving as the relative mobility marker. The curve of Log (molecular weight) vs. Rf is a straight line  $y = -315000x + 343000$  ( $y$ : log molecular weight;  $x$ : Rf) with  $R^2 = 0.890$  (Figure 2-10), and can be used to determine molecular weight of unknown proteins.

*Western Blotting* - Western blotting, i.e. immunoblotting, was used to identify the core protein of BAE P9 PG. Following separation by SDS-PAGE, the core protein of BAE P9 PG was transferred onto a nitrocellulose blotting membrane. The membrane was incubated with a blocking buffer to block all the nonspecific binding sites. The immobilized proteins were then probed with primary antibodies specific for the sample protein followed by secondary antibodies specific for the general class of primary antibodies. A peroxidase or alkaline phosphatase reporter enzyme is usually attached to the secondary antibody.

Finally, antigens, i.e. the core protein of BAE P9 PG, were visualized with chromogenic substrates for peroxidase or alkaline phosphatase.

*Methods and materials* - After separation on 5% SDS-polyacrylamide gel, 2 µg of PG core proteins were transferred onto a cellulose blotting membrane (COSTAR, Cambridge, MA) at 50 V for 2 hr at 4°C. The equipment we used was TE 22 Mighty Small Transphor Unit with transfer cassettes (HOEFER, San Francisco, CA), and the blotting (filter) paper was from SIGMA. 5% Non-Fat Dry Milk (Carnation) in PBST was used as the blocking buffer. The PBST was composed of phosphate buffered saline (GIBCO) and 0.1% Tween (SIGMA). The membrane was incubated in the blocking buffer for 1 hr at room temperature, then incubated with anti-heparan sulfate proteoglycan, i.e. anti-perlecan (Upstate Biotechnology Incorporated, Lake Placid, NY) as the primary antibody at a final concentration of 1 µg/ml in PBST containing 1% Non-Fat Dry Milk for 1 hr at room temperature. The membrane was washed five times with PBST; once for 15 min, 4 times for 5 min each. The membrane was then hybridized for 1 hr at room temperature with anti-rat IgG (whole molecule) with alkaline phosphatase conjugate from goat (SIGMA, St. Louis, MO) with the titer of 1:30,000 in PBST containing 1% milk. Five washes were conducted as before. The membrane was then incubated in the alkaline phosphatase buffer with pH of 9.5 for 2 min, and put into the buffer made with SIGMA FAST™ BCIP/NBT (5-Bromo-4-Chloro-3-indolyl phosphate/nitro blue tetrazolium) buffered substrate tablet. The protein bands stand purple.

*Results and Conclusions* - Several factors have been observed to influence the SDS-PAGE results during the problem solving and gel running phase:

- (1) It was found that Coomassie blue could not be used for determining molecular weight of core proteins of PG due to the detection limit of the Coomassie stain;
- (2) The time length of putting stained gel into development solution in the process of silver staining detection was very critical. If the development was too short, protein band could not be detected visually. But if it was too long, the primary (first appearing) dense band would become smeared;

(3) The loading amount of 1  $\mu\text{g}$  protein was optimal. More than 1 $\mu\text{g}$  produced a dark smeared lane, in which specific protein bands could not be distinguished.

Firstly, the results of SDS-PAGE with silver staining (Figure 2-11 (a)) and with western blotting (Figure 2-12 (a)) for non-digested intact BAE P9 PG and enzyme digested BAE P9 PG were compared. Non-digested intact PG barely entered the gel and appeared as diffuse bands at the top of the gel. After digestion with the combination of Hep I, Hep III and C.ABC, core proteins of PG migrated as a doublet at apparent molecular weight of 320kDa and 300kDa. Western blotting with anti-perlecan showed that the major bands were perlecan, which was previously demonstrated by Forsten, et al. (1997). Perlecan is the primary proteoglycan component of basement membranes (Iozzo, et al., 1994). It was recently reported that perlecan, a secreted HSPG abundant in proliferating transfected NIH 3T3 cells, was capable of inducing bFGF-receptor interactions in vitro and angiogenesis in vivo (Aviezer, et. al., 1997), although most reports indicate an inhibitory response with perlecan (Benitz, et al., 1990). It was noted that in Figure 2-11 (a), there was a second band in the non-digested intact PG lane, which was around 300kDa, the same size as the second band of the doublet in the enzyme digested PG lane. But this band did not show up in the western blotting (Figure 2-12 (a)). This indicated that either the amount of this band was not enough to be detected by western blotting, this protein was not core protein of perlecan, or it is a perlecan fragment that could not be detected by our antibody. We used a monoclonal primary antibody and the fragment may not have the full targeted region accessible.

Many steps are involved in the separation, desalting and concentrating, i.e. ion exchange chromatography on Q-Sepharose column, dialysis and lyophilizing, and PG-I and PG-II appear vulnerable to the process as they could not be detected on the SDS-PAGE (data not shown). It was observed that pure CS and HS GAG (unattached to PG) could not be visualized on SDS-PAGE with silver staining (Figure 2-11 (b)). Therefore, 4 $\mu\text{g}$  CS was added to each PG-I or PG-II sample before lyophilizing with the idea that CS might serve as a stabilizing agent to help keep PG-I and PG-II from being lost during the process of



lyophilizing (Figure 2-11 ( c) and (d)). As to non-digested intact PG-I (Figure 2-11 ( c) ), the major part barely entered the gel and appeared as diffuse bands at the top of the gel, while a small band appeared at around 300kDa. When treated with C.ABC alone, the top band and second band also existed. Treatment with Hep I / Hep III or Hep I / Hep III and C.ABC led to the disappearance of the top band and a darker second band. It was shown that PG-I had a core protein of 300kDa, and could be released by HepI & Hep III. The results of western blotting of PG-I showed that no matter with or without enzyme treatment, with only Hep I/III or C.ABC, or with both, one band was detectable perlecan using our primary antibody (Figure 2-12 (b)). In Figure 2-11 ( c), the bands appeared around 280kDa were probably fragments of core protein or protein products of cells, and they were not those of perlecan. The non-digested intact PG-II also showed two bands (Figure 2-11 (d)). The second band was much darker than the top one, which indicated that many GAG chains might be lost during the multi-step procedure. Treatment with C.ABC alone did not result in the appearance of any new protein bands. Treatment of Hep I & Hep III or Hep I, Hep III and C.ABC made the 320kDa band much darker. Western blotting showed that this band was core protein of perlecan (data not shown). In addition, a third band appeared in PG-II lower than the 300kDa band. It was probably also some protein product of the BAE cells, but not detectable by our antibody. A band appeared at 100kDa, when sample was treated with Hep I & Hep III or Hep I , Hep III and C.ABC, was probably the unreacted Hep III, which showed two bands on SDS-PAGE (Figure 2-11 (b)). The two distinct bands of 200kDa and 130kDa for C.ABC (Figure 2-11 (b)) did not clearly show up in the enzyme treatment of PG-I and PG-II.

## **2.6 Brief Comparison of Proteoglycans from Different Cells Conditioned Media**

### 2.6-1 Introduction of cell lines

Proteoglycan, as a product secreted by living cells, can vary from different cells and at different growth stages in GAG chain contents, GAG chain length, or even core proteins.

PGs produced by the following cells have been studied briefly:

(1) SV40 *cells* - These are MAC-T cells (bovine mammary epithelial cells) transfected with an expression vector containing IGF-I (Insulin-like Growth Factor-I) cDNA under the control of the constitutively active early simian virus 40 (sv 40) promoters. SV40 cells sustain chronic secretion of both IGF-1 and induced-binding protein 3 (INDUCED-BP3) (Romagnolo, et al., 1994). Conditioned media was obtained as a gift from Dr. R. Michael Akers (Diary Science Department of Virginia Tech);

(2) BAE P9 cells - were bovine aortic endothelial cells of passage 9;

(3) BAE P12 cells - were bovine aortic endothelial cells of passage 12; and

(4) SMC/BAE P5 cells - were a mixture of smooth muscle cells and bovine aortic endothelial cells of passage 5.

#### 2.6-2 Purification by ion exchange chromatography of PGs produced by different cells

A Q-Sepharose column (1.0 x 1.8 cm) was used to purify PGs from different cells conditioned media with the aid of the standard Econo<sup>®</sup> system. Under the same salt linear gradient, PGs produced by the four different cell types could be separated into two peaks, but the eluted position and shape of the peaks were varied (Figure 2-13). This suggests that the PGs are different, likely in their charge or size. Moreover, PGs produced by SV40, SMC/BAE P5, and BAE P9 cells can be separated into two peaks under different optimal salt linear gradients (Figure 2-14). PGs from different cells conditioned media under different conditions varied. The different cells could be wild type or transfected cells, same type of cells with different passage, and cell mixture or pure type. The differences observed in various PGs may indicate an ability by cells to alter their environment to fit specific functional needs.

**Table 1**

**Optimal programming method for producing linear salt gradient  
on standard Econo<sup>®</sup> system for purification of BAE P9 PG**

Inflection no.	Accumulated time (min)	% buffer B	Salt concentration (M NaCl)
1	0	0	0.15
2	3	11	0.3
3	21	41	0.7
4	94	78	1.2
5	99	0	0.15
6	107	0	0.15

(Flowrate: 0.5ml/min; fraction collector: 0.5ml/min;  
buffer A: 0.15M TBS; buffer B: 1.5M TBS)

**Table 2**

**Fractionation range for Sepharose CL gels**

Gel	Fractionation range (Globular Protein) (Mr)	Fractionation range (Dextrans) (Mr)
Sepharose CL-2B	$7 \times 10^4 \sim 4 \times 10^7$	$1 \times 10^5 \sim 2 \times 10^7$
Sepharose CL-4B	$6 \times 10^4 \sim 2 \times 10^7$	$3 \times 10^4 \sim 5 \times 10^6$
Sepharose CL-6B	$1 \times 10^4 \sim 4 \times 10^6$	$1 \times 10^4 \sim 1 \times 10^6$

(Data was obtained from Sigma catalog.)

**Table 3****Effect of pH and concentration of Ca<sup>2+</sup> on Heparinase I / Heparinase III  
(Hep I/Hep III) digestion of heparan sulfate**

HS ( $\mu$ l)	Hep I ( $\mu$ l)	Hep III ( $\mu$ l)	buffer 1 ( $\mu$ l)	buffer 2 ( $\mu$ l)	buffer 3 ( $\mu$ l)	buffer 4 ( $\mu$ l)	buffer 5 ( $\mu$ l)	buffer 6 ( $\mu$ l)	average abs@ 525 <sup>a</sup>	digested (%)
10	-	-	42	-	-	-	-	-	0.0705	-
10	5	7	30	-	-	-	-	-	0.0415	41
10	-	-	-	42	-	-	-	-	0.087	-
10	5	7	-	30	-	-	-	-	0.0585	33
10	-	-	-	-	42	-	-	-	0.0805	-
10	5	7	-	-	30	-	-	-	0.0515	36
10	-	-	-	-	-	42	-	-	0.0795	-
10	5	7	-	-	-	30	-	-	0.042	47
10	-	-	-	-	-	-	42	-	0.084	-
10	5	7	-	-	-	-	30	-	0.0695	17
10	-	-	-	-	-	-	-	42	0.0785	-
10	5	7	-	-	-	-	-	30	0.0685	13

Samples were mixed and incubated at 37 °C for 4 hours.

Buffer 1: tris/CaCl<sub>2</sub> with pH 7.52, CaCl<sub>2</sub> 0.2mM;

Buffer 2: tris/CaCl<sub>2</sub> with pH 7.52, CaCl<sub>2</sub> 0.5mM;

Buffer 3: tris/CaCl<sub>2</sub> with pH 7.02, CaCl<sub>2</sub> 0.2mM;

Buffer 4: tris/CaCl<sub>2</sub> with pH 7.02, CaCl<sub>2</sub> 0.5mM;

Buffer 5: tris/CaCl<sub>2</sub> with pH 8.01, CaCl<sub>2</sub> 0.2mM;

Buffer 6: tris/CaCl<sub>2</sub> with pH 8.01, CaCl<sub>2</sub> 0.5mM.

a. This was an arithmetic average of two abs@525 values of two samples from DMB assay for each case.

**Table 4**

**Effect of pH and Ca<sup>2+</sup> on Chondroitin ABC lyase digestion of chondroitin sulfate**

Chondroitin sulfate (μl)	10	10	10	10	10	10
Chondroitin ABC lyase (μl)	-	7	-	7	-	7
buffer 7.02+ (μl)	47	40	-	-	-	-
buffer 8.01+ (μl)	-	-	47	40	-	-
buffer 8.01- (μl)	-	-	-	-	47	40
average abs@525 <sup>a</sup>	0.0705	0.013	0.068	0.011	0.067	0.013
digestion (%)	-	81.6	-	83.8	-	80.6

Samples were mixed and incubated at 37°C for 4 hours.

Buffer 7.02+: tris/CaCl<sub>2</sub> buffer with pH 7.02, CaCl<sub>2</sub> 0.5mM;

buffer 8.01+: tris/CaCl<sub>2</sub> buffer with pH 8.01, CaCl<sub>2</sub> 0.5mM; and

buffer 8.01-: tris buffer with pH 8.01, without CaCl<sub>2</sub>.

a. This was an arithmetic average of two abs@525 values of two samples from DMB assay for each case.

**Table 5****Effect of salt concentration of enzyme digestion of GAG****(a) Effect of salt concentration of Heparinase I and Heparinase III digestion of heparan sulfate**

Salt concentration (M NaCl)	1.5	1.5	0.3	0.3	0.15	0.15	0	0
Heparan sulfate ( $\mu$ l)	10	10	10	10	10	10	10	10
Heparinase I ( $\mu$ l)	12	-	12	-	12	-	12	-
Heparinase III ( $\mu$ l)	14	-	14	-	14	-	14	-
buffer 7.02+ ( $\mu$ l)	100	126	100	126	100	126	100	126
abs@525	0.086	0.086	0.042	0.044	0.032	0.036	0.009	0.027
digestion (%)	0	-	4.5	-	11	-	67	-

**(b) Effect of salt concentration of chondroitin ABC lyase digestion of chondroitin sulfate**

Salt concentration (M NaCl)	1.5	1.5	0.3	0.3	0.15	0.15	0	0
Chondroitin sulfate ( $\mu$ l)	10	10	10	10	10	10	10	10
Chondroitin ABC lyase ( $\mu$ l)	7	-	7	-	7	-	7	-
buffer 8.01+ ( $\mu$ l)	100	107	100	107	100	107	100	107
abs@525	0.078	0.083	0.021	0.046	0.008	0.037	0.002	0.034
digestion (%)	6	-	54	-	78	-	94	-

Samples were mixed and incubated at 37°C for 4 hours.

Buffer 7.02+: tris/CaCl<sub>2</sub> buffer with pH 7.02, CaCl<sub>2</sub> 0.5mM;

buffer 8.01+: tris/CaCl<sub>2</sub> buffer with pH 8.01, CaCl<sub>2</sub> 0.5mM.

**Table 6****Content percentage of heparan sulfate and chondroitin sulfate in BAE P9 PG**

Heparinase I ( $\mu$ l)	-	12	-	12
Heparinase III ( $\mu$ l)	-	14	-	14
Chondroitin ABC lyase ( $\mu$ l)	-	-	7	7
buffer 7.02+ ( $\mu$ l)	126	100	-	100
buffer 8.01+ ( $\mu$ l)	-	-	100	-
BAE P9 PG ( $\mu$ l)	100	100	100	100
average abs@525 <sup>a</sup>	0.131	0.0666	0.09	0.0268
Percentage (%) <sup>b</sup>	0	49.2 $\pm$ 0.9	31.3 $\pm$ 0.7	79.5 $\pm$ 0.9

Samples were mixed and incubated at 37°C for 4 hours.

Buffer 7.02+: tris/CaCl<sub>2</sub> buffer with pH 7.02, CaCl<sub>2</sub> 0.5mM;

buffer 8.01+: tris/CaCl<sub>2</sub> buffer with pH 8.01, CaCl<sub>2</sub> 0.5mM.

a. There were two samples for each case. This is arithmetic average of two abs@525 values from DMB assay for each case.

b. Percentage % = (average abs@525 of control - average abs@525 of sample)/(average abs@525 of control)\*100

error % = [max( abs@525 of two samples)-average abs@525 of the sample]/(average abs@525 of control)\*100

**Table 7****Content percentage of heparan sulfate and chondroitin sulfate in PG-I and PG-II of BAE P9 PG**

	PG-I				PG-II			
Heparinase I (μl)	-	12	-	12	-	12	-	12
Heparinase III (μl)	-	14	-	14	-	14	-	14
Chondroitin ABC lyase (μl)	-	-	7	7	-	-	7	7
buffer 7.02+ (μl)	126	100	-	100	126	100	-	100
buffer 8.01+ (μl)	-	-	100	-	-	-	100	-
PG-I (μl)	100	100	100	100	-	-	-	-
PG-II (μl)	-	-	-	-	100	100	100	100
average abs@525 <sup>a</sup>	0.001	-0.009	0	-0.011	-0.001	-0.006	-0.004	-0.009
digested percentage (%) <sup>b</sup>	0	91	8	100	0	62	38	100

Samples were mixed and incubated at 37°C for 4 hours.

Buffer 7.02+: tris/CaCl<sub>2</sub> buffer with pH 7.02, CaCl<sub>2</sub> 0.5mM;

buffer 8.01+: tris/CaCl<sub>2</sub> buffer with pH 8.01, CaCl<sub>2</sub> 0.5mM.

a. There were two samples for each case. This is arithmetic average of two abs@525 values from DMB assay for each case.

b. Digested percentage % =  $\frac{|\text{average abs@525 of control} - \text{average abs@525 of sample}|}{|\text{average abs@525 of control} - \text{the smallest average abs@525 of sample}|} * 100$



Structure of heparan sulfate repeat unit

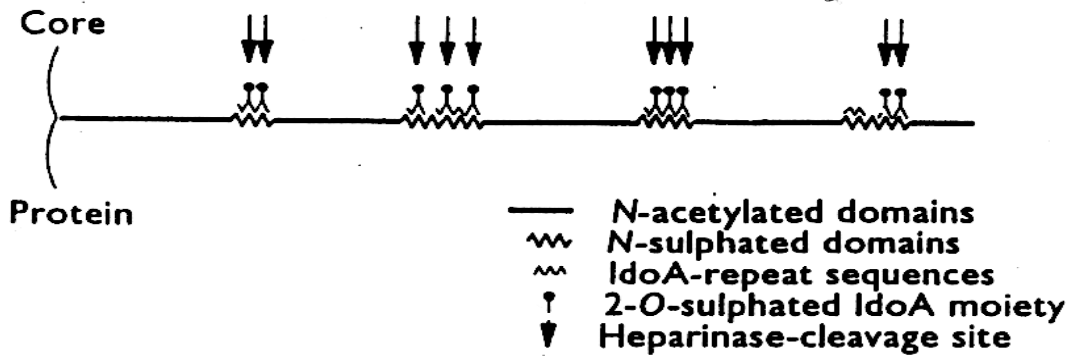
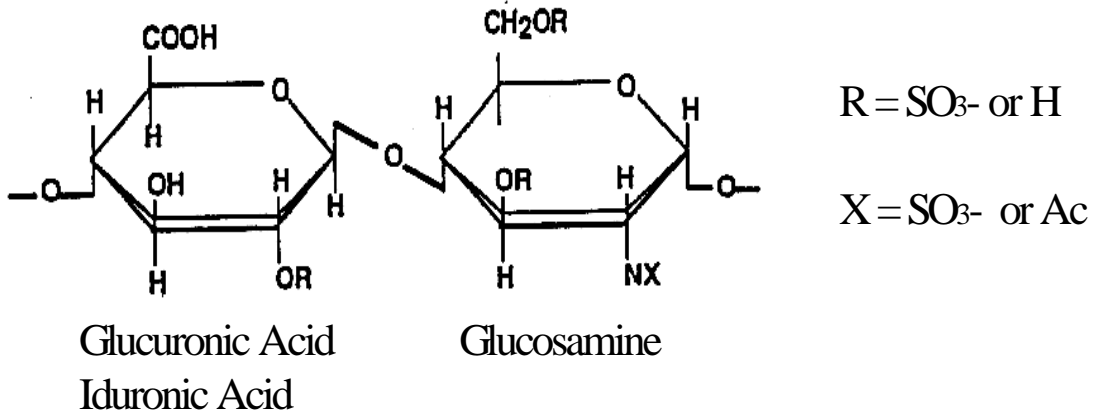
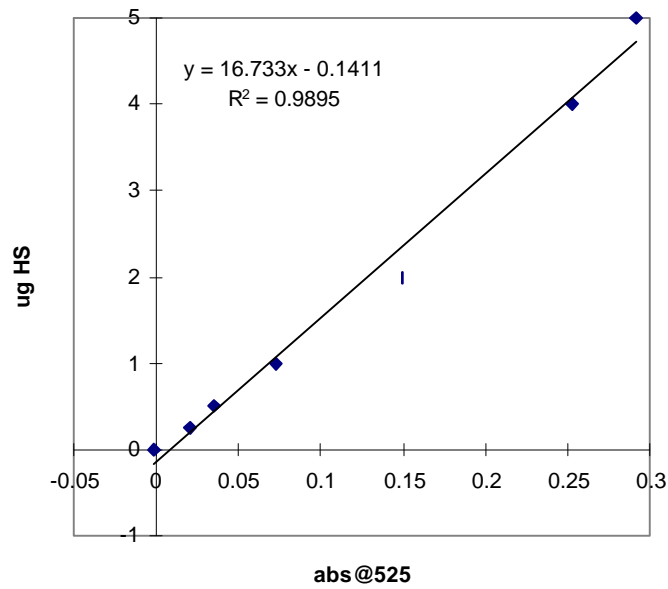


**Figure 2-1 Model of the domain structure of heparan sulfate**  
 (Turnbull and Gallagher, 1993)

**(a) Standard curve for HS**  
**(control: 50 ul 1.5M TBS + 1M urea)**



**(b) Standard curve for HS**  
**(control: 50ul 0.15MTBS)**

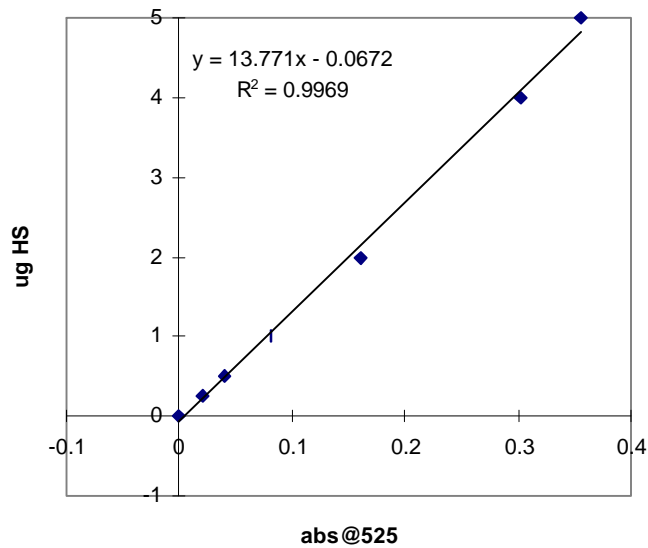


**Figure 2-2 Heparan sulfate (HS) standard curves by DMB assay**  
HS from bovine kidney (Sigma) was used as the standard heparan sulfate. (a) 1.5M TBS with 1M urea or (b) 0.15M TBS was added to bring the final concentration of HS to 0.1  $\mu\text{g}/\mu\text{l}$ . With 1 ml DMB, each 50  $\mu\text{l}$  sample was measured in the spectrophotometer at 525nm wavelength.

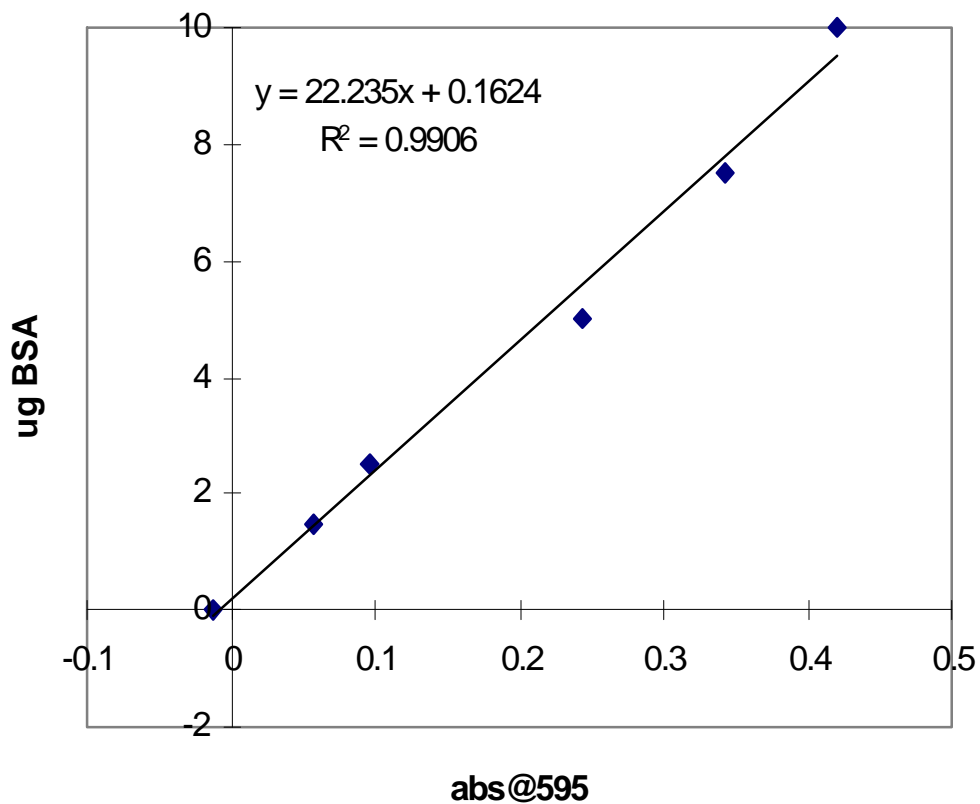


**Figure 2-3 Bovine serum albumin (BSA) standard curve by Bio-Rad protein microassay**

Deionized water was added to bring the final concentration of BSA (Fisher Scientific) to 100  $\mu\text{g}/\text{ml}$ . BSA stock and deionized water totaling 800  $\mu\text{l}$  were mixed with 200  $\mu\text{l}$  Protein Microassay Dye (Bio-Rad) for each sample. Sample absorbance reading at 595nm wavelength were measured in the spectrophotometer.

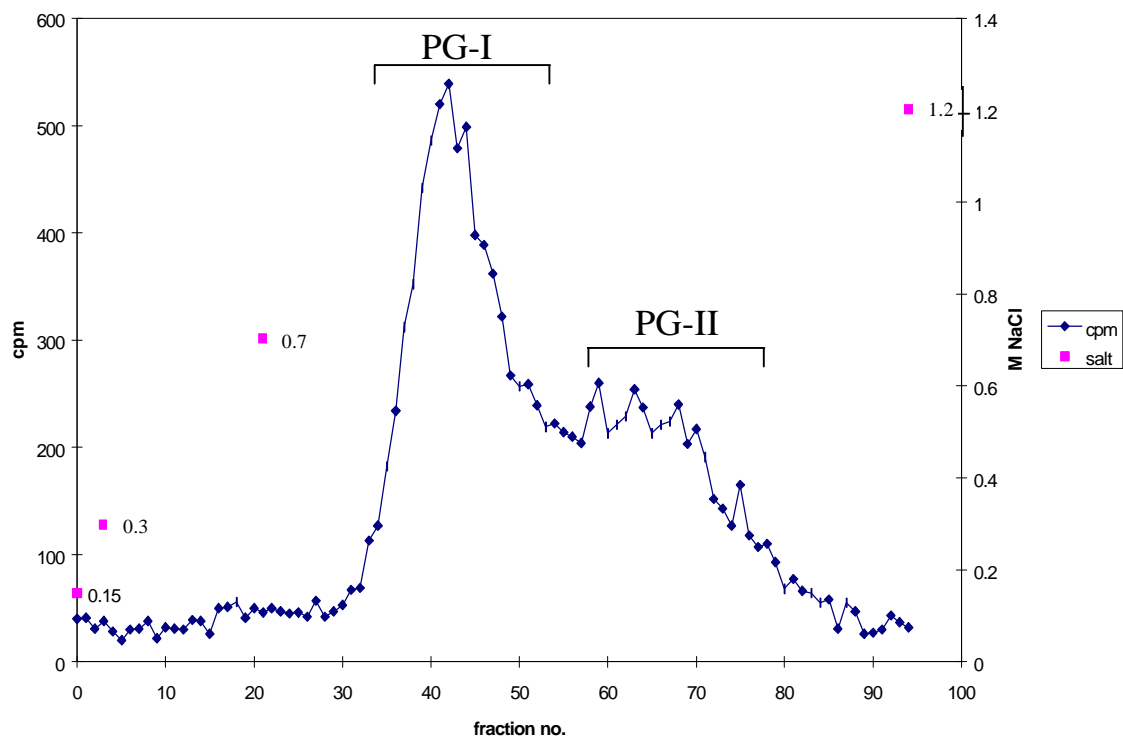
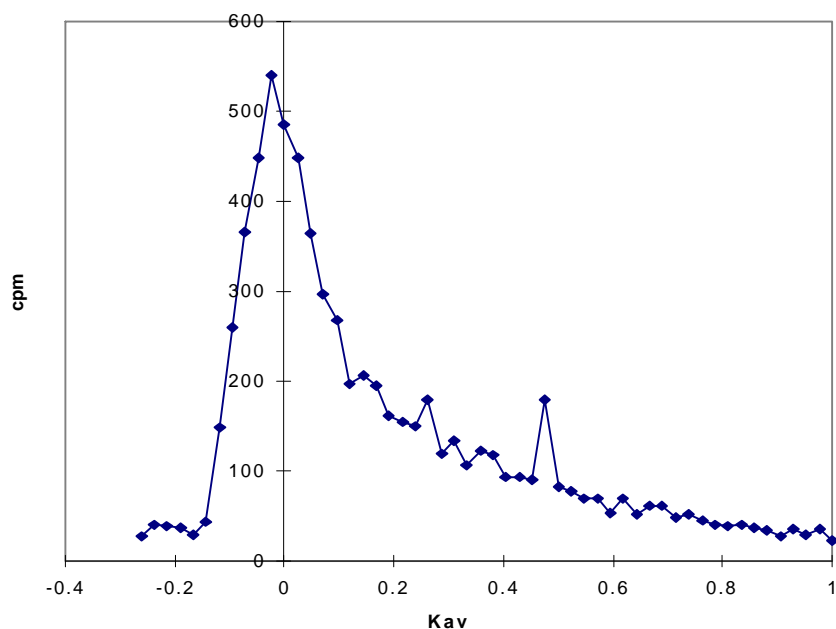


**Figure 2-4 Separation of BAE P9 PG on Q- Sepharose column with linear salt gradient**

BAE P9 PG was separated by a Q-Sepharose column (1.0 x 1.8 cm, Sigma) on the standard Econo<sup>®</sup> System with a linear salt gradient. The flowrate was 0.5 ml/min and fraction collector setting was 0.5 ml/vial.

(a) CL-6B gel filtration of the 1st peak of BAE P9 PG



(b) CL-6B gel filtration of the 2nd peak of BAE P9 PG

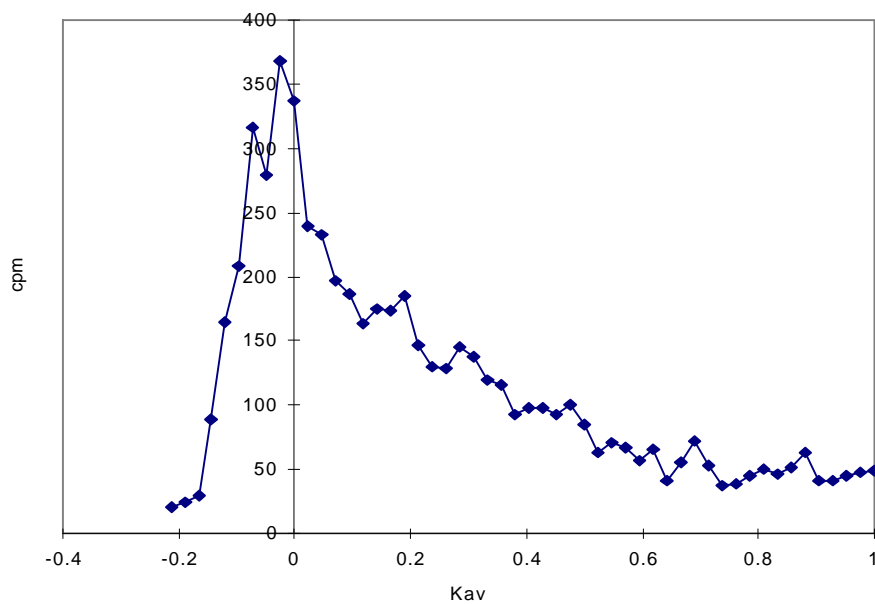
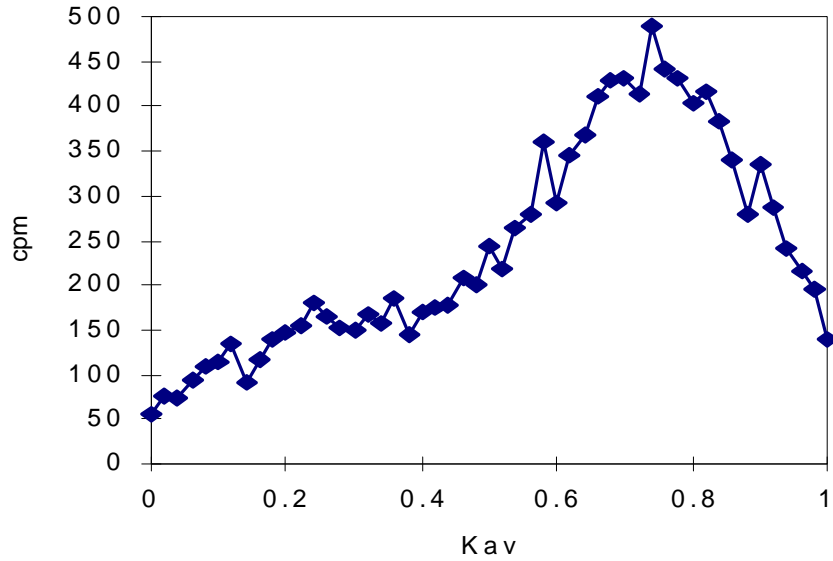


## Figure 2-5 Sepharose CL-6B gel filtration of PG-I and PG-II of BAE P9 PG

(a) PG-I and (b) PG-II of BAE P9 PG following Q-Sepharose column purification were pooled and run over a Sepharose CL-6B column (1.0 x 48 cm, Sigma) in 0.15M TBS at a flowrate of 0.6 ml/min with a fraction collector setting of 0.5 ml/vial.

(a) CL-2B gel filtration of BAE P9 PG



(b) CL-4B gel filtration of BAE P9 PG

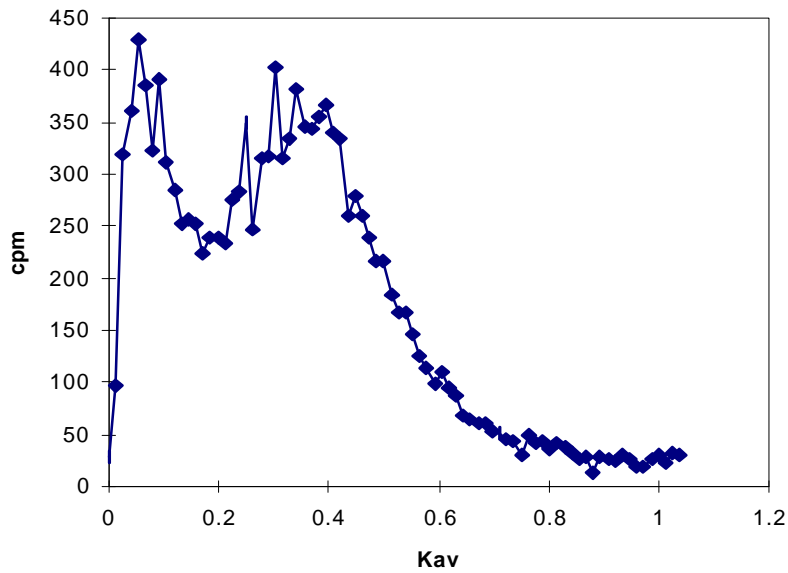


### Figure 2-6 Gel filtration of BAE P9 PG

BAE P9 PG was run over (a) a Sepharose CL-2B column (1.0 x 48 cm, Sigma) and (b) a Sepharose CL-4B column (1.0 x 48 cm, Sigma) in 0.15M TBS at a flowrate of 0.4 ml/min with a fraction collector setting of 0.5 ml/vial.

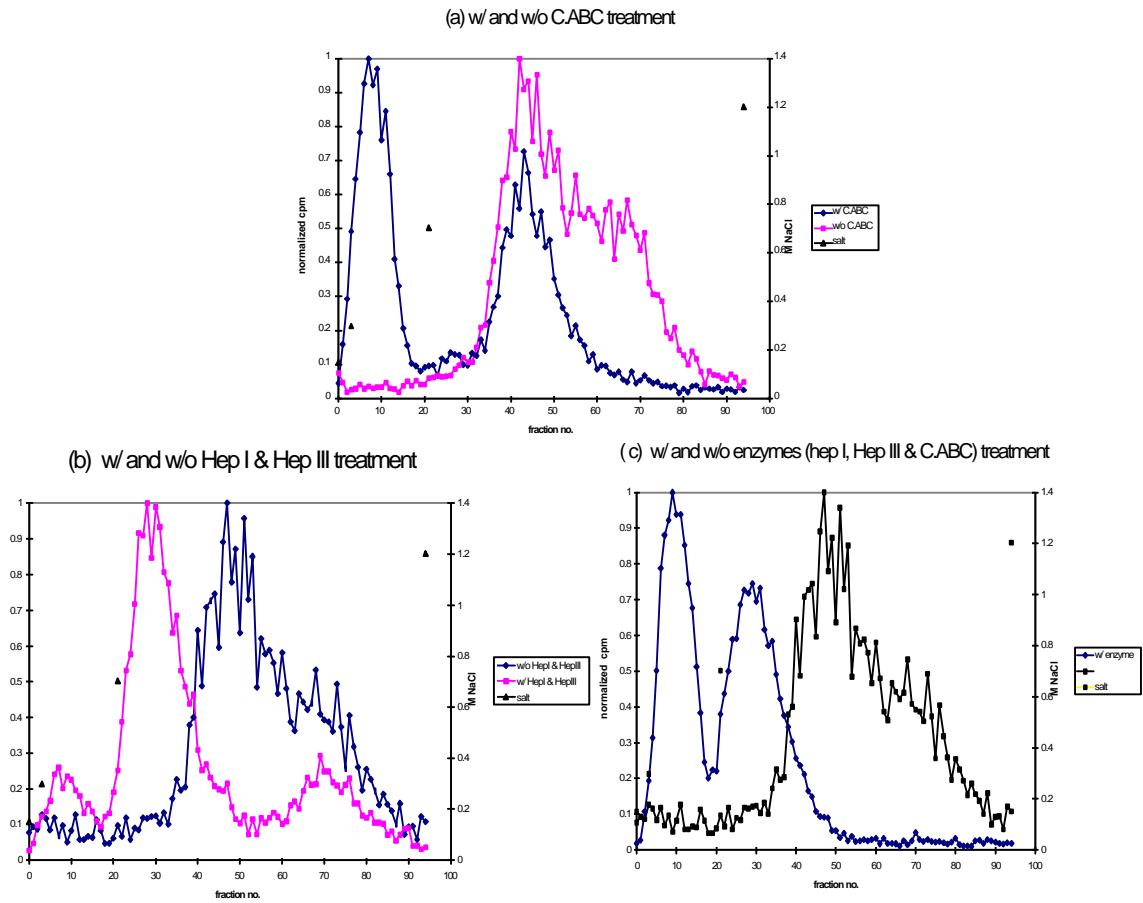


**Figure 2-7 Comparison of salt elution of BAE P9 PG with and without enzyme digestion**

100  $\mu$ l of BAE P9 PG was treated with 12  $\mu$ l of Hep I (Sigma) and 14  $\mu$ l of Hep III (Sigma), or 7  $\mu$ l of C.ABC (Sigma), or 12  $\mu$ l of Hep I , 14  $\mu$ l of Hep III and 7  $\mu$ l of C.ABC (Sigma) at 37  $^{\circ}$ C for 4 hr under the best conditions. Then enzyme digested samples, along with samples without enzyme digestion, were loaded onto a Q-Sepharose column (1.0 x 1.8 cm, Sigma) on the standard Econo<sup>®</sup> System with a linear salt gradient. The flowrate was 0.5 ml/min and fraction collector setting was 0.5 ml/vial.

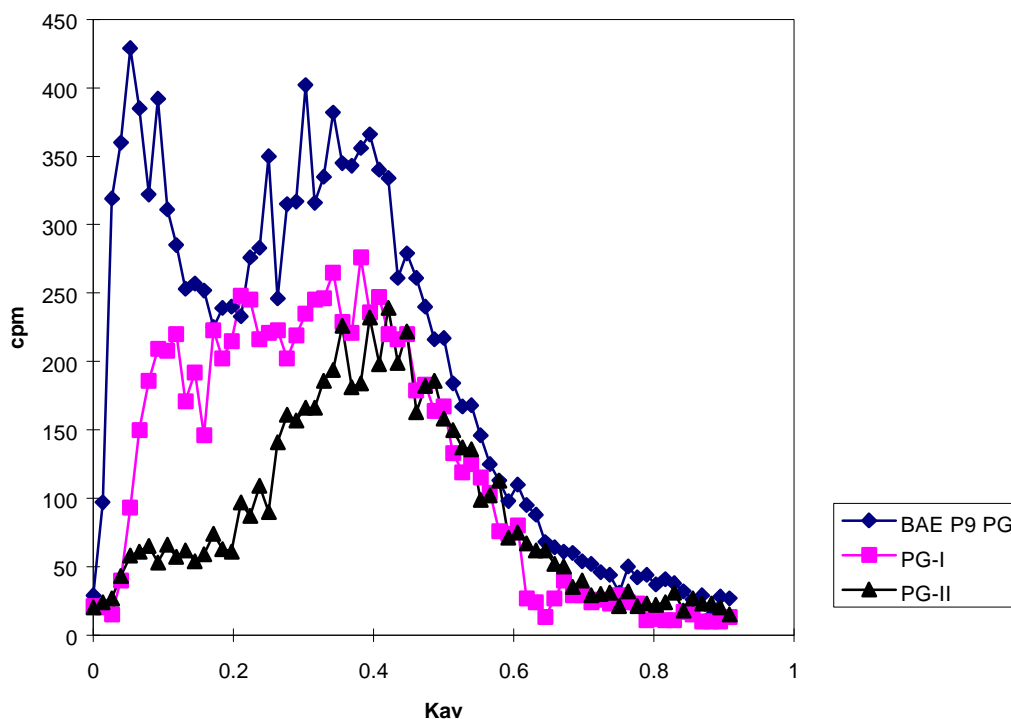


**Figure 2-8 Comparison of non-fractionated BAE P9 PG, PG-I, and PG-II on Sepharose CL-4B**

PG-I and PG-II from BAE P9 PG following Q-Sepharose column purification were pooled and run over a Sepharose CL-4B column (1.0 x 48 cm, Sigma), along with non-fractionated BAE P9 PG, in 0.15M TBS at a flowrate of 0.4 ml/min with a fraction collector setting of 0.5 ml/vial.



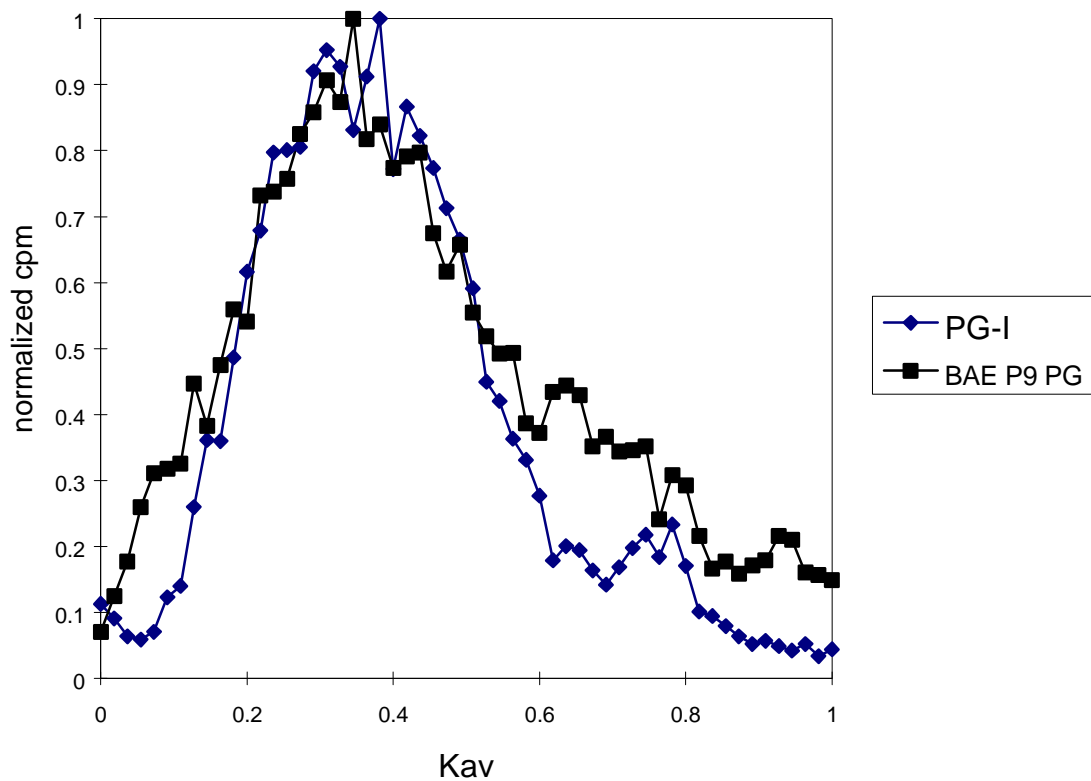


**Figure 2-9 Comparison of non-fractionated BAE P9 PG and PG-I on Sepharose CL-6B after beta-elimination**

PG-I of BAE P9 PG following Q-Sepharose column purification were pooled. After the beta-elimination, PG-I and non-fractionated BAE P9 PG were run over a Sepharose CL-6B column (1.0 x 48 cm, Sigma) in 0.15M TBS at a flowrate of 0.6 ml/min with a fraction collector setting of 0.5 ml/vial.

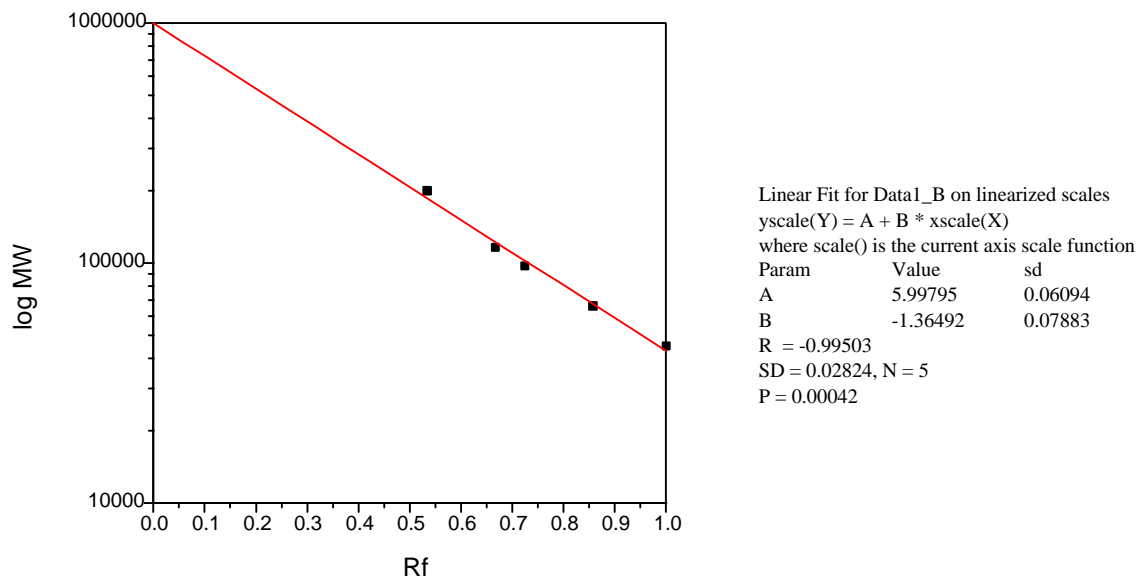


### Figure 2-10 Calibration curve of protein standards on SDS-PAGE

The protein standards (Bio-Rad) consisted of rabbit skeletal muscle myosin (200 kDa), *E. coli*  $\beta$ -galactosidase (116.25 kDa), rabbit muscle phosphorylase b (97.4 kDa), bovine serum albumin (66.2 kDa) and hen egg white ovalbumin (45 kDa). They were run on the SDS-PAGE (3.5% stacking gel and 5% separating gel) for ~ 45 min at 110V. Protein bands were visualized by silver staining.

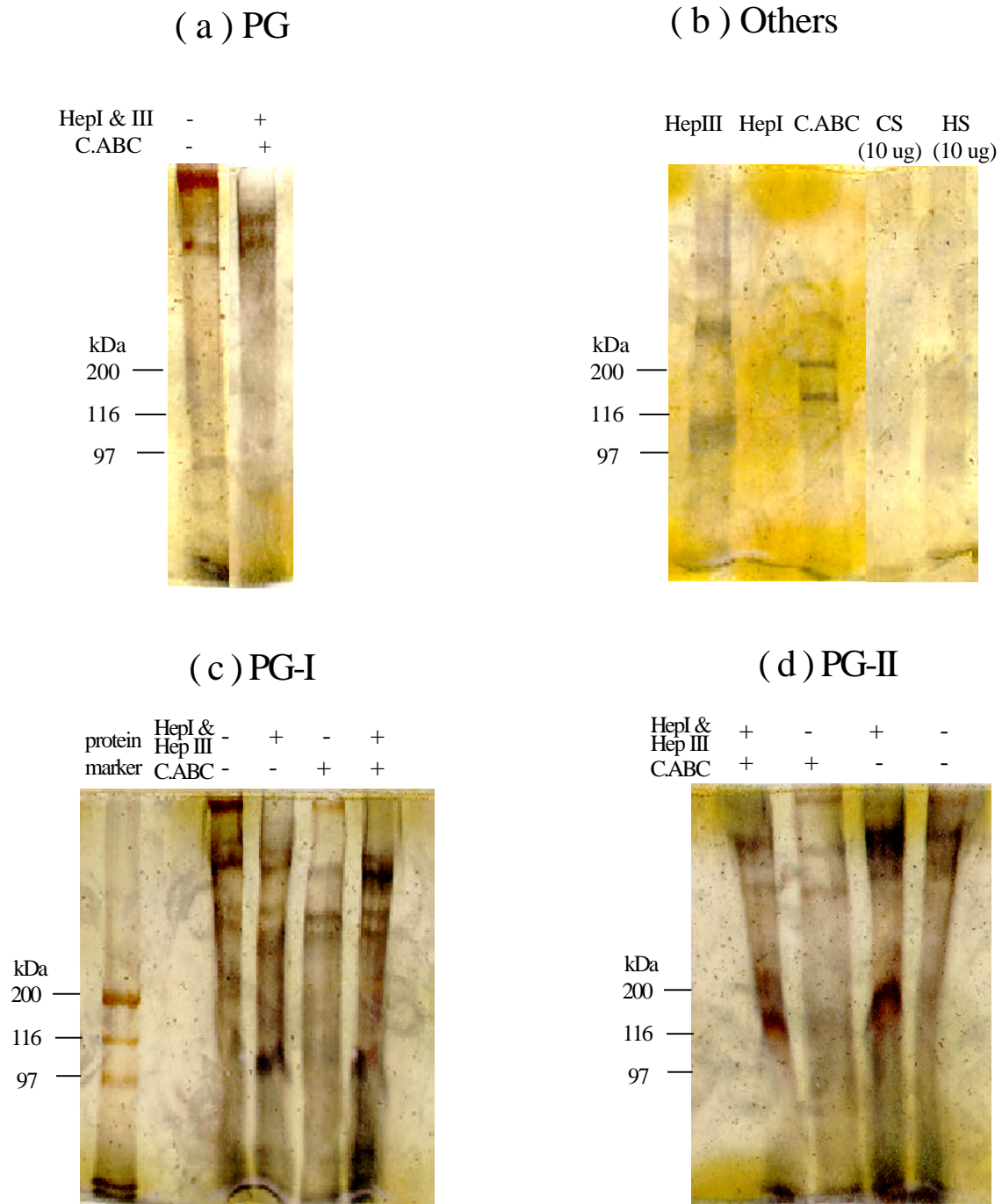
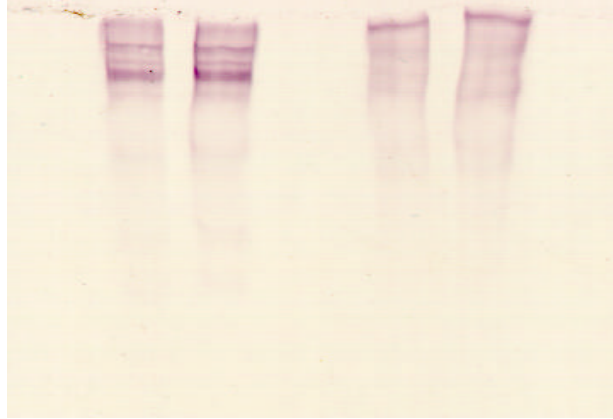


**Figure 2-11 Results of SDS-PAGE with silver staining**

(a) Non-fractionated PG, (b) Hep I, Hep III, C.ABC, 10  $\mu$ g HS and 10  $\mu$ g CS, (c) PG-I, and (d) PG-II were run on the SDS-PAGE (3.5% stacking gel and 5% separating gel) for ~ 45 min at 110V. Bands were visualized by silver staining. Each lane was loaded ~ 1  $\mu$ g protein sample. 100  $\mu$ l PG-I and PG-II following Q-Sepharose column separation with (+) or without (-) enzyme digestion were dialyzed against deionized water. ~ 4  $\mu$ g CS was added to each sample, and they were lyophilized. +: with enzyme digestion; -: without enzyme digestion.

(a) Non-fractionated PG

Hep I/III	+	+	-	-
C. ABC	+	+	-	-



(b) PG-I

Hep I/III	-	+	-	+
C. ABC	-	-	-	+

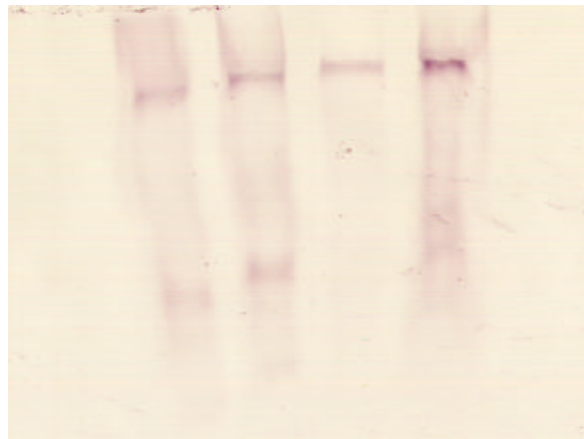


**Figure 2-12 Western blotting with the primary antibody of anti-perlecan**

Following separation on 5% SDS-PAGE, (a) Non-fractionated PG and (b) PG-I core proteins were transferred onto a cellulose blotting membrane at 50V for 2 hr at 4°C. The membrane was incubated in the blocking buffer for 1 hr at room temperature, then incubated with anti-perlecan at a final concentration of 1 µg/ml in PBST containing 1% Non-Fat Dry Milk for 1 hr at room temperature. The membrane was washed five times with PBST and then hybridized for 1 hr at room temperature with anti-rat IgG (whole molecule) with alkaline phosphatase conjugate from goat. Five washes were conducted as before. The membrane was then incubated in the buffer made with SIGMA FAST™ BCIP/NBT buffered substrate tablet. The protein bands stand purple. Each lane was loaded ~ 2 µg protein sample. +: with enzyme digestion; -: without enzyme digestion.

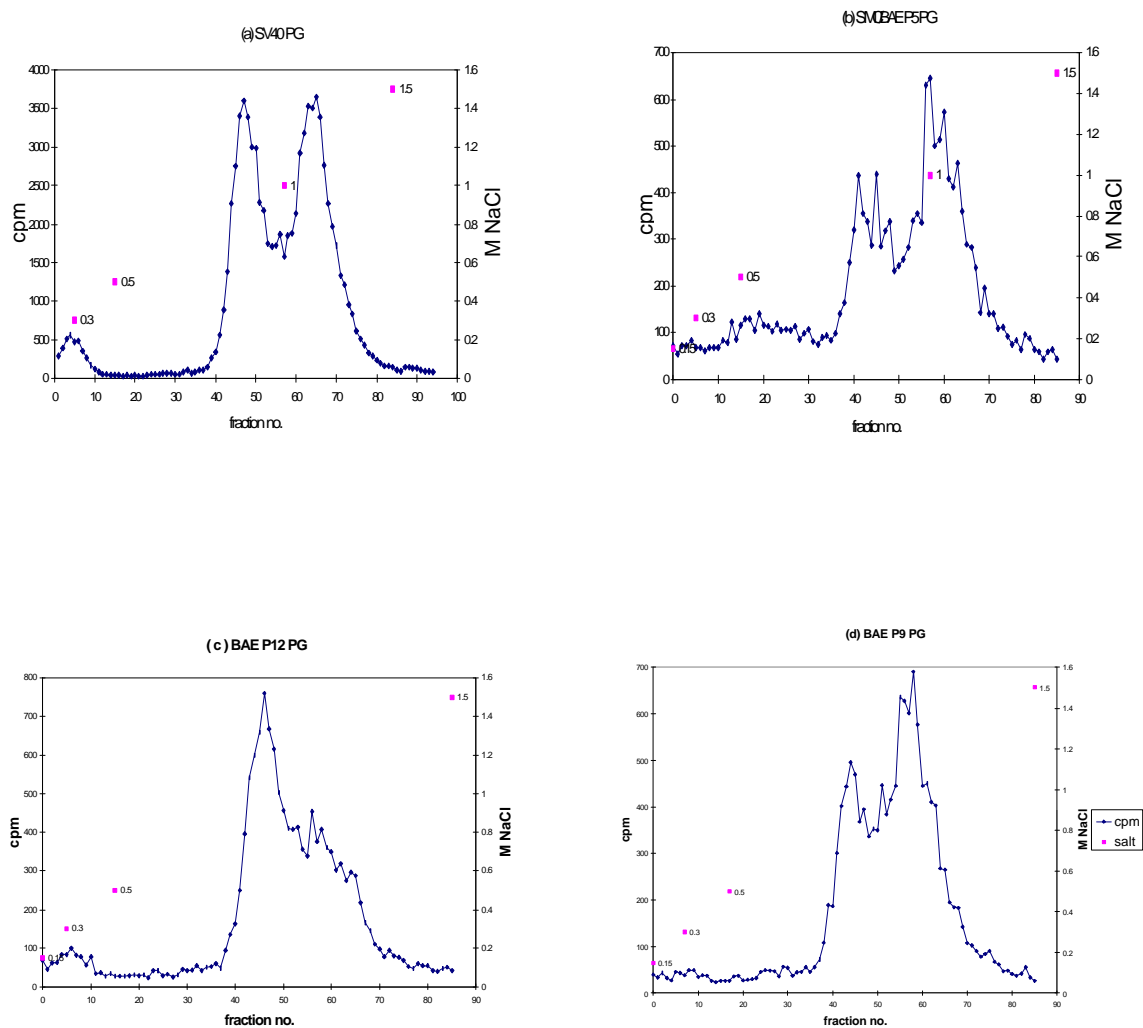


**Figure 2-13 Comparison of PGs on Q-Sepharose column with the same salt linear gradient**

PGs from (a) SV 40 cells, (b) SMC/BAE P5 cell mixture, (c) BAE P12 cells, and (d) BAE P9 cells conditioned media were run over a Q-Sepharose column (1.0 x 1.8 cm, Sigma) on the standard Econo<sup>®</sup> System with the same linear salt gradient. The flowrate was 0.5 ml/min and fraction collector setting was 0.5 ml/vial.

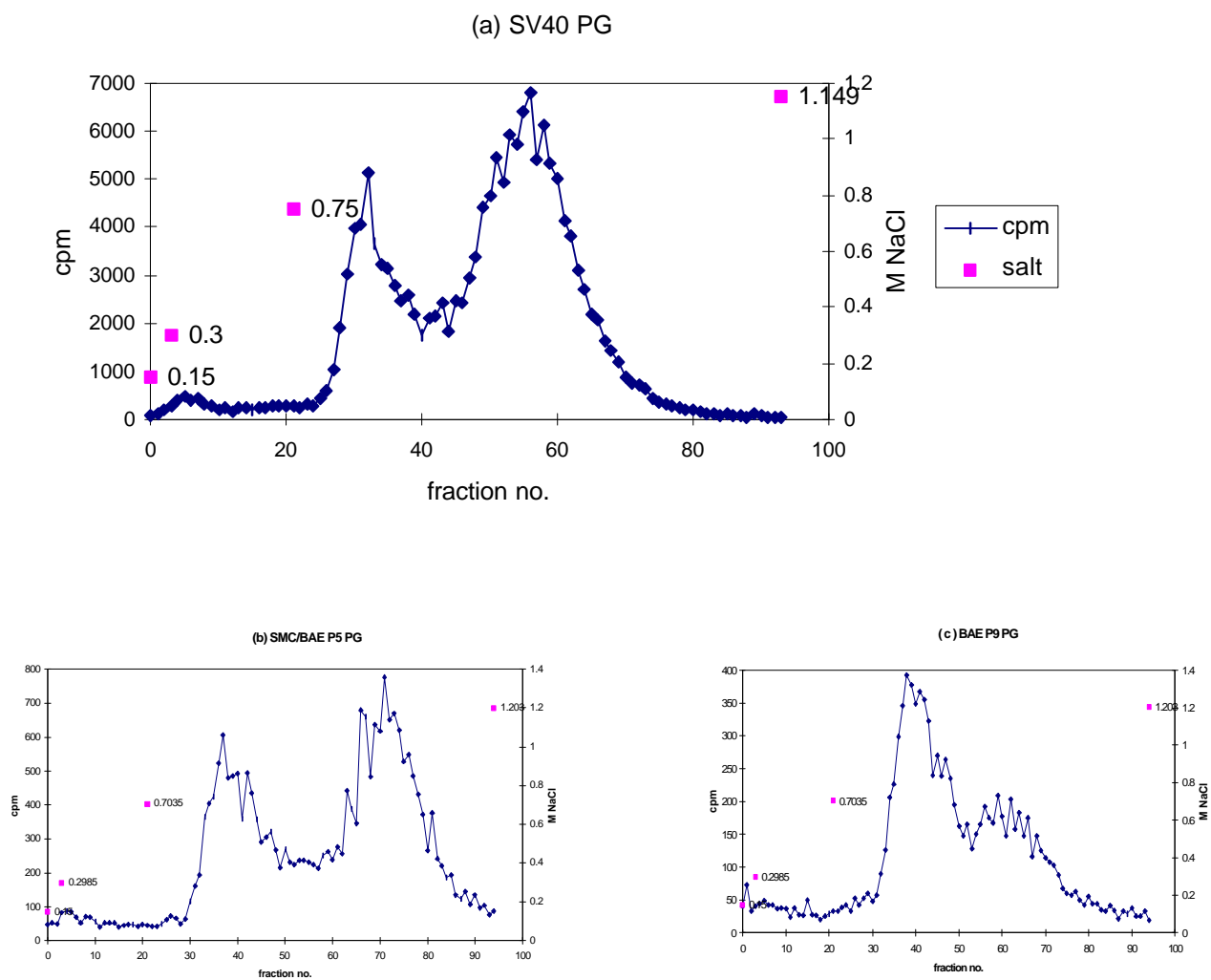


**Figure 2-14 Comparison of PGs on Q-Sepharose column with the optimal salt linear gradient**

PGs from (a) SV 40 cells, (b) SMC/BAE P5 cell mixture, and (c) BAE P9 cells conditioned media were run over a Q-Sepharose column (1.0 x 1.8 cm, Sigma) on the standard Econo<sup>®</sup> System with the optimal linear salt gradient. The flowrate was 0.5 ml/min and fraction collector setting was 0.5 ml/vial.

## **Chapter III**

### **Cell Free Binding Assay**

#### **3.1 Introduction**

There are two primary sets of receptors for bFGF: one is the high affinity receptor, FGFR; the other is the low affinity receptor, HSPG on cell surface. Changes occur in FGFR expression levels during proliferation, differentiation, or malignant transformation. Exponentially growing cells generally express higher receptor levels than do subconfluent or confluent cells (Bikfalvi, et al., 1997). Down-regulation or up-regulation of FGF receptors may also occur according to the cell type and certain biological stage (Bikfalvi, et al., 1997). Focus on bFGF-FGFR interaction has been in three areas: (1) ligand specificity; (2) extracellular conditions that modify ligand/receptor interaction; and (3) interactions between the ligand-activated receptor and substrates generating the intracellular signals (Bikfalvi, et al., 1997). The expression of bFGF and its receptors in normal cells and tissues relies on both temporal and spatial regulation through fine tuning of their molecular interactions. The binding of bFGF with HSPG may have a key role in this fine tuning as well as in the switch to rapid cell proliferation typical of tumor progression. This section addresses our study of the binding properties of extracellular HSPG purified from BAE cell conditioned media with bFGF.

The cell free binding assay for bFGF with purified HSPG from BAE cell conditioned media was conducted in Bio-Dot Microfiltration apparatus (Bio-Rad, Hercules, CA) with Zeta-Probe blotting membrane (Bio-Rad, Hercules, CA), called the cationic filtration assay (CAFAS) thereafter. The Bio-Dot apparatus has a 96-well template that allows various binding combinations to be investigated simultaneously. The Zeta-Probe blotting membrane is a quaternary amine derivatized nylon membrane with the nominal porosity of 0.45  $\mu\text{m}$ . The basic idea is that small positive molecules, such as bFGF, will not bind, and therefore should have a very low retention on the membrane. Large anionic molecules,

such as HSPG, are expected to be fully retained on the membrane due to charge attraction and the size blotting.

### **3.2 The Establishment of Protocol for Cell Free Binding Assay**

General procedures of the cationic filtration assay (CAFAS): The Zeta-Probe blotting membrane was cut into a certain size to fit the Bio-Dot apparatus, and presoaked in 0.15M TBS, 1 mg/ml BSA buffer for at least 20 minutes. Then the Zeta-Probe blotting membrane was clamped between a plastic sealing gasket and the 96-well sample template, and sealed tightly by tightening the four screws in a cross-diagonal fashion. The plastic sealing gasket lies on top of the gasket support plate which sits in the vacuum manifold. The vacuum manifold has a three-way flow valve, which allows for on and off control during the assay (Figure 3-1). After the membrane was secured in the apparatus, 200 $\mu$ l of the buffer was added to each well and pulled via vacuum pump across the membrane to insure that the membrane is completely wet. The vacuum was then turned off, and samples added to individual well. After incubation for a certain time, samples were pulled through the membrane via vacuum and washed with the buffer several times. Finally the amount of  $^{125}$ I-bFGF or  $^{35}$ S-PG retained on the membrane was determined by cutting out individual membrane dot, putting into scintillation vials and counting in a liquid scintillation counter (Tri-Carb 2100TR, Packard, Downers Grove, IL). The presoaking and incubation buffer, the washing buffer, the length of incubation, and the washing times were investigated and optimized for the specified binding system.

Firstly, 0.15M TBS with 1 mg/ml BSA buffer was used for presoaking and incubation. Approximately 2000cpm of  $^{125}$ I-bFGF was incubated in a well with 200 $\mu$ l buffer for 1 hour, then pulled through the membrane, and followed by one wash. The retention of  $^{125}$ I-bFGF was quite high, more than 25%, which was undesirable, and indicated that  $^{125}$ I-bFGF was a very “sticky” molecule and would create high level of non-specific binding. In addition, the transient study of  $^{125}$ I-bFGF behavior in the Bio-Dot apparatus was conducted. 0.15M TBS with 1 mg/ml BSA buffer was used, and approximately 2000cpm



of  $^{125}\text{I}$ -bFGF was separately added to individual wells with 200ul buffer. After 5min, 10min, till 60min of incubation, 100ul of liquid inside of each well was pulled out and counted in the scintillation counter as free  $^{125}\text{I}$ -bFGF (Figure 3-2). It was determined that after 20 min the level of free  $^{125}\text{I}$ -bFGF tended to be stable, and that more than half the amount of  $^{125}\text{I}$ -bFGF had stuck to the membrane or the plastic wall of the wells as non-specific binding. In order to decrease such a high non-specific binding of pure  $^{125}\text{I}$ -bFGF, preliminary experiments were done to determine the optimal assay conditions.

*Effect of BSA concentrations in the buffer on transient study of  $^{125}\text{I}$ -bFGF behavior in Bio-Dot* - BSA serves as a coating agent to prevent bFGF or other molecules studied from sticking to the membrane and the plastic wall of wells. Presoaking the membrane in a buffer with higher BSA concentration might help to put a “coat” on the surface of the membrane, as might washing the membrane with a higher BSA concentration buffer after pulling all samples through the membrane facilitate any molecules sticking on the plastic wall of wells fall off. But the BSA concentration cannot be indefinitely high, because coating might also decrease the retention of PG on the membrane or interfere with bFGF-PG binding. We compared the effect of 1.5M TBS with 1 mg/ml BSA buffer with that of 1.5M TBS with 2 mg/ml BSA buffer on transient  $^{125}\text{I}$ -bFGF sticking behavior in the Bio-Dot apparatus. 2 mg/ml BSA buffer decreased the non-specific binding of  $^{125}\text{I}$ -bFGF when incubated in Bio-Dot well with one wash (Figure 3-3). The binding of  $^{35}\text{S}$ -PG with 2 mg/ml BSA 0.15M TBS buffer in Bio-Dot was investigated. After 20 min, the free  $^{35}\text{S}$ -PG also reached a stable level, and the  $^{35}\text{S}$ -PG retention on the membrane was above 80%. Therefore, 0.15M TBS with 2 mg/ml BSA buffer was chosen as the presoaking and incubation buffer.

*Effect of washes on  $^{125}\text{I}$ -bFGF behavior in Bio-Dot* - Following incubation and vacuum pull through, some sample molecules may remain stuck on the plastic wall of the wells. A single wash with washing buffer can assist in rinsing the walls and membrane, and is necessary for the procedure. More than one wash may be helpful in cleaning off “sticky molecules” on the walls and membrane and decrease the non-specific background binding.

But the binding complex might also be washed off with too many washes. To investigate washing effect on  $^{125}\text{I}$ -bFGF behavior in Bio-Dot,  $^{125}\text{I}$ -bFGF was loaded into individual wells; after one hour incubation, all liquid in some wells was aspirated, while others were pulled through the membrane. No wash, 1 wash, 2 washes, and 3 washes were investigated, and the retention of  $^{125}\text{I}$ -bFGF on the membrane with and without aspiration were determined (Figure 3-4 (a)). Three washes appear the best. Similarly, the washing effect on  $^{35}\text{S}$ -PG behavior in Bio-Dot was also investigated. Figure 3-4 (b) shows that there is no difference for  $^{35}\text{S}$ -PG retention for different numbers of washes. As a result, three washes were used.

*Effect of different washing buffers on retention of  $^{125}\text{I}$ -bFGF,  $^{35}\text{S}$ -PG, and  $^{125}\text{I}$ -bFGF-PG in Bio-Dot* - Four different washing buffers were studied:

0.15M TBS + 2mg/ml BSA;

0.3M TBS + 2mg/ml BSA;

0.15M TBS + 2mg/ml BSA + 0.5M urea; and

0.15M TBS + 2mg/ml BSA + 1.0M urea.

0.25ng  $^{125}\text{I}$ -bFGF alone, 10ng  $^{35}\text{S}$ -PG alone, and 0.25ng  $^{125}\text{I}$ -bFGF with 10ng PG were loaded into Bio-Dot wells. After one hour incubation in 0.15M TBS with 2mg/ml BSA buffer, all liquid was pulled through the membrane and followed by three washes (Figure 3-5). The retention of  $^{125}\text{I}$ -bFGF-PG complex was 33% with 0.15M TBS + 2mg/ml BSA buffer, 26% with 0.3M TBS + 2mg/ml BSA buffer, 27% with 0.15M TBS + 2mg/ml BSA + 0.5M urea buffer, and 27% with 0.15M TBS + 2mg/ml BSA + 1.0M urea buffer. One might predict that high salt concentration, as well as the addition of urea, would disrupt the binding complex, and decrease the retention of the complex on the membrane. Even though the 0.5M urea helped to decrease the background retention of  $^{125}\text{I}$ -bFGF, we chose to use 0.15M TBS + 2mg/ml BSA as washing buffer, because the main purpose of our cationic filtration assay (CAFAS) is to measure the retention of the binding complex  $^{125}\text{I}$ -bFGF-PG, and the disruption of the binding complex in the washing step would lead to erroneous results.

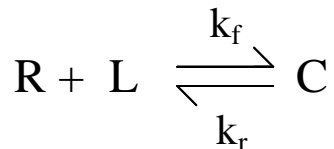
*Binding study of <sup>125</sup>I-bFGF with PG in Bio-Dot* - In one section of the Bio-Dot apparatus, 10ng, 15ng, 20ng PG were loaded into wells respectively. After one hour, all liquid in each well was aspirated, and 0.25ng <sup>125</sup>I-bFGF in buffer (total volume of 200μl) was loaded into each individual well. After one hour incubation, all liquid was pulled through the membrane and three washes followed. The binding retention of 0.25ng <sup>125</sup>I-bFGF with PG pre-incubation was determined (Figure 3-6 (a) ). From the Figure 3-4 (b), we found that about 25% of PG was bound to the membrane after one hour. The retention shown in Figure 3-6 (a) includes the surface binding of <sup>125</sup>I-bFGF with 25% of 10ng, 15ng, and 20ng PG (2-dimension binding) and non-specific binding of <sup>125</sup>I-bFGF on the membrane and the plastic wall of wells. In another section of the Bio-Dot, 0.25ng <sup>125</sup>I-bFGF, 10ng, 15ng or 20ng PG, and the buffer totaling 200μl were loaded into wells. After one hour incubation, all liquid was pulled through and three washes followed. The binding retention of 0.25ng <sup>125</sup>I-bFGF with PG was measured, which included the binding occurring in solution (3-dimension binding), occurring on the surface (2-dimension binding), and non-specific binding on the membrane and the plastic wall of wells (Figure 3-6 (b) ). Comparison of Figure 3-6 (a) and (b) reveals little difference. The involvement of the membrane in the binding study during the incubation period makes it difficult to clearly analyze the results. In order to overcome this disadvantage, we employed an alternative location for the binding step, a separate 0.6ml plastic Eppendorf vial. <sup>125</sup>I-bFGF and PG were loaded into a separate vial with buffer totaling 200μl, incubated for one hour, and then pulled through the membrane directly by placing contents into a well with the vacuum on. The membrane now served as a “net” catching the bound complex which occurred in the solution. In this way, the retention of <sup>125</sup>I-bFGF decreased to 8.7%, and the retention of 10ng PG with 0.25ng <sup>125</sup>I-bFGF was 12.3%. There was around 30% increase of retention due to the presence of 10ng PG. The decreasing of background “noise” of <sup>125</sup>I-bFGF facilitated the analysis of results. And there was little <sup>125</sup>I-bFGF stuck on the surface of the vial. Therefore, a separate vial was incorporated into the cationic filtration assay (CAFAS). Also we noted that the presence of bFGF would not affect the retention of PG on the membrane (Figure 3-7). Different amounts of bFGF without radioactive labeling

was incubated with 10ng <sup>35</sup>S-PG for one hour, and the retention of <sup>35</sup>S-PG measured remained around 80%.

*Determination of incubation length* - The incubation length was determined by the transient study of binding retention of 0.25ng <sup>125</sup>I-bFGF with 40ng PG in Bio-Dot. Figure 3-8 showed that after one hour the binding reaction reached an equilibrium, and the binding retention was on a stable level. One hour was used for steady-state incubation.

### 3.3 The Cell Free Binding Assay of <sup>125</sup>I-bFGF with PG

PG, especially HS, can serve as a low affinity binding element for bFGF. The binding reaction can be assumed as a simple monovalent binding model (Lauffenburger and Linderman, 1993):



in which a monovalent ligand L (bFGF) binds reversibly to a monovalent receptor R (PG) to form a receptor/ligand complex C. We assume that the medium is well-mixed so that the ligand is available at a uniform concentration from a macroscopic point of view. In addition, we assume that PG has homogeneous binding sites with a uniform molecular size of  $5 \times 10^5$ , the average molecular weight of PG we got from the result of Sepharose CL-2B gel filtration experiment. Using principles of mass action kinetics:

$$(1) \quad \frac{dC}{dt} = k_f RL - k_r C$$

wherein:

R: number of free monvalent binding sites of receptor (PG);

L: ligand (<sup>125</sup>I-bFGF);

C: complex of receptor and ligand;

k<sub>f</sub>: association rate constant [M<sup>-1</sup>time<sup>-1</sup>]

the velocity of the second-order interaction between the receptor and ligand;  
 $k_f$ : dissociation rate constant [time<sup>-1</sup>]  
the velocity of the first-order breakdown of the receptor/ligand complex;  
t: time.

Because both R and L change with time, R(t) and L(t), we cannot solve equation (1) for C(t) directly. We assumed that the total number of receptor  $R_T$  was not changed, i.e. there was no degradation and synthesis of PG during the course of the experiment, so that:

$$(2) \quad R_T = R + C \quad (\text{receptor conservation})$$

Then the equation (1) simplifies to:

$$(4) \quad \frac{dC}{dt} = k_f[R_T - C]L - k_rC$$

At equilibrium, i.e. steady state,  $\frac{dC}{dt} = 0$ , therefore

$$(5) \quad C_{eq} = \frac{R_T L}{K_D + L}$$

wherein:  $K_D = k_r / k_f$ , the equilibrium dissociation constant [M].

Rearranging equation (5):

$$(6) \quad \frac{C_{eq}}{L} = -\frac{1}{K_D} C_{eq} + \frac{R_T}{K_D}$$

The Scatchard plot of  $(C_{eq}/L)$ , termed “bound/free”, versus  $C_{eq}$ , termed “bound”, should thus yield a straight line, with slope equal to  $-1/K_D$ , abscissa-intercept equals to  $R_T$ , and ordinate-intercept equals to  $(R_T/K_D)$  (Limbird, 1986).

Increasing  $R_T$  or  $L_0$  (the initial concentration of ligand) should therefore lead to an increase in C. Figure 3-9 (a) shows that with increasing amounts of PG, the retention of the binding complex of <sup>125</sup>I-bFGF and PG increased. The saturation retention occurred at 40ng PG, which might be due to reaching either the reaction equilibrium or the membrane

saturation. In addition, Figure 3-9 (b) shows that with increasing  $^{125}\text{I}$ -bFGF from 0.25ng to 0.5ng, the amount of binding complex increased greatly.

The cell free binding assays of  $^{125}\text{I}$ -bFGF (0.05ng, 0.1ng, 0.15ng, 0.2ng, or 0.25ng) and PG (20ng, 30ng, or 40ng) were conducted with separate vial incubation and using the Bio-Dot apparatus for separation. Retention of the binding complex was measured after one hour incubation (steady-state). The equilibrium dissociation constant,  $K_D$ , was obtained from CAFAS data and equation (6) using FORTRAN and the IMSL subroutine RLINE for least squares analysis (Appendix A). The results showed that

$$K_D = (1.6 \pm 0.8) \times 10^{-10} \text{ M}$$

$$R_T = (1.3 \pm 0.6) \times 10^8 \text{ \#/ng PG.}$$

When we used the estimated average molecular weight of PG,  $5 \times 10^5$ , the  $R_T$  might be converted to  $R_T = 0.1 \sim 0.2$  (# of site)/(molecule of PG). That means 5 ~10 molecules of PG will form a binding site for bFGF.

We noticed that  $L \gg C$ , and since  $L_0 = L + C$ , the assumption that  $L = L_0$  could be made. Then equation (4) becomes:

$$(7) \quad \frac{dC}{dt} = k_f[R_T - C]L_0 - k_r C$$

With the initial condition  $C(t = 0) = C_0$ , we can get the transient solution of  $C(t)$  using standard techniques for solving ordinary differential equations (Ritger and Rose, 1968):

$$(8) \quad C(t) = C_0 \exp[-(k_f L_0 + k_r)t] + \left(\frac{k_f L_0 R_T}{k_f L_0 + k_r}\right) \{1 - \exp[-(k_f L_0 + k_r)t]\}$$

Rearranging the equation (8) with  $K_D = k_r / k_f$  and taking natural logarithm on both sides, we get

$$(9) \quad \ln[C_{eq} - C(t)] = \ln\left[\frac{R_T}{1 + (K_D / L_0)} - C_0\right] - \left[1 + \left(\frac{L_0}{K_D}\right)\right]k_r t$$

It is assumed that  $C(t = 0) = C_0 = 0$ , i.e. at the beginning of the binding experiment,  $t = 0$ , there is no binding complex formed. Equation (9) becomes:

$$(10) \quad \ln[C_{eq} - C(t)] = \ln\left[\frac{R_T}{1 + (K_D / L_0)}\right] - \left[1 + \left(\frac{L_0}{K_D}\right)\right]k_r t$$

Once we can get data of  $C(t) \sim t$ , and  $C_{eq}$ ,  $k_r$  can be obtained from the slope value

$\{-[1 + (\frac{L_0}{K_D})k_r]\}$  of the straight line  $\ln[C_{eq} - C(t)] \sim t$ , since we already knew  $L_0$  and  $K_D$ .

Furthermore,  $k_f$  can be determined, because  $K_D = k_r / k_f$ .

Transient study of binding of 0.2ng  $^{125}$ I-bFGF and 40ng PG was conducted with separate vial incubation and using Bio-Dot apparatus. At  $t = 1\text{min}, 5\text{min}, 10\text{min}, 15\text{min}, 20\text{min}, 30\text{min}$  and  $60\text{min}$ ,  $C(t)$ s were measured as the retention of binding complex on the membrane of Bio-Dot. Retentions of 0.2ng  $^{125}$ I-bFGF alone without PG were also measured at above certain time and deducted as non-specific background binding.  $C_{eq}$  was determined at  $t = 60\text{min}$ . The dissociation rate constant,  $k_r$ , and the association rate constant,  $k_f$ , were obtained from the CAFAS data and equation (10) using FORTRAN and the IMSL subroutine RLINE for least squares analysis (Appendix B). The results showed that

$$k_r = 0.01 \text{ min}^{-1}$$

$$k_f = 6.2 \times 10^7 \text{ M}^{-1}\text{min}^{-1}$$

If we consider  $L = L_0 - C$  instead of using the assumption  $L = L_0$ , the equation (4) becomes:

$$(11) \quad \frac{dC}{dt} = k_f(R_T - C)(L_0 - C) - k_r C, \text{ i.e.}$$

$$(12) \quad \frac{dC}{dt} = k_f R_T L_0 + [-(k_f R_T + k_f L_0 + k_r)]C + k_f C^2,$$

which has a form of the *Riccati* equation (Boyce and DiPrima, 1997). This equation was solved by transforming to second-order differential equation with constant coefficients (Boyce and DiPrima, 1997), and obtaining the general solution (Korn and Korn, 1968). Data from above CAFAS was fitted into the solution by the software “Origin” (version

3.01, Microcal Software, Inc. Northampton, MA), and obtained average  $k_f$  (Appendix C). The results showed that

$$k_f = 5.6 \times 10^7 \text{ M}^{-1}\text{min}^{-1}$$

$$k_r = 0.009 \text{ min}^{-1}$$

The difference of  $k_f$  or  $k_r$  with or without the assumption ( $L = L_0$ ) is within 10%, therefore the assumption  $L = L_0$  is valid in our case.

*Effect of  $\text{Ca}^{2+}$  on binding retention of PG with  $^{125}\text{I}$ -bFGF in Bio-Dot* - Divalent cations, such as  $\text{Ca}^{2+}$  and  $\text{Mg}^{2+}$ , were reported to be required for the high affinity interaction of heparin with FGFR at physiological concentrations (Kan, et al., 1996). We wanted to determine if divalent cations also affect the interaction of HSPG with bFGF. 40ng PG and 0.25ng  $^{125}\text{I}$ -bFGF were incubated in the absence or presence of different concentration of  $\text{CaCl}_2$  (0mM ~ 60mM), and CAFAS was conducted. Figure 3-10 showed that  $\text{Ca}^{2+}$  did not affect the binding of HSPG with bFGF either at physiological concentration (25mM) or at higher concentration. Our results indicate that PG binding to bFGF does not be affected by divalent cations just as heparin binding does not (Kan, et. al., 1996).

*Effect of HS and CS on retention of  $^{125}\text{I}$ -bFGF alone and on binding retention of  $^{125}\text{I}$ -bFGF with PG in Bio-Dot* - PG is composed primarily of HS, and bFGF binds to many HSPG (Bikfalvi, et al., 1997). We wanted to determine if exogenous HS (Sigma) or CS (Sigma) would affect the binding reaction. Firstly we investigated the effect of 40ng HS or 40ng CS on retention of  $^{125}\text{I}$ -bFGF alone at 0.1ng, 0.15ng, 0.2ng and 0.25ng in Bio-Dot. Figure 3-11 (a) demonstrated that, compared with the retention of  $^{125}\text{I}$ -bFGF alone without adding any HS or CS, 40ng HS had no effect on  $^{125}\text{I}$ -bFGF retention on the Bio-Dot, while 40ng CS decreased the retention about 4%. CS reduces the non-specific background binding of  $^{125}\text{I}$ -bFGF. The result indicated that, on zeta-probe membrane, neither HS nor CS would bind, both being pulled though with three washes. Therefore, the effect of HS and CS on binding retention of  $^{125}\text{I}$ -bFGF and PG could be studied using our



CAFAS. 40ng PG and 0.1ng, 0.15ng, 0.2ng or 0.25ng  $^{125}\text{I}$ -bFGF were incubated in separate vials with or without 40ng HS or 40ng CS for 1 hr. Then all liquid in each vial was pulled through the respective well and followed by 3 washes. Figure 3-11 (b) shows that 40ng CS had no effect on the binding retention of 40ng PG with 0.1~0.25ng  $^{125}\text{I}$ -bFGF, 40ng HS had no effect on the binding retention of 40ng PG with 0.15~0.25ng  $^{125}\text{I}$ -bFGF, but decreased the binding retention of 40ng PG with 0.1ng  $^{125}\text{I}$ -bFGF. When  $^{125}\text{I}$ -bFGF was at 0.1ng, 40ng HS competed with 40ng PG for binding with  $^{125}\text{I}$ -bFGF. Our studies indicate that PG has 0.2 binding sites/molecule. 40ng PG has total  $9 \times 10^9$  binding sites, and 0.1ng  $^{125}\text{I}$ -bFGF corresponds to  $3 \times 10^9$  molecules. According to our monovalent binding reaction model, 0.1ng  $^{125}\text{I}$ -bFGF is not enough to saturate the total binding sites of PG, and when exogenous HS is added, the competitive effect dominates. The effect of competition was not apparent, however, when greater than 0.1ng  $^{125}\text{I}$ -bFGF was used. Therefore, 0.1ng  $^{125}\text{I}$ -bFGF and 40ng PG were used to determine the effect of different amount of HS or CS on the binding retention of  $^{125}\text{I}$ -bFGF and PG in Bio-Dot. From Figure 3-12 (a), we see that HS has no effect on retention of 0.1ng  $^{125}\text{I}$ -bFGF alone up to 200ng, while the addition of HS decreased the binding retention of 0.1ng  $^{125}\text{I}$ -bFGF and 40ng PG from 32% without HS to 20% with 120ng HS present. Exogenous HS competed with the PG for binding to  $^{125}\text{I}$ -bFGF ( $P < 0.001$ ). The addition of CS up to 200ng had no effect on retention of 0.1ng  $^{125}\text{I}$ -bFGF alone, and 40ng ~ 120ng of exogenous CS seemed to facilitate the binding of 0.1ng  $^{125}\text{I}$ -bFGF with 40ng PG by slightly increasing their binding retention (Figure 3-12 (b)) ( $P < 0.005$ ). This may mean that CS functions as a stabilizing agent for HSPG and helps it bind to  $^{125}\text{I}$ -bFGF.

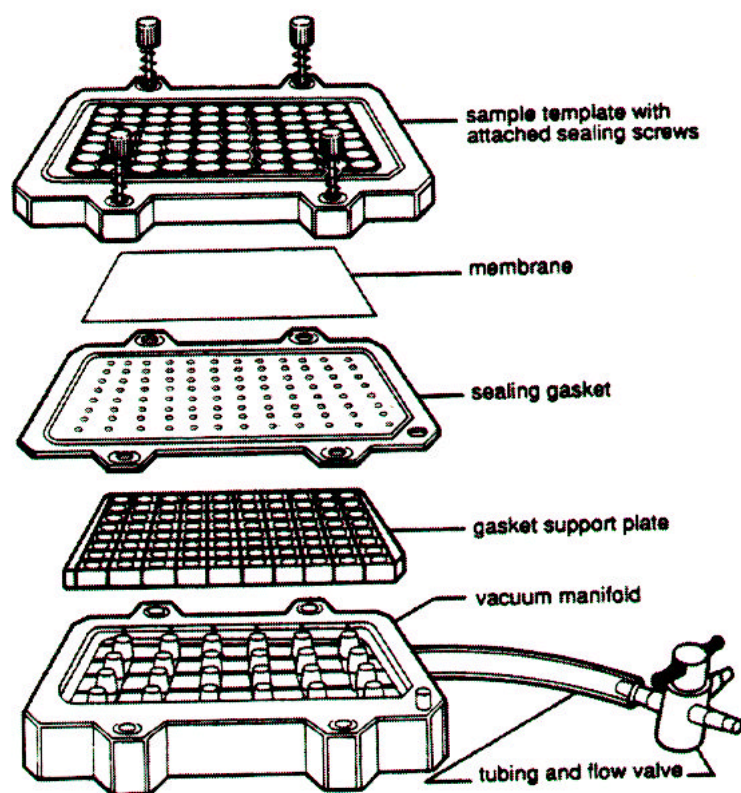


**Figure 3-1 Diagram of the assembly of the Bio-Dot apparatus**  
(Bio-Dot Apparatus Instruction Manual, Bio-Rad, Hercules, CA)

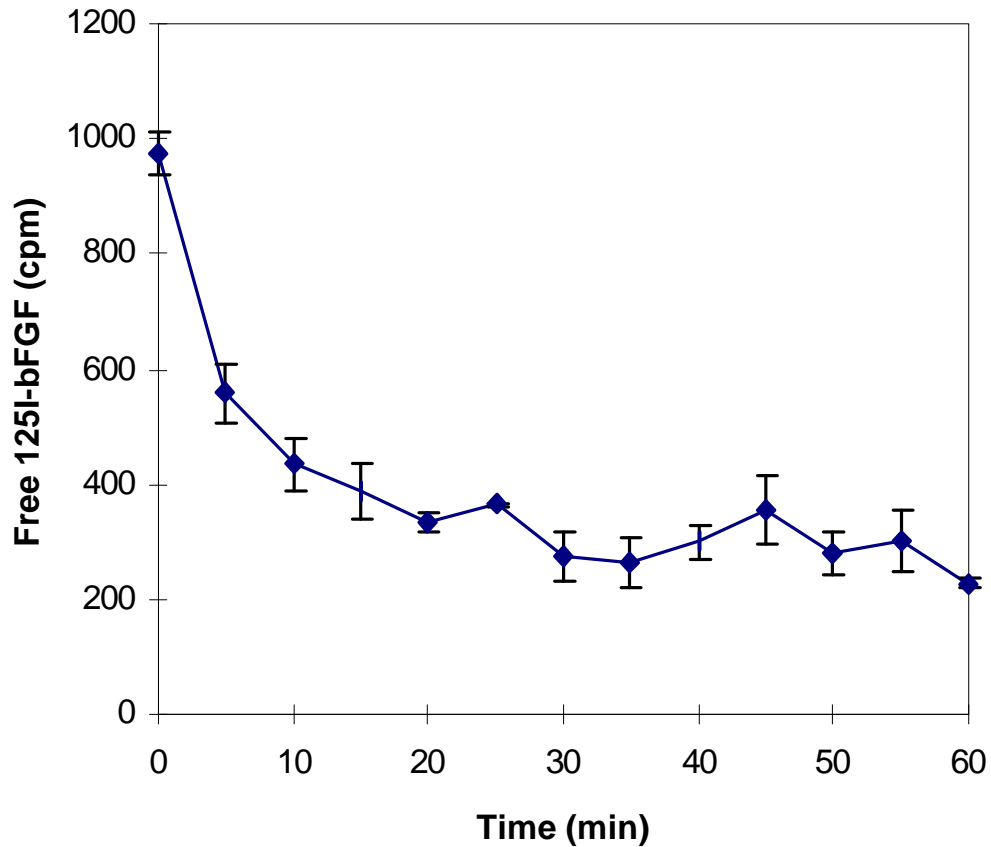


**Figure 3-2 Transient study of <sup>125</sup>I-bFGF with 1mg/ml BSA+0.15MTBS buffer in Bio-Dot**

1800cpm <sup>125</sup>I-bFGF was incubated with 200  $\mu$ l 1mg/ml BSA+0.15M TBS buffer in each well of Bio-Dot. Liquid was aspirated at different time as indicated and counted for cpm as free <sup>125</sup>I-bFGF in the solution. All data was averaged from triple cases, and the error bars showed the standard error of triplicate measurements.

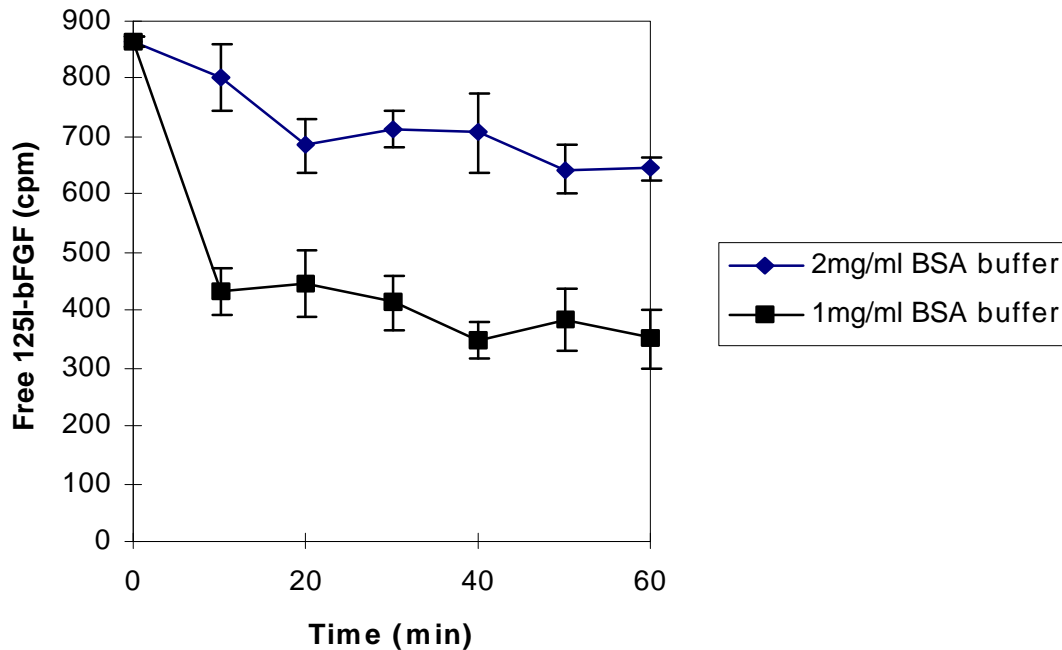
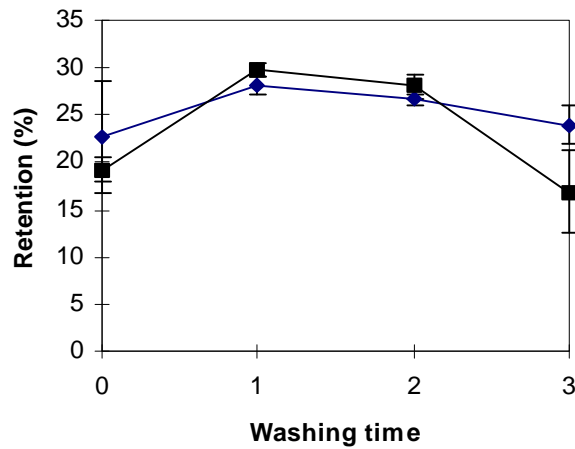


**Figure 3-3 Effect of BSA concentration on transient study of <sup>125</sup>I-bFGF behavior in Bio-Dot**

1800cpm <sup>125</sup>I-bFGF was incubated with 200  $\mu$ l 1mg/ml BSA+0.15M TBS buffer or 2mg/ml BSA+0.15M TBS buffer in each well of Bio-Dot. Liquid was aspirated at different time as indicated and counted for cpm as free <sup>125</sup>I-bFGF in the solution. All data was averaged from triple cases, and the error bars showed the standard error of triplicate measurements.

(a)  $^{125}\text{I}$ -bFGF



(b)  $^{35}\text{S}$ -PG

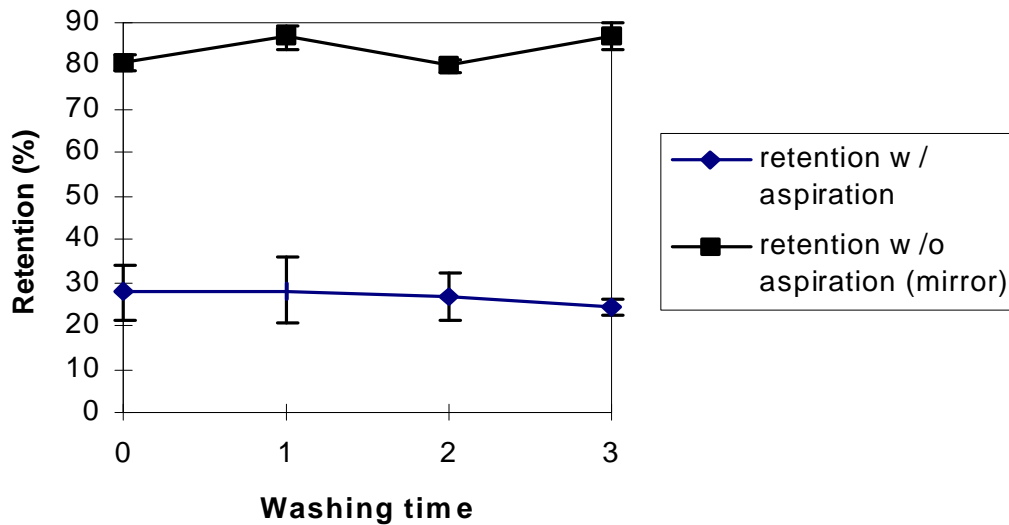


**Figure 3-4 Study of washing effect on  $^{125}\text{I}$ -bFGF and  $^{35}\text{S}$ -PG behavior in Bio-Dot**  
(a) 1800cpm  $^{125}\text{I}$ -bFGF or (b) 400cpm  $^{35}\text{S}$ -PG was incubated with 200  $\mu\text{l}$  2mg/ml BSA+0.15M TBS buffer in each well of Bio-Dot for 1 hr. All liquid in each well was pulled through the zeta-probe membrane without wash or with 1 wash, 2 washes or 3 washes of 2mg/ml BSA+0.15M TBS buffer. Each dot on the membrane was cut off and counted in a scintillation counter. All data was averaged from triple cases, and the error bars showed the standard error of triplicate measurements.

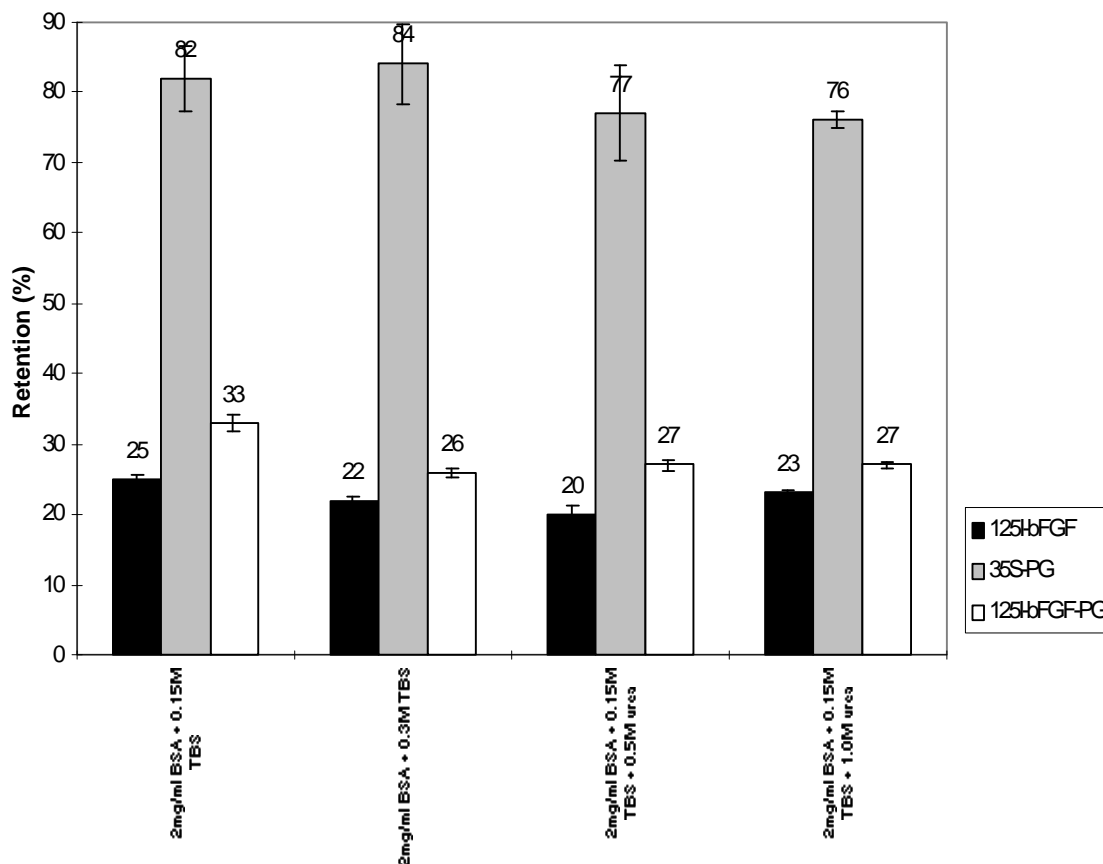
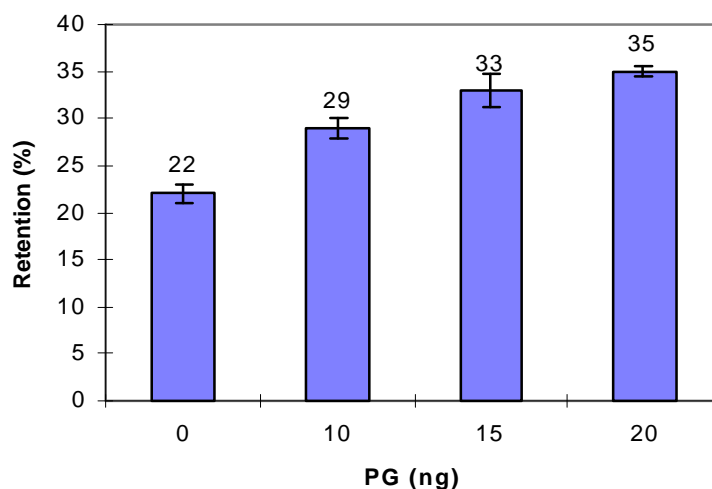


**Figure 3-5 Effect of different washing buffers on retention of <sup>125</sup>I-bFGF, <sup>35</sup>S-PG, and <sup>125</sup>I-bFGF-PG in Bio-Dot**

0.25ng <sup>125</sup>I-bFGF, 10ng <sup>35</sup>S-PG, or 0.25ng <sup>125</sup>I-bFGF + 10ng PG was incubated with 2mg/ml BSA+0.15M TBS buffer totaling 200 µl in each well of Bio-Dot for 1 hr. All liquid in each well was pulled through the zeta-probe membrane with 3 washes of 2mg/ml BSA+0.15M TBS buffer, 2mg/ml BSA+0.3M TBS buffer, 2mg/ml BSA+0.15M TBS+0.5M urea buffer or 2mg/ml BSA+0.15M TBS+1.0M urea buffer. Each dot on the membrane was cut off and counted in a scintillation counter. All data was averaged from triple cases, and the error bars showed the standard error of triplicate measurements.

**(a) Binding of  $^{125}\text{I}$ -bFGF with PG bound on the membrane**



**(b) Binding of  $^{125}\text{I}$ -bFGF and PG**

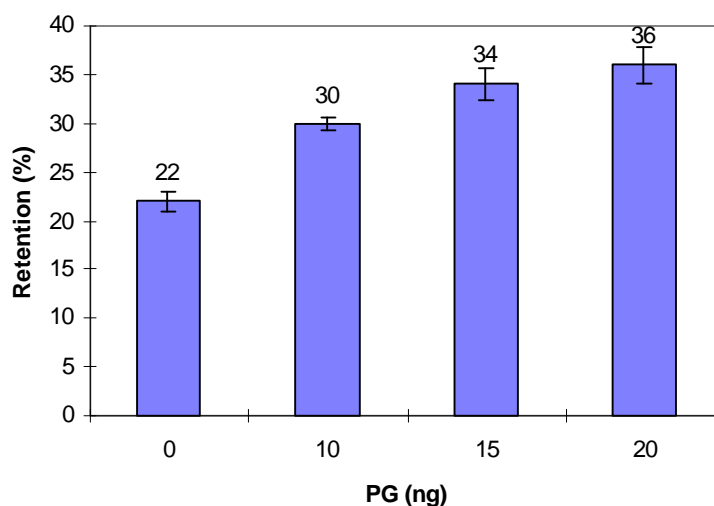


**Figure 3-6 Binding retention of  $^{125}\text{I}$ -bFGF with PG in Bio-Dot**

(a) 0ng, 10ng, 15ng, or 20ng PG was incubated with 2mg/ml BSA+0.15M TBS buffer totaling 200  $\mu\text{l}$  in each well of Bio-Dot for 1 hr, then all liquid in each well was aspirated. Then 0.25ng  $^{125}\text{I}$ -bFGF with 2mg/ml BSA+0.15M TBS buffer totaling 200  $\mu\text{l}$  was added in each well. Incubated for 1 hr. (b) 0.25ng  $^{125}\text{I}$ -bFGF and 0ng, 10ng, 15ng, or 20ng PG were incubated with 2mg/ml BSA+0.15M TBS buffer totaling 200  $\mu\text{l}$  in each well of Bio-Dot for 1 hr. All liquid in each well was pulled through the zeta-probe membrane with 3 washes of 2mg/ml BSA+0.15M TBS buffer. Each dot on the membrane was cut off and counted in a scintillation counter. All data was averaged from triple cases, and the error bars showed the standard error of triplicate measurements.

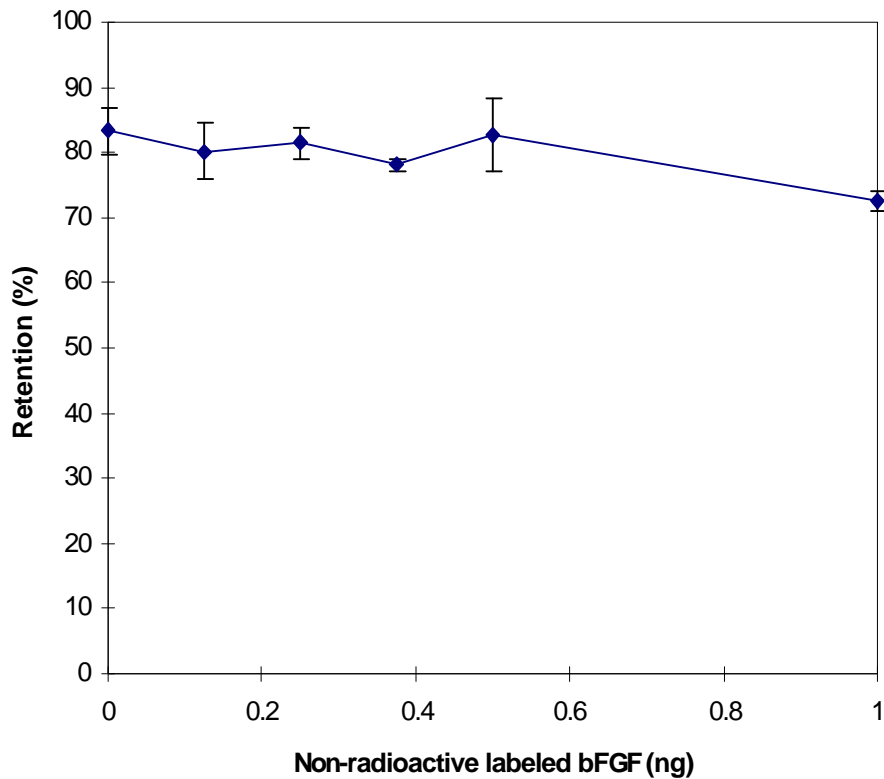


**Figure 3-7 Effect of non-labeled bFGF on <sup>35</sup>S-PG retention in Bio-Dot**

0ng, 0.125ng, 0.25ng, 0.375ng, 0.5ng or 1.0ng non-radioactive labeled bFGF and 10ng <sup>35</sup>S-PG were incubated in separate 0.6ml eppendorf vials with 2mg/ml BSA+0.15M TBS buffer totaling 200 µl for 1 hr. All liquid in each vial was aspirated out and pulled through the zeta-probe membrane with 3 washes of 2mg/ml BSA+0.15M TBS buffer. Each dot on the membrane was cut off and counted in a scintillation counter. All data was averaged from triple cases, and the error bars showed the standard error of triplicate measurements.



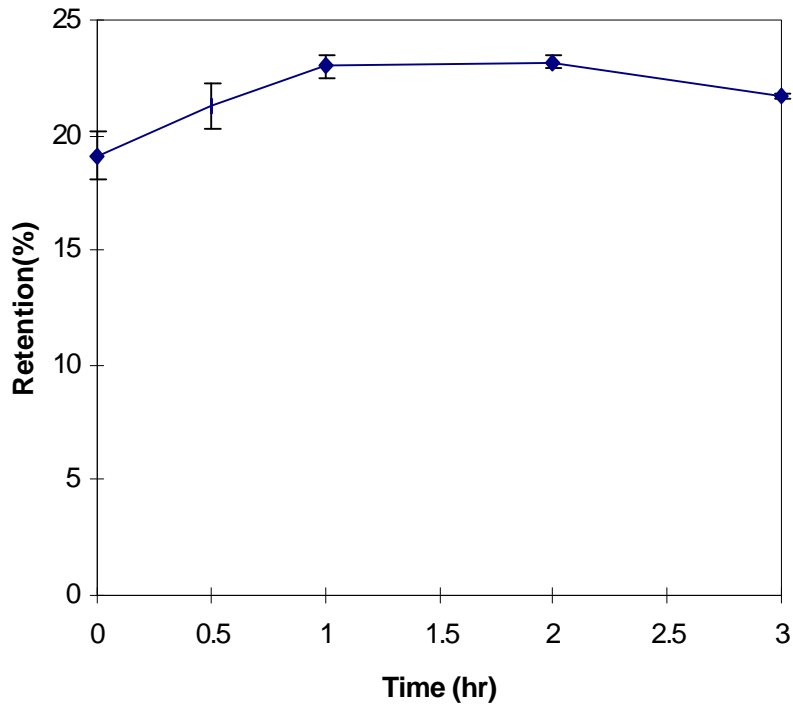
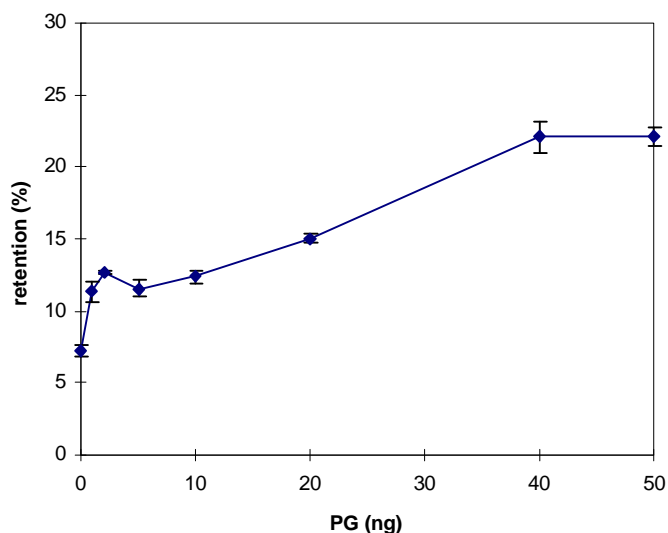


**Figure 3-8 Transient study of binding of  $^{125}\text{I}$ -bFGF with PG in Bio-Dot**

0.25ng  $^{125}\text{I}$ -bFGF and 40ng PG were incubated in separate 0.6ml eppendorf vials with 2mg/ml BSA+0.15M TBS buffer totaling 200  $\mu\text{l}$ . After certain time indicated above, all liquid in vials was aspirated out and pulled through the zeta-probe membrane with 3 washes of 2mg/ml BSA+0.15M TBS buffer. Each dot on the membrane was cut off and counted in a scintillation counter. All data was averaged from triple cases, and the error bars showed the standard error of triplicate measurements.

(a) 0.25ng 125I-bFGF



(b) 0.25ng 125I-bFGF and 0.5ng 125I-bFGF

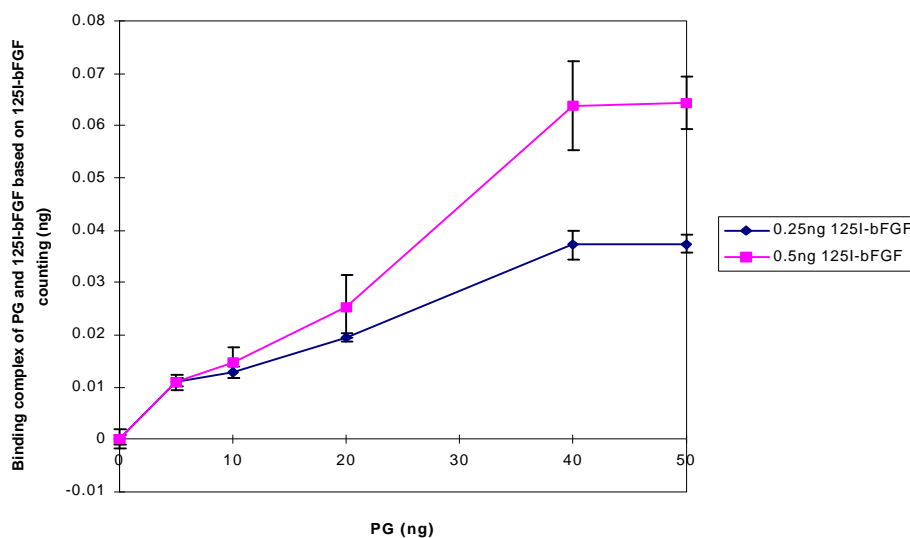


**Figure 3-9 Effect of PG on <sup>125</sup>I-bFGF retention in Bio-Dot**

(a) 0.25ng <sup>125</sup>I-bFGF or (b) 0.25ng <sup>125</sup>I-bFGF or 0.5ng <sup>125</sup>I-bFGF and different amount of PG as indicated were incubated in separate 0.6ml eppendorf vials with 2mg/ml BSA+0.15M TBS buffer totaling 200  $\mu$ l for 1 hr. All liquid in each vial was aspirated out and pulled through the zeta-probe membrane with 3 washes of 2mg/ml BSA+0.15M TBS buffer. Each dot on the membrane was cut off and counted in a scintillation counter. All data was averaged from triple cases, and the error bars showed the standard error of triplicate measurements.

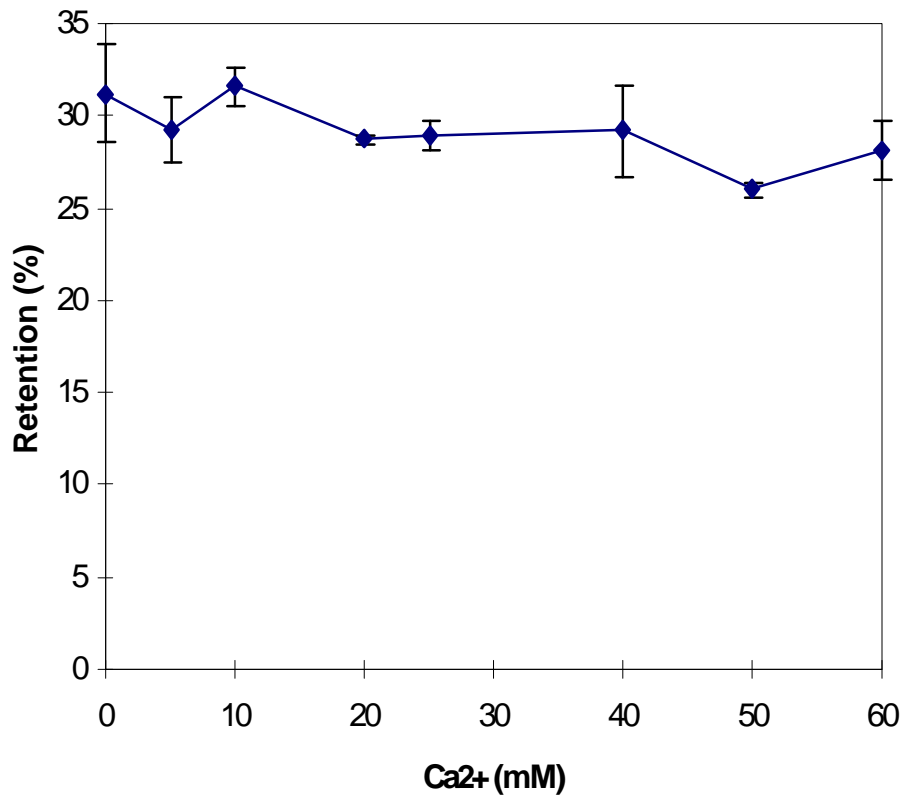
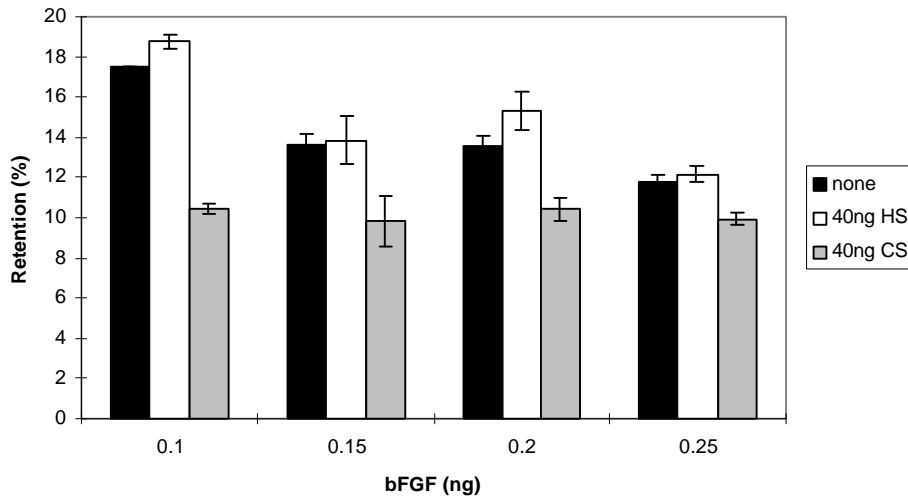


**Figure 3-10 Effect of Ca<sup>2+</sup> on binding retention of PG with <sup>125</sup>I-bFGF in Bio-Dot**

0.25ng <sup>125</sup>I-bFGF and 40ng PG along with different concentration of Ca<sup>2+</sup> as indicated were incubated in separate 0.6ml eppendorf vials with 2mg/ml BSA+0.15M TBS buffer totaling 200 µl for 1 hr. All liquid in each vial was aspirated out and pulled through the zeta-probe membrane with 3 washes of 2mg/ml BSA+0.15M TBS buffer. Each dot on the membrane was cut off and counted as cpm in scintillation counter. All data was averaged from triple cases, and the error bars showed the standard error of triplicate measurements.

**(a) Effect of 40ng HS or 40ng CS on retention of  $^{125}\text{I}$ -bFGF on Bio-Dot**



**(b) Effect of 40ng HS or 40ng CS on binding retention of 40ng PG with  $^{125}\text{I}$ -bFGF on Bio-Dot**

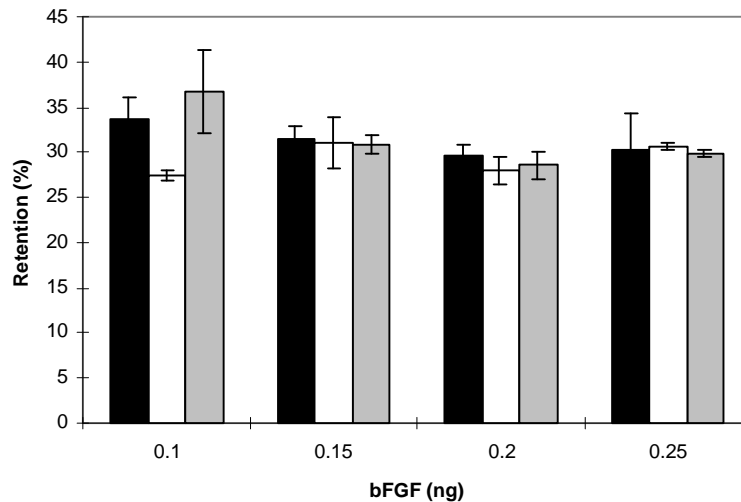
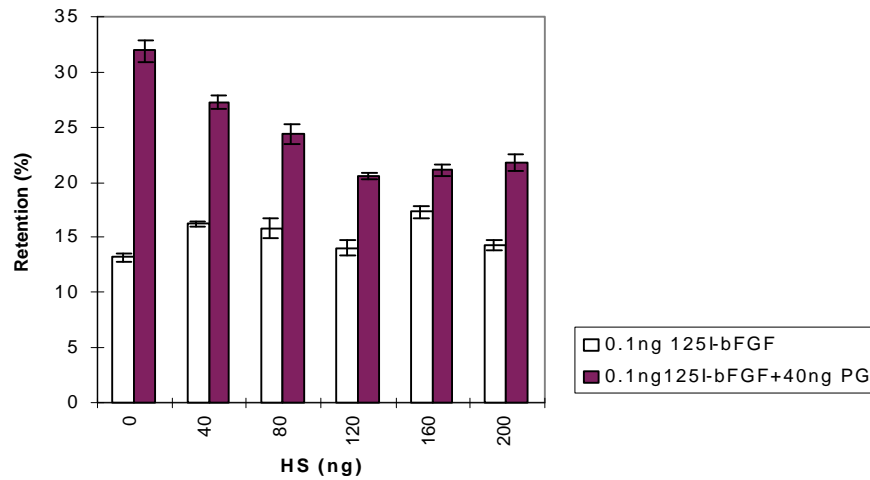


**Figure 3-11 Effect of HS and CS on retention of  $^{125}\text{I}$ -bFGF alone and on binding retention of  $^{125}\text{I}$ -bFGF with PG**

(a) 0.1ng, 0.15ng, 0.2ng or 0.25ng  $^{125}\text{I}$ -bFGF or (b) 0.1ng, 0.15ng, 0.2ng or 0.25ng  $^{125}\text{I}$ -bFGF and 40ng PG, along with 40ng HS or 40ng CS, were incubated in separate 0.6ml eppendorf vials with 2mg/ml BSA+0.15M TBS buffer totaling 200  $\mu\text{l}$  for 1 hr. All liquid in each vial was aspirated out and pulled through the zeta-probe membrane with 3 washes of 2mg/ml BSA+0.15M TBS buffer. Each dot on the membrane was cut off and counted as cpm in scintillation counter. All data was averaged from triple cases, and the error bars showed the standard error of triplicate measurements.

**(a) Effect of HS on retention of 0.1ng  $^{125}$ I-bFGF alone and of 0.1ng  $^{125}$ I-bFGF binding with 40ng PG**



**(b) Effect of CS on retention of 0.1ng  $^{125}$ I-bFGF alone and of 0.1ng  $^{125}$ I-bFGF binding with 40ng PG**

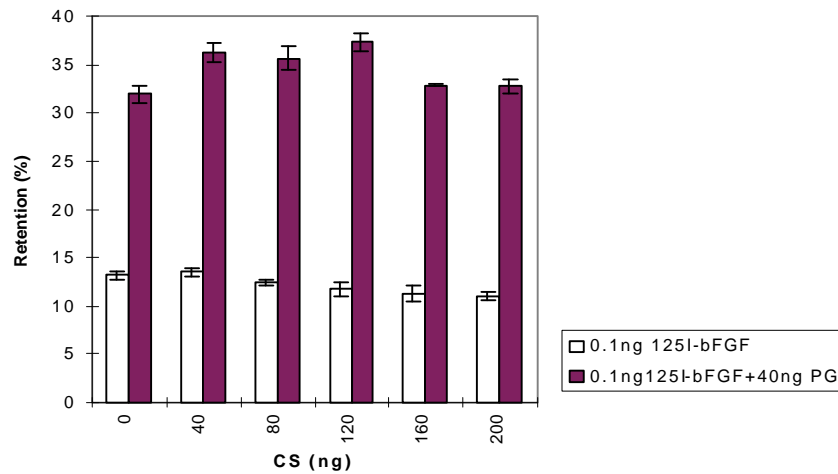


**Figure 3-12 Effect of HS and CS on retention of 0.1ng  $^{125}$ I-bFGF alone and on binding retention of 0.1ng  $^{125}$ I-bFGF with 40ng PG**

(a) 0.1ng  $^{125}$ I-bFGF or (b) 0.1ng  $^{125}$ I-bFGF and 40ng PG, along with different amount of HS or CS as indicated, were incubated in separate 0.6ml eppendorf vials with 2mg/ml BSA+0.15M TBS buffer totaling 200  $\mu$ l for 1 hr. All liquid in each vial was aspirated out and pulled through the zeta-probe membrane with 3 washes of 2mg/ml BSA+0.15M TBS buffer. Each dot on the membrane was cut off and counted as cpm in scintillation counter. All data was averaged from triple cases, and the error bars showed the standard error of triplicate measurements. HS inhibits the binding of PG and  $^{125}$ I-bFGF ( $P < 0.001$ ), while CS seems to facilitate the binding ( $P < 0.005$ ).

## Chapter IV

### Discussion , Conclusions and Future Work

#### 4.1 Discussion

Most growth factors do not simply diffuse passively from the site of their release in order to interact with the nearest cell surface receptor. Rather, many of these proteins contain structural features that foster their interaction with other molecules within the extracellular environment. These interactions confine the action of the growth factor to an appropriate place and time. Thus, the specificity of growth factor signaling is derived not only from its binding to cell surface receptors but also through critical interactions with other components of the extracellular environment (Flaumenhaft and Rifkin, 1992). PG from BAE cells conditioned media is a major component of the extracellular environment of BAE cells. Understanding the structural characteristics of the molecules will be of great assistance if we want to understand the full biological significance.

##### 4.1-1 Purification and characterization of BAE P9 PG

By ion exchange chromatography (Q-Sepharose column) with linear salt gradient, we obtained, from the BAE P9 cells conditioned media, two proteoglycan peaks which eluted at 0.85 M salt and 1.0 M salt respectively. Each fraction was pooled (PG-I and PG-II), the two peaks were dialyzed against 0.15M TBS using Spectra/Por cellulose membrane (MWCO of 1,000) for desalting, and then concentrated by lyophilization. Post concentrating, the final salt concentration of PG-I and PG-II was ~ 0.6 M. Because high salt concentration (> 0.15M) inhibited both Hep I / Hep III digestion and C.ABC digestion, the dialysis step was altered to be against deionized water using Spectra/Por cellulose membrane (MWCO of 10,000), and then concentrated by lyophilization. The resulting final salt concentration of PG-I and PG-II was less than 0.15 M. SDS-PAGE with silver staining of PG-I and PG-II showed that the smear bands which appeared on the top of gel without enzyme digestion was less dense than the lower band. In addition, the

appearance of the core protein bands of PG-I and PG-II did not change with or without enzyme treatment on Western blotting. If there were long GAG chains attached to the core proteins or sufficient amount of the primary active material, a dense smear band should have appeared on the top of the gel or the blotting membrane without enzyme digestion, since large GAG chains tend to be hydrated and prevent the migration of core proteins on the gel. We suspect that PGs with long GAG chains are lost during the purification procedures. In addition, the cationic filtration assay (CAFAS) with PG-I or PG-II and <sup>125</sup>I-bFGF showed that the addition of PG-I and PG-II up to 90 ng did not result in an increase in the retention of <sup>125</sup>I-bFGF on the zeta-probe membrane (Figure 4-1). This indicates that PG-I and PG-II have little biological activity with regard to <sup>125</sup>I-bFGF binding. It has been shown that proteoglycans with five disaccharide units (degree of polymerization (dp) = 10) or less in size are unable to bind and activate bFGF (Walker, et al., 1993). The CAFAS results of PG-I and PG-II may be due to a lack of GAG chains of sufficient length or the loss of the active material. Furthermore, the negative values obtained with the DMB assay after enzyme digestion of PG-I and PG-II also indicate that there is not enough GAG chains in our purified samples. There are several reasons which may account for these results.

We have noticed that exposure time in developing solution for silver staining is very critical for detecting bands. Longer exposure time made more bands appear but the initial dense bands would fade. The less dense band which appeared on the top of gel without enzyme digestion might be due to the inappropriate length of exposure time. On the other hand, the purification procedure probably accounts for loss of major active materials. First, as to the further separation step with a linear salt gradient, many have reported using a DEAE-Sephacel or DEAE-Sepharose column, a weak anion exchanger, instead of Q-Sepharose column, a strong anion exchanger for purification of PG by ion-exchange chromatography with linear salt gradient (Kinsella, M.G. and Wight, T.N., 1988, Benitz, et al., 1990 and Bonneh-Barkay, et al., 1997). Two fractions of PG, PG-I and PG-II, may exist as random polymer coils held together by weak force, such as van der Waals packing, by which they could be separated depending on the charge difference. Once

separated on the strong ion exchange column, the whole conformation of PG may change. The more negative charged chain, usually longer chains, may be exposed and then stick to the column without being eluted, as we noticed that the efficiency of Q-Sepharose column for the separation was as low as 30%. In addition, during dialysis and lyophilizing, absorption to the dialysis tubing or lyophilizing vials is possible. Second, the samples later used for enzyme digestion were dialyzed against deionized water, and ended up with a very low salt concentration. This might deteriorate the stability of PG-I and PG-II, and make loss of material more likely.

#### 4.1-2 Comparison of experimental data with model data

The comparison of experimental data with data calculated from the model is helpful for gaining understanding regarding the binding between bFGF and PG. In Chapter III, we set up a simple model along with several assumptions, and obtained the equation

$$(4) \quad \frac{dC}{dt} = k_f[R_T - C]L - k_rC .$$

Because  $L = L_0 - C$ , and at steady state,  $\frac{dC}{dt} = 0$ , equation (4) becomes

$$(13) \quad k_f(R_T - C)(L_0 - C) = k_rC .$$

Rearranging equation (13) using  $K_D = k_r / k_f$ , we get

$$(14) \quad L_0R_T - (R_T + L_0 + K_D)C + C^2 = 0$$

Because we already obtained from Appendix A

$$K_D = (1.6 \pm 0.8) \times 10^{-10} \text{ M}$$

$$R_T = (1.3 \pm 0.6) \times 10^8 \text{ \# / ng PG,}$$

the equation (14) serves as a model equation for calculating binding complex ( C ) from the initially added  $^{125}\text{I}$ -bFGF ( $L_0$ ). A cell free binding assay in Bio-Dot of  $^{125}\text{I}$ -bFGF (0.1ng, 0.2ng, 0.5ng, 0.8ng, 1.0ng, 1.5ng) with 10ng PG was conducted by our protocol set up in Chapter III. The results, as well as the binding complex ( C ) obtained from the model equation, were compared in Table 8 and Figure 4-2. Model data showed an approaching saturation trend, while the experimental data indicated an increase (Figure 4-



2). They are not compatible. The basic assumption for the model is that the binding between bFGF and PG is monovalent, i.e. one binding site on PG can only bind one bFGF molecule. When we compared the total binding sites of 10 ng PG and the number of  $^{125}\text{I}$ -bFGF molecules initially added, it was shown that at 0.1ng  $^{125}\text{I}$ -bFGF, the number of bFGF molecules was similar as the total binding sites provided by 10 ng PG. The ratio satisfied our assumption, and experiment results matched with the model data (Table 8 and Figure 4-2). Above 0.2ng  $^{125}\text{I}$ -bFGF, the number of  $^{125}\text{I}$ -bFGF molecules was much greater than the total binding sites of 10ng PG, i.e.  $^{125}\text{I}$ -bFGF was in excess. According to our monovalent model, the binding complex would reach a saturation with increasing  $L_0$  given certain number of binding sites. In fact, more than one bFGF molecule probably binds in each binding site when it is excessive in the system. It has been reported that bFGF preferentially self-associates, which could lead to the formation of bFGF dimers or oligomers from the examination of bFGF crystal structures (Venkataraman, et al., 1995 and Arakawa, et al., 1994). We postulate that this is the reason why our experimental data has an increasing trend without reaching a saturation up to  $L_0 = 1.5\text{ng}$  and does not fit our model when  $L_0 \geq 0.2\text{ng}$ . To confirm our hypothesis, we further compared experimental data and model data of binding between 40ng PG and  $^{125}\text{I}$ -bFGF (0.1 ~ 0.25ng) and between 80ng PG and  $^{125}\text{I}$ -bFGF (0.1 ~ 1.5ng). In the first case, PG provided more binding sites than the number of bFGF molecules available. The experimental data fit with the model (Table 9 and Figure 4-3). In the second case (Table 10 and Figure 4-4), the experimental data curve has the same trend as model curve when  $L_0 < 0.8\text{ng}$ , i.e. the binding sites provided by PG has similar number as the bFGF molecules added; and when  $L_0 \geq 0.8\text{ng}$ , the binding sites provided by PG exceeds the number of bFGF molecules, and our model is not satisfied. The experimental data curve increases instead of following the model curve, and there probably are more than one bFGF molecule in each binding site. Therefore, we proposed that the ratio of binding site number and bFGF molecule might determine if the binding is a simple monovalent reaction. We define a ratio  $R = (\text{Binding site provided by PG}) / (\text{Number of bFGF molecule})$ . When  $R \geq 1$ , the monovalent model is satisfied; and when  $R < 1$ , the model is not satisfied.

#### 4.1-3 Proposed model for BAE P9 PG

In our present study, we find that the PG has an average molecular weight of  $5 \times 10^5$  Da from size exclusion chromatography (Sephacrose CL-2B column), and the core protein is  $\sim 3 \times 10^5$  Da from SDS-PAGE with silver staining and appears to be perlecan by Western blotting. GAG chains of PG were eluted as a single peak with estimated MW of  $< 2 \times 10^5$  Da from Sepharose CL-6B column (Figure 2-9), and were mainly composed of HS. Two parameters were also calculated from the monovalent model with experimental data:  $K_D = (1.6 \pm 0.8) \times 10^{-10}$  M and  $R_T = 0.1 \sim 0.2$  (# of site)/(molecule of PG). Therefore, we propose that BAE P9 PG is a large molecule with a large core protein (perlecan) and a long HS GAG chain, and that only a cluster of PG molecules can form a dynamic binding site for bFGF with a very high affinity.

HSPG on the cell surface and in the extracellular matrix have been shown to be binding sites for bFGF (Moscatelli, 1988 and Bashkin et al., 1989). By using the isothermal titrating calorimetry for obtaining  $K_a$ , and the calculation of Gibbs free energy change upon binding of heparin with bFGF ( $\Delta G^\circ = -RT \ln K_a$ ), it has been reported that pure electrostatic interactions contribute only 30% of the binding free energy as analyzed by polyelectrolyte theory (Thompson, et al., 1994). More specific nonionic interactions, such as hydrogen bonding and van der Waals packing, contribute the majority of the free energy of this binding reaction (Thompson, et al., 1994). It is expected that due to similarities between heparin and HSPG, the interaction of bFGF and HSPG is dynamic, i.e. the binding reversible. We may view PGs moving around in an extracellular matrix which forms a “net” for “holding” bFGF. Once a binding site is formed by a cluster of PGs, the binding site has a high affinity. bFGF will rapidly associate and dissociate but still hang onto the PG net. Individual PG can also bind with bFGF but with low affinity. bFGF binds with individual PG, then dissociates readily or even diffuses. When bFGF molecules are in excess, there may be more than one bFGF as dimer or oligomer binding within a binding site. Since the PG net is composed of HS and the binding interaction is dynamic, the

exogenous addition of HS should compete with HSPG for the binding with bFGF, which agrees with our HS addition results from the CAFAS.

After  $\beta$ -elimination, small GAG chains may aggregate or pack together and appear as a relatively big molecule (single peak) in the elution from Sepharose CL-6B column. Another possible model for PG is that PG has many small GAG chains instead of a single long chain. The inadequate length of the small chains may not support bFGF binding to individual PG molecule, so at least 5 molecules of PG are required to form a binding site. To investigate if the second model is true, we might use high concentration of urea with 0.15M TBS buffer for eluting GAG chains from Sepharose CL-6B column after  $\beta$ -elimination to see if there is any change in the profile. If we verified that PG had only small GAG chains, then another question must be posed: does PG originally have only small or moderate size of GAG chains or exist with many much longer GAG chains in the BAE cells conditioned media before purification? (i.e. Does our purification step just catch one part of PG originally secreted by BAE cells and lose PG with longer GAG chains?) Proteoglycans secreted into extracellular matrix can have short, moderate or long GAG chains depending on the cell type and their environments. PG from BAE cells conditioned media may indeed exist without long GAG chains, although it is doubtful (Forsten et al., 1997). We must investigate whether our purification process selects certain PGs. In addition, we want to point out here that our assumption that PG has homogeneous binding sites with a uniform molecule size is used in our calculation of  $R_T$  and may be incorrect. Since PG has a broad range of size distribution (Figure 2-6). However, the assumption gives us a simple model for estimating parameters. The sensitivity of our experimental methods does currently not warrant a more complex model.

#### 4.1- 4 Effects of CS and $Ca^{2+}$

Our data indicate that CS may have a role in assisting with the activity of HSPG. Firstly, in the CAFAS, the addition of CS up to 200ng had no effect on retention of 0.1ng  $^{125}I$ -bFGF alone, but 40ng ~ 120ng of exogenous CS seemed to facilitate the binding of 0.1ng  $^{125}I$ -

bFGF with 40ng PG by slightly increasing their binding retention ( $P < 0.005$ ) (Figure 3-12 (b)). This implies that CS may function to help in the binding activity of HSPG with  $^{125}\text{I}$ -bFGF. Secondly, the addition of CS served as a stabilizing agent before the lyophilizing and helped to eliminate the loss of proteoglycan during the lyophilizing, so that PGs were detected in SDS-PAGE gel with silver staining. From the structural viewpoint of BAE P9 PG, ~ 30% of GAG chains are CS and are the secondary GAG, besides the major component of HS. The small amount of CS of PG is probably very important for the biological functions of HS, though we have not yet explored the mechanism for such an effect.

In addition, we examined the effect of  $\text{Ca}^{2+}$  addition. The CAFAS showed that  $\text{Ca}^{2+}$  had no effect on binding of HSPG with bFGF either at physiological concentration or the higher concentration. It has been reported that divalent cations, such as  $\text{Ca}^{2+}$  and  $\text{Mg}^{2+}$ , are required for the high affinity interaction of heparin with FGF receptors at physiological concentrations (Kan, et al., 1996). This indicates that PG may bind bFGF in a different manner than FGFR. The presence of  $\text{Ca}^{2+}$  inside of the cell environment deserves our attention during future cell-based experiments.

#### 4.1- 5 Comparison of BAE P9 PG with similar molecules

The goal of using the mathematical model is to characterize the binding so that we may compare BAE P9 PG with other similar molecules.

*Comparison of BAE P9 PG with heparin* - Heparin is a very clinically useful agent. The application of heparin as an inhibitor for restenosis after angioplasty or bypass surgery for treating coronary disease has been attempted. It is similar in size to HS, but with a higher degree of sulfation than HS (Jorpes and Gardell, 1948). The equilibrium dissociation constant  $K_D$  for heparin is  $10^{-8} \sim 10^{-9}$  M (Arakawa, et al., 1994 and Ornitz, et al., 1995), which is larger than the  $K_D$  for BAE P9 PG, indicating that the PG has a higher affinity for binding with bFGF than heparin. This is likely due to the fact that PG is a large molecule

and has longer HS chains for binding bFGF, or a cluster of PG molecules stabilize the binding site, or CS in the GAG chain composition of PG aids for binding. It has been reported that low-molecular-weight heparin ( $M_r = \sim 5000$ ) binds an average 2.2 bFGF per molecule and high-molecular-weight heparin ( $M_r = 15,000$ ) binds an average 6.3 bFGF per molecule using size exclusion chromatography with on-line light scattering, absorbance and refractive index detection (Arakawa, et al., 1994). It is proposed that bFGF tends to be self-associated to form bFGF cascade, and heparin helps to stabilize the bFGF dimer and oligomer forms. This may also play a role in PG binding.

*Comparison of BAE P9 PG with HSPG on the cell surface and cell surface receptor (CSR) -* The association and dissociation kinetics of bFGF with cell surface receptor (CSR) and HSPG sites on Balb/c3T3 cells, Balb/c3T3 cells digested with heparinase to remove the heparin-like bFGF binding component, and with detergent-extracted HSPG without CSR had been measured. And it was found that the difference in  $K_D$  for the two affinity classes of bFGF binding, high affinity with CSR and low affinity with HSPG, resulted primarily from a difference in  $k_r$  and not  $k_f$  (Nugent and Edelman, 1992). bFGF binding seems to be controlled by HSPG as a result of stabilization of the bFGF-CSR complex, producing a “high-affinity” interaction. Based on a simple model and several assumptions, we calculated the equilibrium dissociation constant ( $K_D$ ), the association rate constant ( $k_f$ ) and the dissociation rate constant ( $k_r$ ) for BAE P9 PG with bFGF by least squares analysis (Appendix A and B). These compare with results from Nugent and Edelman as following:

	HSPG <sup>a</sup>	BAE P9 PG	CSR <sup>a</sup>
$K_D$ (M)	$7.5 \times 10^{-10}$	$1.6 \times 10^{-10}$	$1.3 \times 10^{-11}$
$k_f$ ( $M^{-1} \text{ min}^{-1}$ )	$9 \times 10^7$	$6.2 \times 10^7$	$2.27 \times 10^8$
$k_r$ ( $\text{min}^{-1}$ )	0.068	0.01	0.003

a.  $k_f$  and  $k_r$  for HSPG and CSR were measured on intact cells.

Parameters for BAE P9 PG are intermediate between the cell surface HSPG and the cell surface receptor. In terms of  $K_D$ , the PG can compete with HSPG on the cell surface for

binding with bFGF but would not likely compete with CSR, which has higher affinity, on equal molar basis. Higher  $k_f$  indicates the association of bFGF is much quicker, while a lower  $k_f$  indicates the dissociation of bFGF will be slower. The PG, located in extracellular matrix, was purified from BAE cells conditioned media, while HSPG is on the intact Balb/c3T3 cell surface. The structural variability of PG molecules in different tissues, species, states of cellular differentiation and cell locations might account for their kinetic differences. In addition, binding of bFGF with HSPG in extracellular matrix is different from that of bFGF with HSPG on cell surface. The extracellular matrix has been proposed to act as a storage site for bFGF in vivo (Baird and Ling, 1987; Bashkin et al., 1989; and Flaumenhaft et al., 1989). The HSPG in extracellular matrix may act as high-frequency bFGF sites which bind, release, and rebind bFGF in a three-dimension volume, providing a dynamic storage system for bFGF (Nugent and Edelman, 1992). The bFGF in such a dynamic reservoir may bind randomly with HSPG or receptors on the cell surface. HSPG in extracellular matrix can serve as a carrier and safe-guard for the biological function of bFGF and prevent it from deactivation and proteolytic cleavage during the process of transport. However, the low affinity receptor, HSPG on the cell surface, reduces the dimensionality of ligand diffusion from three to two dimensions. The abundant HSPG on the cell surface that are restricted to two dimensions will increase the local concentration of the bound ligands at the plasma membrane, and the probability of their interaction with a high affinity receptor will be greatly enhanced (Schlessinger, et al., 1995). Moreover, cell surface HSPG may first bind free bFGF and then bring the bFGF to the vicinity of an unbound high affinity receptor (FGFR) to form a FGFR-bFGF complex if FGFR is present. This conforms to the ligand carrier mechanism of the role of low affinity receptors (Forsten and Lauffenburger, 1994). Concentration of bFGF presented in extracellular matrix and the amount ratio of HSPG and FGF receptors on the cell surface may also lead to different binding phenomena. Compared with bFGF-deficient environments, the extracellular matrix storage of bFGF will create a diffusion gradient and release bFGF to the low bFGF concentration area without physical degradation of the extracellular matrix. In addition, if the HSPG on the cell surface is in great excess to FGF receptors, the binding of bFGF-HSPG and bFGF-HSPG-FGF receptor is more likely to occur than the

binding of bFGF-FGF receptor. Therefore, all these factors will affect the binding kinetics and the transport of bFGF. Mathematical modeling needs to be used to clearly decipher what is occurring.

## 4.2 Conclusions

PG, purified from different types of cells conditioned media, or from the same cell type under different growth stage, may differ in chemical structure, components and function. It has been shown in this study that PG from BAE P9 cells conditioned media is primarily composed of HS, which is accessible to the HepI / HepIII digestion and nitrous acid treatment; and a small amount of CS, which can be digested by C.ABC. BAE P9 PG can be separated into two fractions, PG-I and PG-II, by ion exchange chromatography on a Q-Sepharose column using a linear salt gradient from 0.15M to 1.2M. PG-I and PG-II elute at 0.85M salt and 0.1M salt respectively. In addition, results from Sepharose CL-2B and CL-4B size exclusion columns show that BAE P9 PG consists of two different components depending on the size, and its average molecular weight is  $5 \times 10^5$  Da. SDS-PAGE with silver staining shows that BAE P9 PG has two core protein bands of estimated sizes 300kDa and 320kDa, corresponding to core protein of PG-I and PG-II respectively. Similarly, it was shown that fetal bovine pulmonary arteries basement membrane HSPG also had doublet protein bands (Benitz, et al., 1990). Western blotting with anti-perlecan primary antibody demonstrates that the core proteins of BAE P9 PG are perlecan, which is the same as reported (Forsten, et al., 1997). Size exclusion chromatography of Sepharose CL-6B column following  $\beta$ -elimination shows that PG has GAG chains estimated as a size of  $< 2 \times 10^5$ .

The cationic filtration assay (CAFAS) was developed for studying the binding between bFGF and purified BAE P9 PG. A protocol has been set up for the “uniquely sticky” molecule of bFGF: incubate PG and bFGF in a buffer (2 mg/ml BSA + 0.15M TBS) in a separate 0.6ml eppendorf vials for 1 hr in order to reach steady state. The material is then pulled through the zeta-probe membrane under vacuum, followed by 3 washes with the

buffer. Using a simple monovalent binding model, we obtained values for the equilibrium dissociation constant,  $K_D$  as  $(1.6 \pm 0.8) \times 10^{-10}$  M; the dissociation rate constant,  $k_r$  as  $0.01 \text{ min}^{-1}$ ; the association rate constant,  $k_f$  as  $6.2 \times 10^7 \text{ M}^{-1}\text{min}^{-1}$  and the total binding sites of PG,  $R_T$  as  $(1.3 \pm 0.6) \times 10^8$  (# of site)/(ng PG) from the results of cell free CAFAS by least squares analysis (Appendix A and B).  $\text{Ca}^{2+}$  has no effect on binding of HSPG with bFGF at either physiological or higher concentration. Exogenous HS competes with the PG for binding with bFGF by decreasing the binding retention of PG and bFGF with increasing amount of added HS from 0 ng to 120ng. The addition of 40ng ~ 120ng CS seems to facilitate the binding of PG and bFGF by slightly increasing the binding retention.

Comparison of experimental data with model data indicates that when the number of binding sites provided by PG is similar or greater than that of bFGF, the monovalent binding model is valid; while when the number of binding sites is less than that of bFGF, the binding might not be a simple monovalent reaction, and bFGF might bind to PG as dimers or oligomers. We also propose that PG, which has a large core protein, has a long HS GAG chain. 5 ~ 10 PG molecules can form a binding site for bFGF with a high affinity.

In the design of an analogy compound to PG, a new regulatory agent for bFGF, the characteristics of BAE P9 PG may be beneficial. For example, the incorporation of certain amount of CS into the HSPG macromolecule may increase the binding affinity of HSPG to bFGF, so that the inhibiting effect of HSPG on bFGF function may be more efficient.

### **4.3 Future Work**

4.3-1 Purification of PG and the study of biological functions of its two components



Due to the strong ion exchange chromatography on Q-Sepharose column, and the use of dialysis and lyophilizing, we have lost the biological activities of PG-I and PG-II. The use of a weak anion exchange column, such as DEAE-Sephacel or DEAE-Sepharose column, may alleviate some troubles. There may be disadvantages though, such as some samples may flow through without binding on the column at the beginning of sample loading, or we may not get distinct separation peaks by a linear salt gradient. Alternatively, other types of chromatography may apply. It was shown that the sulfate content and molecular weight of the glycosaminoglycans correlated with their binding properties to hydroxyapatite, and hydroxyapatite columns facilitated rapid separation of the glycosaminoglycans, especially dermatan sulfate and chondroitin sulfate (Narita, et al., 1995). At present, we are not sure if hydroxyapatite column will work for our PG samples, but it deserves our attention. Furthermore, a Tube-O-Dialyzer™ (Research Products International Corp., Mount Prospect, IL) was used in our lab for testing its ability for eliminating sample loss. More than 80% of labeled samples was recovered after dialysis against 0.15M TBS by Tube-O-Dialyzer™ with regard to radioactive counts and percentage of TCA precipitation. Though the capacity of Tube-O-Dialyzer™ is small, up to 3ml, it is a good candidate for replacing the Spectra/Por cellulose membrane (Spectrum, Houston, TX) for dialysis in order to reduce the loss of PG.

The good separation and recovery of PG-I and PG-II will provide us samples with biological functions for investigating their structural characteristics, and functions individually. We may conduct cell free binding assay of each component with bFGF, calculate values of  $K_D$ ,  $k_r$  and  $k_f$ , and figure out their cooperative effect on binding with bFGF. In this way, we will well understand the functional properties and secretion differences of HSPG as a major component in extracellular matrix.

The results we got from SDS-PAGE were not clear enough to show the bands because of the limitation of silver staining. We may get clearer bands if we incorporate radioactive labeled amino acids, such as  $^{35}\text{S}$ -Methionine (including Cysteine) into BAE cells. Labeled

amino acids are absorbed by cells and may appear in the core proteins of PG secreted by the cell. Then the core protein bands can be clearly visualized by autoradiography.

#### 4.3-2 The system of bFGF, HSPG, and FGFR

In the present study, we only studied the binding activities of bFGF and isolated extracellular HSPG. bFGF contains 12 anti-parallel  $\beta$ -sheets organized into a trigonal pyramidal structure, and has receptor-binding sites and section for modulation of mitogenicity. There are two potential phosphorylation sites in bFGF, which can activate receptor (FGFR) on the cell surface to transfer signals for its biological activities (Bikfalvi, et al., 1997). In addition, HSPG is located primarily on the cell surface and in the extracellular matrix. It has been shown that approximately half of porcine aortic endothelial cell surface associated HSPG is releasable with soluble heparin, and the remaining cell surface HSPG, as well as HSPG in extracellular matrix, cannot be removed from the cells with heparin core (Lowe-Krentz, et al., 1991). The heparin releasable and nonreleasable cell surface HSPG are also different in size. It has been concluded that cultured porcine aortic endothelial cells contain at least two distinct types of cell surface HSPG, one of which appears to be associated with the cells through its GAG chains, the other (which is more tightly associated) is probably linked via a membrane intercalated protein core (Lowe-Krentz, et al., 1991). Therefore, the system of bFGF, HSPG (on the cell surface or in the extracellular matrix) and cell surface FGFR will expose us to a full picture of the mechanism of how bFGF functions in BAE cells.

It was reported that FGFR-1 binds both aFGF and bFGF, but FGFR-3 preferentially binds aFGF as judged using the cloned murine homologues of fibroblast growth factor receptors 1 and 3 (FGFR-1 and FGFR-3) (Ornitz and Leder, 1992). In addition, the use of a genetically engineered soluble form of FGFR-1 fused to placental alkaline phosphatase provided a way for demonstrating that heparin is required for cell-free binding of bFGF to a soluble receptor (Ornitz et al., 1992). We may further use the Bio-Dot to do cell free assay with bFGF, HSPG and soluble FGF receptors, such as FGFR-1, to see the

interaction among these three components. Furthermore, binding study with BAE cells will elucidate much more information. Three different mechanisms for the modulation of FGF activity by HS were proposed: (1) FGF may be inactive unless it binds to cell-surface HS, which induces a conformational change that activates FGF and enables it to bind to the signal-transducing receptors (FGFR); (2) signal transduction may require binding of HS to both FGF and the FGFR. The induction of conformational changes in FGF or the receptor may or may not be required; (3) HS facilitates the formation of FGF dimer, and this could promote FGFR dimerization, which may be required for signal transduction (Turnbull and Gallagher, 1993). Venkataraman et al. (1996) have shown that monomeric bFGF preferentially self-associates and forms bFGF dimers, and heparin-like polysaccharides can readily bind to self-associated bFGF without causing a conformational change in bFGF or disrupting the bFGF self association, but that the bound polysaccharides only additionally stabilize the bFGF self-association. It will be of interest to know which mechanism is proper for our BAE cell system, and how bFGF and FGFR dimerizations are affected by the binding with regard to the presence of HSPG.

Finally, two special cases will be important for study. Treatment of Balb/c3T3 fibroblast cells with sodium chlorate, an inhibitor of cell surface proteoglycan sulfation, can greatly inhibit the binding of bFGF to HSPG, since the sulfation of GAG chain of HSPG is needed for bFGF binding (Fannon and Nugent, 1996). Also, a non-sulfated polyanionic aromatic compound, which mimics functional features of heparin/HS, inhibited bFGF binding to soluble- and cell surface-FGFR-1 (Miao, et al., 1997). In addition, after removal of the cell surface HS by heparinase, an effective inhibition of tyrosine phosphorylation induced by bFGF on cell surface FGFR-1 was observed (Miao, et al., 1997) . Also, it was reported that HS with less than eight sugar residues, produced by heparinase or nitrous acid digestion, is insufficient to support the activities of bFGF, such as bFGF-receptor binding and bFGF-induced mitogenic activity (Ornitz, et al., 1992 and Walker, et al., 1993). Treatment with sodium chlorate or Hep I / Hep III to BAE cells will provide us a case for studying the binding of bFGF and FGFR with HSPG deficiency.

#### 4.3-3 Biological functions of HSPG

It has recently been demonstrated that glypican, a proteoglycan purified from rat myoblasts, inhibits the binding of the keratinocyte growth factor (KGF), but enhances the binding of aFGF to the KGF receptor both in keratinocytes and rat myoblasts; augments the binding of aFGF and bFGF to human FGFR-1 in a cell-free system; and inhibits the mitogenic response to KGF while enhancing the response to aFGF in keratinocytes (Bonneh-Barkay, et al., 1997). The dual modulator of the biological activity of growth factors implies that proteoglycans can have different functions on various growth factors depending on species differences and the differences of target cells and growth factors. In this study, we showed that PG from BAE cells conditioned media was primarily perlecan. It was reported that perlecan represented a major storage site for bFGF in the blood vessel wall (Whitelock, et al., 1996). The blood vessel wall is composed of two major cell types: endothelial cells and smooth muscle cells. HSPG from endothelial cells may either stimulate bFGF binding and mitogenic activity (Ornitz et al., 1992; Yayon et al., 1991), or have inhibitory effects on proliferation of smooth muscle cells (Benitz, et al., 1990 and Forsten, et al., 1997). It is of great importance to identify under what kind of conditions HSPG will have inhibitory or stimulating effects on bFGF activities, so that therapeutics can be created and administrated under the determined conditions to obtain the desired response from bFGF, and to cure different diseases caused by the malfunction of bFGF.

#### 4.3-4 Mathematical models

Experiments cannot always be successfully done under many extreme circumstances and with given financial research support. The set up of a reliable mathematical model will help us to predict results we cannot easily obtain from experiments and to better understand our experimental results. How the system of bFGF, HSPG (on cell surface and in extracellular matrix), and cell surface FGFR within BAE cells works may be clarified by setting up a mathematical model based on reasonable assumptions, and utilizing parameters we obtain from experiments and from literature. For example, the

mathematical model will help us to predict how the change of available ligand concentration, and ratio of HSPG and FGFR on the cell surface will affect the binding kinetics and transport phenomena of bFGF; under what kind of conditions, HSPG will inhibit or facilitate the signal transduction of bFGF through FGFR; how the system responds with the exogenous heparin, with respect to binding of bFGF, HSPG (both in the extracellular and on the cell surface) and FGFR, and to the following biological functions of bFGF on its releasing cells and the neighbor cells. The primary goal is to understand how a natural regulator (BAE P9 PG) works and to use this information to design better “man-made” versions.

**Table 8**

**Comparison of model data with experiment data of the binding  
between 10 ng PG with <sup>125</sup>I-bFGF (0.1ng ~ 1.5ng)**

		PG (ng)	<sup>125</sup> I-bFGF (L <sub>0</sub> ) (ng)					
		10	0.1	0.2	0.5	0.8	1.0	1.5
Binding sites (#) <sup>a</sup> ( x 10 <sup>9</sup> )		2.4	-	-	-	-	-	-
Molecule (#) <sup>b</sup> ( x 10 <sup>9</sup> )		-	3.3	6.6	16.5	26.4	33	49.5
Binding Complex (ng)	Experiment <sup>c</sup>	-	0.006 ± 0.0018	0.022 ± 0.0015	0.0728 ± 0.0063	0.096 ± 0.0091	0.122 ± 0.01	0.185 ± 0.01
	Model <sup>d</sup>	-	0.0059 ± 0.003	0.0011 ± 0.005	0.0022 ± 0.0011	0.003 ± 0.0015	0.0034 ± 0.0017	0.0041 ± 0.002

- a. The binding sites was calculated based on  $R_T = 0.2$  sites / molecule of PG and the molecular weight of PG 500 kDa;
- b. The molecule was calculated based on the molecular weight of bFGF 18 kDa;
- c. Experiment was conducted in Bio-Dot and the Binding complex =  $L_0 \times$  modified retention;
- d. Data was obtained from model equation (14).

**Table 9**

**Comparison of model data with experiment data of the binding  
between 40 ng PG with <sup>125</sup>I-bFGF (0.1ng ~ 0.25ng)**

		PG (ng)	<sup>125</sup> I-bFGF (L <sub>0</sub> ) (ng)			
		40	0.1	0.15	0.2	0.25
Binding sites (#) <sup>a</sup> ( x 10 <sup>9</sup> )		9.6	-	-	-	-
Molecule (#) <sup>b</sup> ( x 10 <sup>9</sup> )		-	3.3	5	6.6	8.2
Binding Complex (ng)	Experiment <sup>c</sup>	-	0.0204 ± 0.0017	0.0219 ± 0.0037	0.0286 ± 0.0036	0.0333 ± 0.01
	Model <sup>d</sup>	-	0.019 ± 0.0042	0.0274 ± 0.0054	0.0348 ± 0.0066	0.0415 ± 0.0072

a. The binding sites was calculated based on  $R_T = 0.2$  sites / molecule of PG and the molecular weight of PG 500 kDa;

b. The molecule was calculated based on the molecular weight of bFGF 18 kDa;

c. Experiment was conducted in Bio-Dot and the Binding complex =  $L_0 \times$  modified retention;

d. Data was obtained from model equation (14).

**Table 10**

**Comparison of model data with experiment data of the binding  
between 80 ng PG with <sup>125</sup>I-bFGF (0.1ng ~ 1.5ng)**

		PG (ng)	<sup>125</sup> I-bFGF (L <sub>0</sub> ) (ng)					
		80	0.1	0.2	0.5	0.8	1.0	1.5
Binding sites (#) <sup>a</sup> ( x 10 <sup>9</sup> )		19.2	-	-	-	-	-	-
Molecule (#) <sup>b</sup> ( x 10 <sup>9</sup> )		-	3.3	6.6	16.5	26.4	33	49.5
Binding Complex (ng)	Experiment <sup>c</sup>	-	0.0173 ± 0.01	0.031 ± 0.014	0.0848 ± 0.0164	0.125 ± 0.027	0.146 ± 0.018	0.211 ± 0.022
	Model <sup>d</sup>	-	0.0326 ± 0.009	0.061 ± 0.017	0.123 ± 0.034	0.163 ± 0.045	0.182 ± 0.05	0.214 ± 0.06

a. The binding sites was calculated based on  $R_T = 0.2$  sites / molecule of PG and the molecular weight of PG 500 kDa;

b. The molecule was calculated based on the molecular weight of bFGF 18 kDa;

c. Experiment was conducted in Bio-Dot and the Binding complex =  $L_0 \times$  modified retention;

d. Data was obtained from model equation (14).



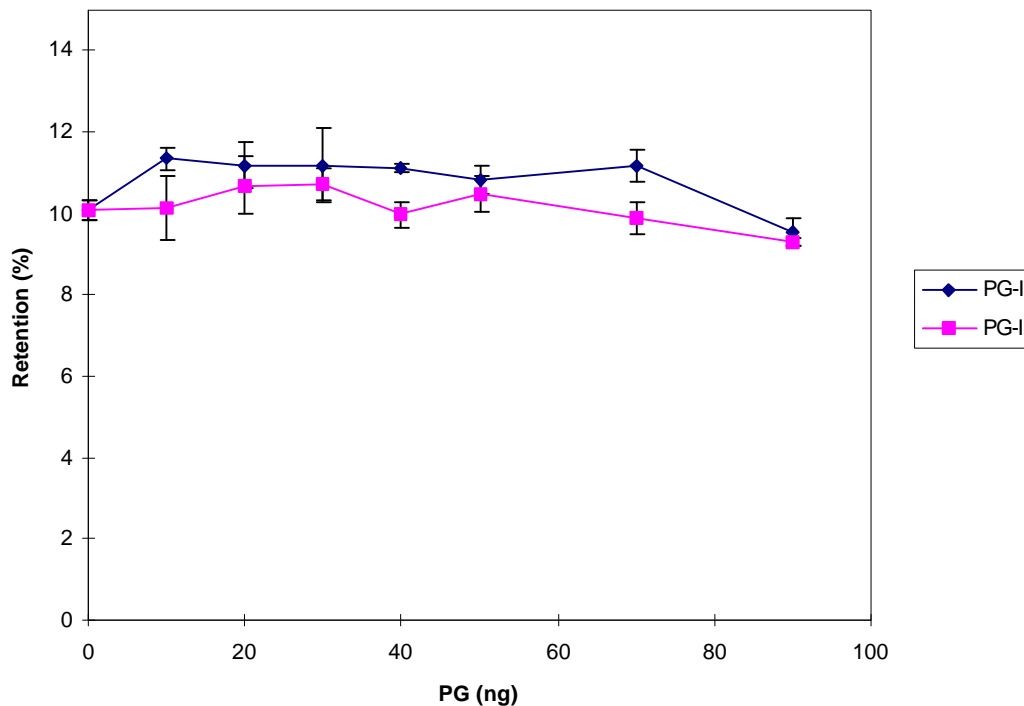


**Figure 4-1 Effect of PG-I and PG-II on  $^{125}\text{I}$ -bFGF retention in Bio-Dot**

PG-I and PG-II were pooled following Q-Sepharose column separation. 0.25ng  $^{125}\text{I}$ -bFGF and different amount of PG-I or PG-II as indicated were incubated in separate 0.6ml eppendorf vials with 2mg/ml BSA+0.15M TBS buffer totaling 200  $\mu\text{l}$  for 1 hr. All liquid in each vial was aspirated out and pulled through the zeta-probe membrane with 3 washes of 2mg/ml BSA+0.15M TBS buffer. Each dot on the membrane was cut off and counted as cpm in scintillation counter. All data was averaged from triple cases, and the error bars showed the standard error of triplicate measurements.

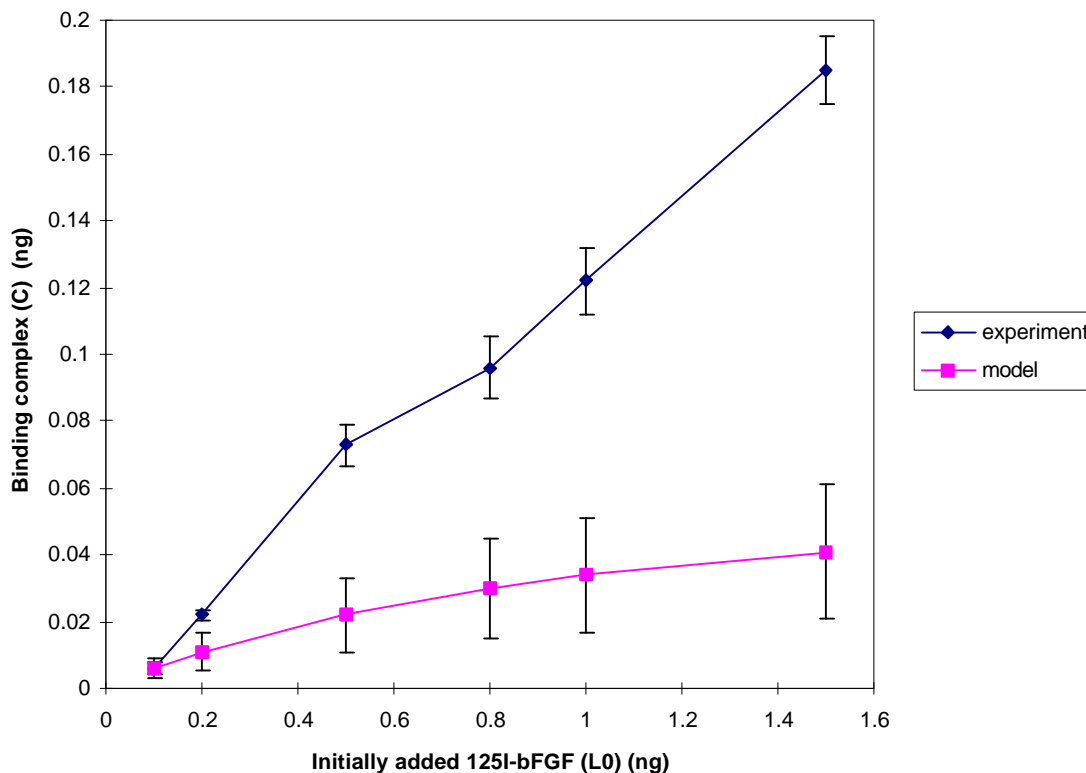


**Figure 4-2 Comparison of experimental data with model data  
- Binding of 10 ng PG with  $^{125}\text{I}$ -bFGF**

Different amount of  $^{125}\text{I}$ -bFGF as indicated and 10ng PG were incubated in separate 0.6ml eppendorf vials with 2mg/ml BSA+0.15M TBS buffer totaling 200  $\mu\text{l}$  for 1 hr. All liquid in each vial was aspirated out and pulled through the zeta-probe membrane with 3 washes of 2mg/ml BSA+0.15M TBS buffer. Each dot on the membrane was cut off and counted as cpm in scintillation counter. All data was averaged from triple cases, and the error bars showed the standard error of triplicate measurements. Model data was from model equation (14).

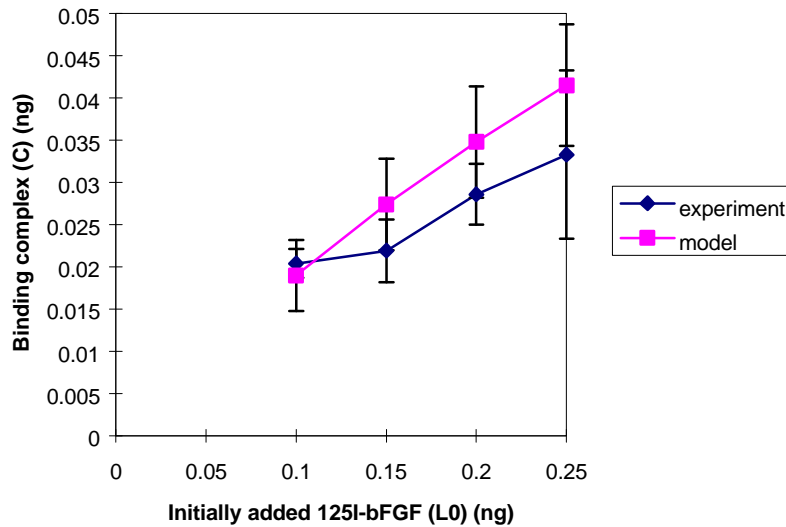


**Figure 4-3 Comparison of experimental data with model data**

**- Binding of 40 ng PG with  $^{125}\text{I}$ -bFGF**

Different amount of  $^{125}\text{I}$ -bFGF as indicated and 40ng PG were incubated in separate 0.6ml eppendorf vials with 2mg/ml BSA+0.15M TBS buffer totaling 200  $\mu\text{l}$  for 1 hr. All liquid in each vial was aspirated out and pulled through the zeta-probe membrane with 3 washes of 2mg/ml BSA+0.15M TBS buffer. Each dot on the membrane was cut off and counted as cpm in scintillation counter. All data was averaged from triple cases, and the error bars showed the standard error of triplicate measurements. Model data was from model equation (14).

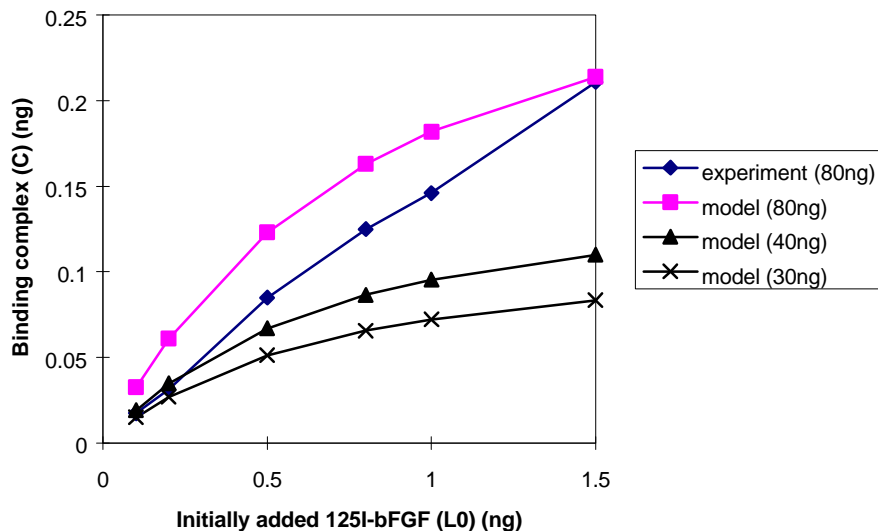
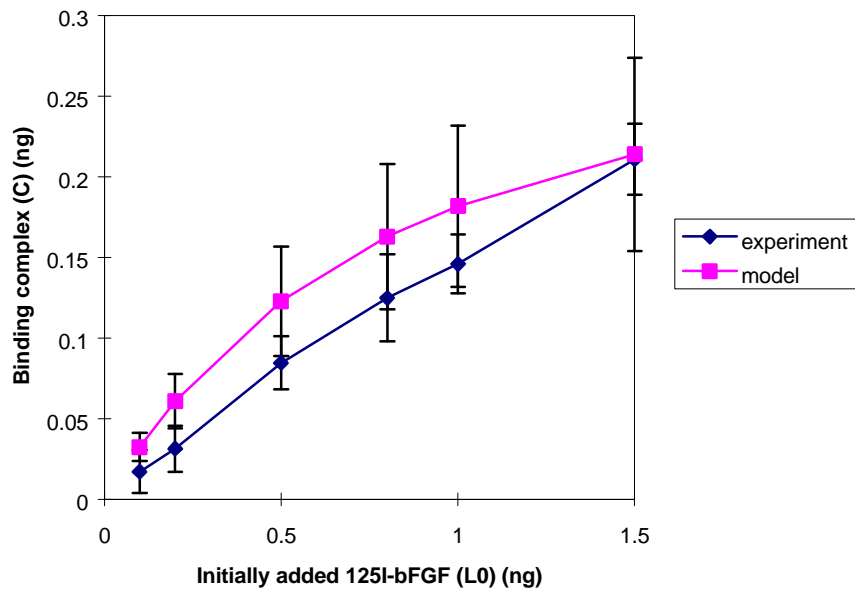


**Figure 4-4 Comparison of experimental data with model data  
- Binding of 80 ng PG with <sup>125</sup>I-bFGF**

Different amount of <sup>125</sup>I-bFGF as indicated and 80ng PG were incubated in separate 0.6ml eppendorf vials with 2mg/ml BSA+0.15M TBS buffer totaling 200  $\mu$ l for 1 hr. All liquid in each vial was aspirated out and pulled through the zeta-probe membrane with 3 washes of 2mg/ml BSA+0.15M TBS buffer. Each dot on the membrane was cut off and counted as cpm in scintillation counter. All data was averaged from triple cases, and the error bars showed the standard error of triplicate measurements. Model data was from model equation (14).

## References

- Akira, S., Hirano, T., Taga, T., and Kishimoto, T. (1990) Biology of multifunctional cytokines: IL-6 and related molecules (IL-1 and TNF). *FASEB J.* 4: 2860-2867.
- Arakawa, T., Wen, J. and Philo, J.S. (1994) Stoichiometry of heparin binding to basic fibroblast growth factor. *Archives of Biochemistry and Biophysics* 308: 267-273.
- Aviezer, D., Iozzo, R.V., Noonan, D.M. and Yayon, A. (1997) Suppression of autocrine and paracrine functions of basic fibroblast growth factor by stable expression of perlecan antisense cDNA. *Mol. Cell. Biol.* 17:1938-1946.
- Baird, A. and Ling, N. (1987) Fibroblast growth factors are present in the extracellular matrix produced by endothelial cells in vitro: implications for a role of heparinase-like enzymes in the neovascular response. *Biochem. Biophys. Res. Commun.* 142: 428-435.
- Bashkin, P., Doctrow, S., Klagsbrun, M., Svahn, C.M., Folkman, J., and Vlodavsky, I. (1989) Basic fibroblast growth factor binds to subendothelial extracellular matrix and is released by heparitinase and heparin-like molecules. *Biochemistry* 28: 1737-1743.
- Bassols, A. and Massague, J. (1988) Transforming growth factor b regulates the expression and structure of extracellular matrix chondroitin/dermatan sulfate proteoglycans. *J. Biol. Chem.* 263: 3039-3045.
- Bellot, F., Crumley, G., Kaplow, J.M., Schlessinger, J., Jaye, M., and Dionne, C.A. (1991) Ligand-induced transphosphorylation between different FGF receptors. *EMBO J.* 10: 2849-2854.
- Benitz, W.E., Kelley, R.T., Anderson, C.M., Lorant, D.E. and Bernfield, M. (1990) Endothelial heparan sulfate proteoglycan. I. Inhibitory effects on smooth muscle cell proliferation. *Respir. Cell Mol. Biol.* 2: 13-24.
- Bikfalvi, A., Klein, S., Pintucci, G., and Rifkin, D. (1997) Biological roles of fibroblast growth factor-2. *Endocrine Reviews* 18: 26-45.
- Bonneh-Barkay, D., Shlissel, M., Berman, B., Shaoul, E., Admon, A., Vlodavsky, I., Carey, D.J., Asundi, V.K., Reich-Slotky, R., and Ron, D. (1997) Identification of glypican as a dual modulator of the biological activity of fibroblast growth factors. *J. Biol. Chem.* 272: 12415-12421.
- Boyce, W.E. and DiPrima, R.C. (1977) Elementary differential equations and boundary value problems. Third edition, John Wiley & Sons, Inc.
- Casscells, W. (1992) Migratin of smooth muscle and endothelial cells: critical events in restenosis. *Circulation.* 86: 723-729.

- Castellot, J.J., Addonizio, M.L., Rosenberg, R. and Karnovsky, M.J. (1981) Cultured endothelial cells produce a heparinlike inhibitor of smooth muscle cell growth. *J. Cell Biol.* 90:372-379.
- Castellot, J.J., Wright, T.C. and Karnovsky, M. (1987) Regulation of vascular smooth muscle cell growth by heparin and heparan sulfate. *Semin. Thromb. Hemostasis.* 13: 489-503.
- Cook, P.W., Ashton, N.M., Karkaria, C.E., Siess, D.C. and Shipley, G.D. (1995) Differential effects of a heparin antagonist (hexadimethrine) or chlorate on amphiregulin, basic fibroblast growth factor, and heparin-binding EGF-like growth factor activity. *J. Cell. Physiol.* 163: 418-429.
- Dionne, C.A., Crumley, G., Bellot, F., Kaplow, J.M., Searfoss, G., Ruta, M., Burgess, W.H., Jaye, M., and Schlessinger, J. (1990) Cloning and expression of two distinct high-affinity receptors cross-reacting with acidic and basic fibroblast growth factor. *EMBO J.* 9: 2685-2692.
- Edelman, E.R. and Karnovsky, M.J. (1994) Contrasting effects of the intermittent and continuous administration of heparin in experimental restenosis. *Circulation.* 89:770-776.
- Fannon, M. and Nugent, M.A. (1996) Basic fibroblast growth factor binds its receptors, is internalized, and stimulates DNA synthesis in Balb/c3T3 cells in the absence of heparan sulfate. *J. Biol. Chem.* 271: 17949-17956.
- Farndale, R.W., Buttle, D.J. and Barrett, A.J. (1986) Improved quantitation and discrimination of sulfated glycosaminoglycans by use of dimethylmethylene blue. *Biochem. Biophys. Acta.* 883: 173-177.
- Flaumenhaft, R., Moscatelli, D., Saksela, O., and Rifkin, D.B. (1989) Role of extracellular matrix in the action of basic fibroblast growth factor: matrix as a source of growth factor for long-term stimulation of plasminogen activator production and DNA synthesis. *J. Cell. Physiol.* 140: 75-81.
- Flaumenhaft, R., Moscatelli, D., and Rifkin, D.B. (1990) Heparin and heparan sulfate increase the radius of diffusion and action of basic fibroblast growth factor. *J. Cell Biol.* 111: 1651-1659.
- Flaumenhaft, R. and Rifkin, D.B. (1992) The extracellular regulation of growth factor action. *Molecular Biology of the Cell.* 3:1057-1065.
- Forsten, K.E. and Lauffenburger, D.A. (1994) The role of low-affinity interleukin-2 receptors in autocrine ligand binding: alternative mechanisms for enhanced binding effect. *Molecular Immunology.* 31:739-751.

Forsten, K.E., Courant, N.A. and Nugent, M.A. (1997) Endothelial proteoglycans inhibit bFGF binding and mitogenesis. *J. Cell. Physiol.* 172:209-220.

Gallagher, J.T. (1989) The extended family of proteoglycans: social residents of the pericellular zone. *Curr. Opin. Cell Biol.* 1: 1201-1218.

Gannoun-Zaki, L., Pieri, I., Badet, J., Moenner, M., and Barritault, D. (1991) Internalization of basic fibroblast growth factor by Chinese hamster lung fibroblast cells: involvement of several pathways. *Exp. Cell Res.* 197: 272-279.

Gospodarowicz, D., and Cheng, J. (1986) Heparin protects basic and acidic FGF from inactivation. *J. Cell. Physiol.* 128: 475-484.

Hadley, M.E. (1996) *Endocrinology*, 4<sup>th</sup> edition

Harada, K., Friedman, M., Lopez, J.J., Wang, S.Y., Li, J., Prasad, P.V., Pearlman, J.D., Edelman, E.R., Sellke, F.W. and Simons, M. (1996) Vascular endothelial growth factor administration in chronic myocardial ischemia. *Am. J. Physiol.* 270: H1791-1802.

Hardingham, T.E. and Fosang, A.J. (1992) Proteoglycans: many forms and many functions. *FASEB J.* 6:861-870.

Hardingham, T.E. and Bayliss, M.T. (1990) Proteoglycans of articular cartilage changes in aging and in joint disease. *Semin. Arth. Rheum., Suppl.* 1: 12-33.

Hofer (1994) *Protein electrophoresis applications guide*. Hoefer Scientific Instrument

Hook, M., Kjellen, L., Johansson, S. and Robinson, J. (1984) Cell-surface glycosaminoglycans. *Annu. Rev. Biochem.* 53: 847-869.

Hovingh, P. and Linder, A. (1974) The disaccharide repeating units of heparan sulfate. *Carbohydr. Res.* 37: 181-192

Hughes, S.E. and Hall, P.A. (1993) Overview of the fibroblast growth factor and receptor families: complexity, functional diversity, and implications for future cardiovascular research. *Cardiovascular Research.* 27: 1199-1202.

Iozzo, R. (1988) Cell surface heparan sulfate proteoglycan and the neoplastic phenotype. *J. Cell Biochem.* 37: 61-78.

Iozzo, R.V., Cohen, I.R., Grassel, S. and Muirdoch, A.D. (1994) The biology of perlecan: the multifaceted heparan sulphate proteoglycan of basement membranes and pericellular matrix. *Biochem. J.* 302:625-639.

Jackson, R.L., Busch, S.J. and Cardin, A.D. (1991) Glycosaminoglycans: molecular properties, protein interactions, and role in physiological processes. *Physiological Rev.* 71: 481-539.

Jaye, M., Schlessinger, J. and Dionne, C.A. (1992) Fibroblast growth factor receptor tyrosine kinase: molecular analysis and signal transduction. *Biochim. Biophys. Acta* 1135: 185-199.

Jorpes, J.E. and Gardell, S. (1948) On heparin monosulfuric acid. *J. Biol. Chem.* 176: 267-275.

Kan, M., Wang, F., Kan, M., To, B., Gabriel, J.L., and McKeehan, W.L. (1996) Divalent cations and heparin/heparan sulfate cooperate to control assembly and activity of the fibroblast growth factor receptor complex. *J. Biol. Chem.* 271: 26143-26148.

Kawano M., Hirano T., Matsuda T., Taga T., Horii Y., Iwato K. et al. (1988) Autocrine generation and essential requirement of BSF-2/IL-6 for human multiple myelomas. *Nature.* 332: 83-85.

Kinsella, M.G. and Wight, T.N. (1988) Structural characterization of heparan sulfate proteoglycan subclasses isolated from bovine aortic endothelial cell cultures. *Biochemistry* 27:2136-2144.

Korn, G.A. and Korn, T.M. (1968) *Mathematic handbook for scientists and engineers.* 2<sup>nd</sup> edition, McGraw-Hill Book Inc.

Kramer, R.H., Vogel, K.G., and Nicolson, G.L. (1982) Solubilization and degradation of subendothelial matrix glycoproteins and proteoglycans by metastatic tumor cells. *J. Biol. Chem.* 257: 2678-2686.

Lauffenburger, D.A. and Linderman, J.J. (1993) *Receptors: models for binding, trafficking, and signaling.* Oxford University Press.

Linker, A. and Hovingh, P. (1984) Structural studies on heparin: tetrasaccharides obtained by heparinase digestion. *Carbohydr. Res.* 127: 75-94.

Linker, A. and Hovingh, P. (1972) Heparinase and heparitinase from *flavobacteria*. *Methods Enzymol.* 28: 902-907.

Liu, M.W., Roubin, G.S. and King, S.B. III (1989) Restenosis after coronary angioplasty: potential biologic determinants and role of intimal hyperplasia. *Circulation.* 79: 1374-1387.



Lowe-Krentz, L.J., Thompson, K. and Patton II, W.A. (1991) Heparin releasable and nonreleasable forms of heparan sulfate proteoglycan are found on the surfaces of cultured porcine aortic endothelial cells. *Molecular and Cellular biochemistry* 109: 51-60.

Luciano, D.S., Vander, A.J. and Sherman, J.H. (1983) Human anatomy and physiology-structure and function, 2<sup>nd</sup> edition, McGraw-Hill book company.

Mansukhani, A., Moscatelli, D., Talarico, D., Levytska, V., and Basilico, C. (1990) A murine fibroblast growth factor (FGF) receptor expressed in CHO cells is activated by basic FGF and kaposi FGF. *Proc. Natl. Acad. Sci. U.S.A.* 87: 4378-4382.

Mansukhani, A., Dell'Era, P., Moscatelli, D., Kornbluth, S., Hanafusa, H., and Basilico, C. (1992) Characterization of murine BEK fibroblast growth factor (FGF) receptor: activation by three members of the FGF family and requirement for heparin. *Proc. Natl. Acad. Sci. U.S.A.* 89: 3305-3309.

Mason, I.J. (1994) The ins and outs of fibroblast growth factors. *Cell*, 78: 547-552.

Miao, H., Ornitz, D.M., Aingorn, E., Ben-Sasson, S.A. and Vlodavsky, I. (1997) Modulation of fibroblast growth factor-2 receptor binding, dimerization, signaling, and angiogenic activity by a synthetic heparin-mimicking polyanionic compound. *J. Clin. Invest.* 7: 1565-1575.

Moscatelli, D. (1987) High affinity and low affinity binding sites for basic fibroblast growth factor on cultured cells: absence of a role for low affinity binding in the stimulation of plasminogen activator production by bovine capillary endothelial cells. *J. Cell. Physiol.* 131: 123-130.

Moscatelli, D. (1988) Metabolism of receptor-bound and matrix-bound basic fibroblast growth factor by bovine capillary endothelial cells. *J. Cell Biol.* 107: 753-760.

Moscatelli, D. (1992) *J. Biol. Chem.* 267: 25803-25809.

Narita, H., Takeda, Y., Takagaki, K., Nakamura, T., Harata, S. and Endo, M. (1995) Identification of glycosaminoglycans using high performance liquid chromatography on a hydroxyapatite column. *Analytical Biochemistry* 232: 133-136.

Nathan, A., Nugent, M.A. and Edelman, E.R. (1995) Tissue engineered perivascular endothelial cell implants regulate vascular injury. *Proc. Natl.Acad.Sci.* 92:8130-8134.

Neufeld, G. and Gospodarowicz, D. (1985) The identification of partial characterization of the fibroblast growth factor receptor of baby hamster kidney cells. *J. Biol. Chem.* 260: 13860-13868.

- Neufeld, G. and Gospodarowicz, D. (1986) Basic and acidic fibroblast growth factors interact with the same cell surface receptors. *J. Biol. Chem.* 261: 5631-5637.
- Nugent, M.A. and Edelman, E.R. (1992) Kinetics of basic fibroblast growth factor binding to its receptor and heparan sulfate proteoglycan: a mechanism for cooperativity. *Biochemistry*, 31: 8876-8883.
- Nugent, M.A., Karnovsky, M.J. and Edelman, E.R. (1993) Vascular cell-derived heparan sulfate sows coupled inhibition of basic fibroblast growth factor binding and mitogenesis in vascular smooth muscle cells. *Circ. Res.* 73:1051-1060.
- Ohno, H., Blackwell, J., Jamieson, A.M., Carrino, D.A. and Caplan, A.I. (1986) Calibration of the relative molecular mass of proteoglycan subunit by column chromatography on Sepharose CL-2B. *Biochem. J.* 235:553-557.
- Olwin, B.B. and Rapraeger, A. (1992) Repression of myogenic differentiation by aFGF, bFGF, and K-FGF is dependent on cellular heparan sulfate. *J. Cell Biol.* 118: 631-639.
- Oohira, A., Wight, T.N. and Bornstein, P. (1983) Sulfated proteoglycans synthesized by vascular endothelial cells in culture. *J. Biol. Chem.* 258:2014-2021.
- Ornitz, D.M., Herr, A.B., Nilsson, M., Westman, J., Svahn, C.M., and Waksman, G. (1995) FGF binding and FGF receptor activation by synthetic heparan-derived di- and trisaccharides. *Science* 268: 432-436.
- Ornitz, D.M. and Leder, P. (1992) Ligand specificity and heparin dependence of fibroblast growth factor receptors 1 and 3. *J. Biol. Chem.* 267: 16305-16311.
- Ornitz, D.M., Yayon, A., Flanagan, J.G., Svahn, C.M., Levi, E. and Leder, P. (1992) Heparin is required for cell-free binding of basic fibroblast growth factor to a soluble receptor and for mitogenesis in whole cells. *Mol. Cell. Biol.* 12: 240-247.
- Presta, M., Maier, J.A.M., Rusnati, M., and Ragnotti, G. (1989) Basic fibroblast growth factor is released from endothelial extracellular matrix in a biologically active form. *J. Cell. Physiol.* 140: 68-74.
- Rapraeger, A.C., Krufka, A. and Olwin, B.B. (1991) Requirement of heparan sulfate for bFGF-mediated fibroblast growth and myoblast differentiation. *Science.* 252: 1705-1708.
- Richard, C., Liuzzo, J.P., and Moscatelli, D. (1995) Fibroblast growth factor-2 can mediate cell attachment by linking receptors and heparan sulfate proteoglycans on neighboring cells. *J. Biol. Chem.* 270: 24188-24196.
- Rifkin, D.B. and Moscatelli, D. (1989) Recent developments in the cell biology of basic fibroblast growth factor. *J. Cell Biol.* 109: 1-6.

- Ritger, P.D. and Rose, N.J. (1968) Differential equations with applications. New York: McGraw-Hill.
- Roghani, M. and Moscatelli, D. (1992) Basic fibroblast growth factor is internalized through both receptor-mediated and heparan sulfate-mediated mechanisms. *J. Biol. Chem.* 267: 22156-22162.
- Roghani, M., Mansukhani, A., Dell'Era, P., Bellosta, P., Basilico, C., Rifkin, D.B. and Moscatelli, D. (1994) Heparin increases the affinity of basic fibroblast growth factor for its receptor but is not required for binding. *J. Biol. Chem.* 269: 3976-3984.
- Romagnolo, D., Akers, R.M., Byatt, J.C., Wong, E.A. and Turner, J.D. (1994) Regulation of expression of IGF-I induced IGFBP-3 and IGF-I receptor by constitutive versus regulated expression of recombinant IGF-I in transfected mammary epithelial cells. *Endocrine J.* 2: 375-384.
- Ruoslahti, E. (1989) Proteoglycans in cell regulation. *J. Biol. Chem.* 264: 13369-13372.
- Ruoslahti, E. and Yamaguchi, Y. (1991) Proteoglycans as modulators of growth factor activities. *Cell* 64: 867-869.
- Rusnati, M., Urbinati, C., and Presta, M. (1993) Internalization of basic fibroblast growth factor (bFGF) in cultured endothelial cells: role of the low affinity heparin-like bFGF receptors. *J. Cell. Physiol.* 154: 152-161.
- Saksela, O., Moscatelli, D., Sommer, A., and Rifkin, D.B. (1988) Endothelial cell-derived heparan sulfate binds basic fibroblast growth factor and protects it from proteolytic degradation. *J. Cell Biol.* 107: 743-751.
- San Antonio, J., Winston, B.M. and Tuan, R.S. (1987) Regulation of chondrogenesis by heparan sulfate and structurally related glycosaminoglycans. *Dev. Biol.* 123: 17-24.
- Sato, Y. and Rifkin, D.B. (1988) Autocrine activities of basic fibroblast growth factor: regulation of endothelial cell movement, plasminogen activator synthesis, and DNA synthesis. *J. Cell Biol.* 107: 1199-1205.
- Schlessinger, J., Lax, I. and Lemmon, M. (1995) Regulation of growth factor activation by proteoglycans: what is the role of the low affinity receptors? *Cell.* 83: 357-360.
- Schweigerer, L., Neufeld, G., Friedman, J., Abraham, J.A., Fiddes, J.C. and Gospodarowicz, D. (1987) Capillary endothelial cells express basic fibroblast growth factor, a mitogen that promotes their own growth. *Nature (Lond.)*. 325: 257-259.

- Shively, J.E. and Conrad, H.E. (1976) Formation of anhydrosugars in the chemical depolymerization of heparin. *Biochemistry* 18: 3932-3942.
- Spron M.B., and Roberts, A.B. (1990) TGF- $\beta$ : Problems and prospects. *Cell Regulation*. 1: 875-882.
- Suzuki, S. (1972) Chondroitinases from *Proteus vulgaris* and *flavobacterium heparinum*. *Methods Enzymol.* 28: 911-917.
- Thesleff, I., Jalkanen, M., Vainio, S. and Bernfield, M. (1989) Cell surface proteoglycan expression correlates with epithelial-mesenchymal interaction during tooth morphogenesis. *Dev. Biol.* 129: 565-572.
- Thompson, L.D., Pantoliano, M.W. and Springer, B.A. (1994) Energetic characterization of the basic fibroblast growth factor-heparin interaction: identification of the heparin binding domain. *Biochemistry* 33: 3831-3840.
- Turnbull, J.E. and Gallagher, J.T. (1993) Heparan sulphate: functional role as a modulator of fibroblast growth factor activity. *Biochemical Society Transactions*. 21: 477-482.
- Vigny, M., Ollier-Hartmann, M.P., Lavigne, M., Fayein, N., Jeanny, J.C., Laurent, M., and Courtois, Y. (1988) Specific binding of basic fibroblast growth factor to basement membrane-like structures and to purified heparan sulfate proteoglycan of the EHS tumor. *J. Cell. Physiol.* 137: 321-328.
- Vlodavsky, I., Bar-Shavit, R., Ishai-Michaeli, R., Bashkin, P. and Fuks, Z. (1991) Extracellular sequestration and release of fibroblast growth factor: a regulatory mechanism? *Trends Biochem. Sci.* 16: 268-271.
- Walker, A., Turnbull, J.E. and Gallagher, J.T. (1993) Specific heparan sulfate saccharides mediate the activity of basic fibroblast growth factor. *J. Biol. Chem.* 269: 931-935.
- Whitelock, J.M., Murdoch, A.D., Iozzo, R.V. and Underwood, P.A. (1996) The degradation of human endothelial cell-derived perlecan and release of bound basic fibroblast growth factor by stromelysin, collagenase, plasmin, and heparanases. *J. Biol. Chem.* 271: 10079-10086.
- Yanagishita, M. and Hascall, V.C. (1992) Cell surface heparan sulfate proteoglycans. *J. Biol. Chem.* 267: 9451-9454.
- Yayon, A., Klagsburn, M., Esko, J.D., Leder, P. and Ornitz, D.M. (1991) Cell surface, heparin-like molecules are required for binding of basic fibroblast growth factor to its high affinity receptor. *Cell.* 64: 841-848.

Zimmer, Y., Givol, D. and Yayon, A. (1993) Multiple structural elements determine ligand binding of fibroblast growth factor receptors. *J. Biol. Chem.* 268: 7899-7903.

## Appendix A

Here it is shown how the equilibrium dissociation constant,  $K_D$ , and the total number of binding site of per ng PG,  $R_T$ , were determined from CAFAS data and equation

$$(6) \quad \frac{C_{eq}}{L} = -\frac{1}{K_D} C_{eq} + \frac{R_T}{K_D}$$

using least squares analysis. The CAFAS data from our cell free binding assay of  $^{125}\text{I}$ -bFGF (0.05ng, 0.1ng, 0.15ng, 0.2ng, or 0.25ng) with PG (20ng, 30ng or 40ng) is shown below:

PG (ng)	20			30			40			
$^{125}\text{I}$ -bFGF ( $L_0$ ) (ng)	0.05	0.1	0.15	0.1	0.15	0.2	0.1	0.15	0.2	0.25
Binding complex $C \times 10^2$ (ng)	0.6	1.16	1.36	1.67	2.43	2.89	2.04	2.09	2.86	3.33
Free ligand $L \times 10^2$ (ng)	4.4	8.84	13.6	8.33	12.6	17.1	7.96	12.9	17.1	21.7
Bound/Free $C/L \times 10^2$	14	13	10	20	19	17	26	16	17	15

Wherein:

$$L = L_0 - C$$

FORTRAN Program: (an example with 40ng PG)

C This program is using subroutine RLINE in IMSL to fit a line to  
C a set of (x,y) data points by the method of least squares.

C Parameters:

C NOBS = number of data points

C XDATA =C (binding complex)

C YDATA = C/L (bound/free)

C B0 = ( $R_T/K_D$ )

C B1 =  $-(1/K_D)$

C

INTEGER NOBS

```

PARAMETER (NOBS = 4)
C
INTEGER  NOUT
DOUBLE PRECISION B0, B1, STAT(12), XDATA(NOBS), YDATA(NOBS)
CHARACTER  CLABEL(13)*15, RLABEL(1)*4
EXTERNAL  DRLINE, UMACH, DWRRRL
C
DATA XDATA/2.04D2,2.09D2,2.86D2,3.33D2/
DATA YDATA/26D2,16D2,17D2,15D2/
DATA RLABEL/'NONE', CLABEL/' ', 'Mean of X', 'Mean of Y',
&  'Variance X', 'Variance Y', 'Corr.', 'Std. Err. B0',
&  'Std. Err. B1', 'DF Reg.', 'SS Reg.', 'DF Error',
&  'SS Error', 'Pts. with NaN'/
C
CALL DRLINE (NOBS, XDATA, YDATA, B0, B1, STAT)
C
CALL UMACH (2, NOUT)
WRITE (NOUT,99) B0, B1
99 FORMAT (' B0 = ', D7.2, ' B1 = ', D14.5)
CALL DWRRRL ('%/STAT', 1, 12, STAT, 1, 0, '(12W10.4)', RLABEL,
&  CLABEL)
C
END

```

Result:

B0 = 2.54D-01 B1 = - .327D+01

From B1 we obtained  $K_D = 0.306$  ng. Then from B0,  $R_T = 0.0777$  ng.

Because the calculated C(ng) and L(ng) were based on initial amount of  $^{125}\text{I}$ -bFGF and its retention, the  $K_D$ (ng) and  $R_T$ (ng) we obtained were also found on the basis of  $^{125}\text{I}$ -bFGF counting. Converting the unit of  $K_D$  and  $R_T$  by using the molecular weight of bFGF, 18kDa, we obtained

$K_D = 8.49 \times 10^{-11}$  M;  $R_T = 6.49 \times 10^{-7}$  #/ng PG

In the same way, we obtained the B0 and B1 for each cell free binding assay of  $^{125}\text{I}$ -bFGF (0.05ng, 0.1ng, 0.15ng, or 0.2ng) with 20ng PG, or 30ng PG, and further calculated  $K_D$  and  $R_T$  for each case. The following is the summary of calculated data:

PG (ng)	20	30	40
B0	0.163	0.203	0.254
B1	-3.86	-0.859	-3.27
K <sub>D</sub> (M)	7.2 x 10 <sup>-11</sup>	3.23 x 10 <sup>-10</sup>	8.49 x 10 <sup>-11</sup>
R <sub>T</sub> (#/ng PG)	7.06 x 10 <sup>7</sup>	2.63 x 10 <sup>8</sup>	6.49 x 10 <sup>7</sup>

Then the average value and standard error was calculated for K<sub>D</sub> and R<sub>T</sub>:

$$K_D = (1.6 \pm 0.8) \times 10^{-10} \text{ M}$$

$$R_T = (1.3 \pm 0.6) \times 10^8 \text{ \#/ng PG.}$$



## Appendix B

Here it is shown that, when we assume  $L = L_0$ , how the dissociation rate constant,  $k_r$ , and the association rate constant  $k_f$ , were determined from CAFAS data and equation

$$(10) \ln[C_{eq} - C(t)] = \ln\left[\frac{R_r}{1 + (K_D / L_0)}\right] - \left[1 + \left(\frac{L_0}{K_D}\right)\right]k_r t$$

using least squares analysis. The cell free binding assay with 0.2ng  $^{125}$ I-bFGF and 40ng PG was conducted. At times were equal to 1min, 5min, 10min, 15min, 20min, 30min and 60min,  $C(t)$  was measured as the retention of binding complex on the membrane.

Retention of 0.2ng  $^{125}$ I-bFGF alone without PG was also measured at the given times and deducted as non-specific background binding.  $C_{eq}$  was determined at  $t = 60$ min. The data is shown below:

Time (min)	Modified Retention (%)	Binding Complex ( C ) (ng)	$C_{eq}-C(t)$ (ng)	$\ln[C_{eq}-C(t)]$
1	9.9	0.0198	0.0196	-3.932
5	12.1	0.0242	0.0152	-4.186
10	16.8	0.0336	0.0058	-5.15
15	14.4	0.0288	0.0106	-4.55
20	13.5	0.027	0.0124	-4.39
30	14.4	0.0288	0.0106	-4.55
60	19.7	0.0394	0	-

Wherein:

$$L_0 = 0.2\text{ng}$$

$$C = L_0 \times \text{modified retention}$$

$$C_{eq} = C (t = 60)$$

FORTTRAN Program:

C This program is using subroutine RLINE in IMSL to fit a line to  
C a set of (x,y) data points by the method of least squares.

C Parameters:

```

C NOBS=number of data points
C XDATA=t (time)
C YDATA=ln[Ceq-C(t)]
C B0=ln[RT/(1+KD/L0)]
C B1=[1+(L0/KD)]kr

INTEGER NOBS

PARAMETER (NOBS=6)
C
INTEGER NOUT
DOUBLE PRECISION B0, B1, STAT(12), XDATA(NOBS), YDATA(NOBS)
CHARACTER CLABEL(13)*15, RLABEL(1)*4
EXTERNAL DRLINE, UMACH, DWRRRL
C
DATA XDATA/1.0D0,5.0D0,10.0D0,15.0D0,20.0D0,30.0D0/
DATA YDATA/-3.932D0,-4.186D0,-5.15D0,-4.55D0,-4.39D0,-4.55D0/
DATA RLABEL/'NONE/', CLABEL/' ', 'Mean of X', 'Mean of Y',
& 'Variance X', 'Variance Y', 'Corr.', 'Std. Err. B0',
& 'Std. Err. B1', 'DF Reg.', 'SS Reg.', 'DF Error',
& 'SS Error', 'Pts. with NaN'/
C
CALL DRLINE (NOBS, XDATA, YDATA, B0, B1, STAT)
C
CALL UMACH (2, NOUT)
WRITE (NOUT,99999) B0, B1
99999 FORMAT (' B0 = ', D14.5, ' B1 = ', D14.5)
CALL DWRRRL ('%/STAT', 1, 12, STAT, 1, 0, '(12W10.4)', RLABEL,
& CLABEL)
C
END

```

Result:

B0 = -.42743D+01 B1 = -.13663D-01

Therefore, the intercept  $\ln\left[\frac{R_T}{1 + \left(\frac{L_0}{K_D}\right)}\right] = -4.3$ , and the slope  $-[1 + \left(\frac{L_0}{K_D}\right)]k_r = -0.014$ .

When we substitute  $K_D = 1.6 \times 10^{-10}$  M into the slope equation  $-[1 + \left(\frac{L_0}{K_D}\right)]k_r = -0.014$ ,

$k_r = 0.01\text{min}^{-1}$  is obtained, since we know  $L_0 = 0.2\text{ng}$ . Because  $K_D = k_r / k_f$ ,  $k_f = 6.2 \times 10^7 \text{ M}^{-1}\text{min}^{-1}$  could be determined.

## Appendix C

In Appendix B, the assumption we made was  $L = L_0$ , in which we neglected the decrease of ligand concentration due to the formation of binding complex, since  $L_0 \gg C$ . However, we wanted to know the effect of the depletion of ligand was on parameter estimation. Here it is shown, when we use  $L = L_0 - C$  instead of the assumption  $L = L_0$ , how the dissociation rate constant,  $k_r$ , and the association rate constant  $k_f$ , were determined from CAFAS data and equation

$$(12) \quad \frac{dC}{dt} = k_f R_T L_0 + [-(k_f R_T + k_f L_0 + k_r)]C + k_f C^2.$$

The cell free binding assay with the Bio-Dot apparatus was conducted with 0.2ng  $^{125}\text{I}$ -bFGF and 40ng PG. At times of 1min, 5min, 10min, 15min, 20min, 30min and 60min,  $C(t)$  was measured as the retention of binding complex on the membrane of Bio-Dot. Retention of 0.2ng  $^{125}\text{I}$ -bFGF alone without PG was also measured at indicated times and deducted as non-specific background binding. The data is shown below (same as that shown in Appendix B):

Time (min)	1	5	10	15	20	30	60
Binding Complex ( C ) (ng)	0.0198	0.0242	0.0336	0.0288	0.027	0.0288	0.0394

The equation (12) has a form of general *Riccati* equation,

$$\frac{dw}{dx} = q_0(x) + q_1(x)w + q_2(x)w^2 \text{ (Boyce and DiPrima, 1977). As to our case,}$$

$$q_0 = k_f R_T L_0;$$

$$q_1 = -(k_f R_T + k_f L_0 + k_r); \text{ and}$$

$$q_2 = k_f.$$

Therefore, the equation (12) can be transformed by a transformation factor  $w = -y'/(yq_2)$  to a second order linear homogeneous equation

$$C''(t) - q_1 C'(t) + q_0 q_2 C(t) = 0, \text{ which matches the second-order ordinary differential}$$

equation with constant coefficients  $a_0 y''(t) + a_1 y'(t) + a_2 y = 0$  ( $a_0 \neq 0$ ) (Boyce and DiPrima, 1977). In our case,

$$a_0 = 1;$$

$$a_1 = k_f L_0 + R_T k_f + k_r; \text{ and}$$

$$a_2 = k_f^2 L_0 R_T. \text{ Then the general solution can be obtained as } C = A_1 e^{at} + A_2 e^{bt}$$

wherein

$$a, b = \frac{-a_1 \pm \sqrt{a_1 a_1 - 4a_0 a_2}}{2a_0} \quad (a_1 a_1 - 4a_0 a_2 \neq 0) \quad (\text{Korn and Korn, 1968}).$$

We used the software MicroCal Origin (version 3.01, Microcal Software, Inc.

Northampton, MA) to fit our data  $C \sim t$  as exponential decay with two terms, and got the following results:

Fit  $y_0 + A_1 e^{-x/t_1} + A_2 e^{-x/t_2}$  to Data1\_B

X offset (x0) = 1

Y offset (y0) = 0

```
-----
t1=12.91      A1=-0.07971
t2=19.19      A2=0.09933
```

In our case,  $a = -1/t_1$  and  $b = -1/t_2$ .

With our initial condition,  $C = 0$  when  $t = 0$ , we got  $A_1 = -A_2$  in our general solution, which matched with the data fitting results.

With the parameter  $L_0 = 0.2 \text{ ng}$ ,  $K_D = 1.6 \times 10^{-10} \text{ M}$  and  $R_T = 1.3 \times 10^8 \text{ (#/ng PG)}$  and the relation  $K_D = k_r / k_f$ , we obtained the average  $k_f = 5.6 \times 10^7 \text{ M}^{-1} \text{ min}^{-1}$  based on molecular weight of bFGF. Then the  $k_r = 0.009 \text{ min}^{-1}$  was obtained from  $k_r = K_D k_f$ .

## Curriculum Vitae

### NINGLING WANG

#### **Campus Address:**

Department of Chemical Engineering  
Virginia Polytechnic Institute and State University  
Blacksburg, VA 24061-0211

#### **Home Address:**

609 North Main St. #3  
Blacksburg, VA 24060  
(540)961-2187

#### **EDUCATION**    **Virginia Polytechnic Institute and State University,** Blacksburg, VA

M.S., Chemical Engineering, August 1997 (expected)  
Q.C.A.: 3.8

#### **Beijing University of Chemical Technology, Beijing, P.R.CHINA**

B.S., Chemical Engineering, July 1994  
GPA:    overall: 3.8                    major: 3.95

#### **EXPERIENCE**    **Virginia Polytechnic Institute And State University** Department of Chemical Engineering, Blacksburg, VA **teaching assistant:**

- Process and Plant Design (Fall semester, 1995)
- Unit Operation lab (2<sup>nd</sup> summer session, 1996)
- Transport Phenomena (Spring semester, 1996; Fall semester, 1996)
- Chemical Process Modeling (Spring semester, 1997)

#### **research assistant:**

- in Dr. Forsten's lab (January 1996 - present)

#### **Liu, Shen & Associates, Beijing, P.R.CHINA**

**legal assistant:** July 1994 - July 1995

#### **HONORS**

Finalist of the graduate student representative to the Board of Visitors  
at Virginia Tech, 1996  
Dean's list at Beijing University of Chemical Technology, 1990-1994  
Award for most distinguished student (ten total), 1993  
DuPont company scholarship, 1993  
Excellence in science and technology scholarship by  
Beijing High Education Bureau, 1992

#### **ACTIVITIES**

Secretary of Graduate Student Assembly (GSA) at Virginia Tech,  
1997-1998  
Representative of GSA to University Council at Virginia Tech,  
1997-1998  
Member of Phi Beta Delta, Honor Society for International scholars,

1997-1998

Officer in Council of International Student Organizations (CISO)  
at Virginia Tech, 1996-1997

Representative of CISO to Graduate Student Assembly and to  
Commission of Students Affairs at Virginia Tech, 1996-1997

Officer of the Student Union at Beijing University of Chemical  
Technology, 1992-1994

Vice-president of the English club at Beijing University of Chemical  
Technology, 1992-1994